

**NAPO**  
**AS A NOVEL APOPTOSIS MARKER**

**A THESIS SUBMITTED TO**  
**THE DEPARTMENT OF MOLECULAR BIOLOGY AND GENETICS**  
**AND THE INSTITUTE OF ENGINEERING AND SCIENCE OF**  
**BILKENT UNIVERSITY**  
**IN PARTIAL FULFILLMENT OF THE REQUIREMENTS**  
**FOR THE DEGREE OF DOCTOR OF PHILOSOPHY**

**BY**  
**BERNA S. SAYAN**  
**AUGUST, 2002**

THESIS

QH  
671  
.S29  
2002

**NAPO**  
**AS A NOVEL APOPTOSIS MARKER**

**A THESIS SUBMITTED TO**  
**THE DEPARTMENT OF MOLECULAR BIOLOGY AND GENETICS**  
**AND THE INSTITUTE OF ENGINEERING AND SCIENCE OF**  
**BILKENT UNIVERSITY**  
**IN PARTIAL FULFILLMENT OF THE REQUIREMENTS**  
**FOR THE DEGREE OF DOCTOR OF PHILOSOPHY**

**BY**  
**BERNA S. SAYAN**  
**AUGUST, 2002**

B067490

QH  
671  
.529  
2002

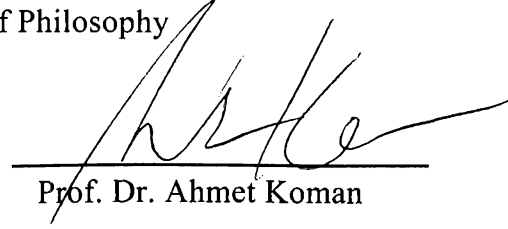
**TO MY HUSBAND EMRE...**

I certify That I read this thesis and in my opinion it is fully adequate, in scope and quality, as thesis for the degree of Doctor of Philosophy



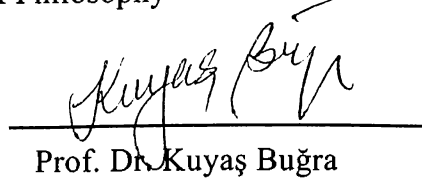
Prof. Dr. Mehmet Öztürk

I certify That I read this thesis and in my opinion it is fully adequate, in scope and quality, as thesis for the degree of Doctor of Philosophy



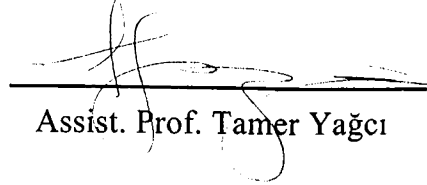
Prof. Dr. Ahmet Koman

I certify That I read this thesis and in my opinion it is fully adequate, in scope and quality, as thesis for the degree of Doctor of Philosophy



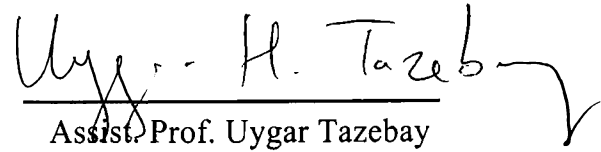
Prof. Dr. Kuyuş Buğra

I certify That I read this thesis and in my opinion it is fully adequate, in scope and quality, as thesis for the degree of Doctor of Philosophy



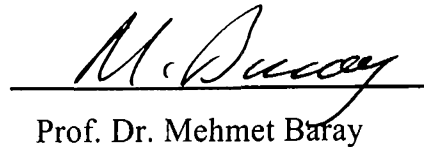
Assist. Prof. Tamer Yağcı

I certify That I read this thesis and in my opinion it is fully adequate, in scope and quality, as thesis for the degree of Doctor of Philosophy



Assist. Prof. Uygur Tazebay

Approved for the Institute of Engineering and Science



Prof. Dr. Mehmet Baray

## **ABSTRACT**

### **NAPO as a novel apoptosis marker**

**Berna S. Sayan**

**Ph.D. in Molecular Biology and Genetics**

**Supervisor: Prof. Dr. Mehmet Öztürk**

**2002, 128 pages**

Apoptosis or programmed cell death plays a pivotal role in embryonic development and maintenance of homeostasis. It is also involved in the etiology and of pathophysiological conditions such as cancer, neurodegenerative, autoimmune, infectious and heart diseases. Consequently, the study of apoptosis is now at center of both basic and clinical research applications. Therefore sensitive and simple apoptosis detection techniques are required. This study involves identification and characterization of a monoclonal antibody-defined novel antigen, namely *NAPO* (negative in apoptosis), which is specifically lost during apoptosis. The anti-*NAPO* antibody recognizes two nuclear polypeptides of 60 kD and 70 kD. The antigen is maintained in quiescent and senescent cells, as well as in different phases of the cell cycle including mitosis. Thus, immunodetection of *NAPO* antigen provides a specific, sensitive and easy method for differential identification of apoptotic and non-apoptotic cells.

## ÖZET

### Yeni bir apoptoz belirteci: NAPO

Berna S. Sayan

Doktora Tezi, Moleküler Biyoloji ve Genetik Bölümü

Tez yöneticisi: Prof. Dr. Mehmet Öztürk

2002, 128 sayfa

Apoptoz veya programlanmış hücre ölümü embriyonik gelişimde ve homeostazın sağlanmasında çok önemli bir role sahiptir. Ayrıca kanser, nörodejeneratif hastalıklar, otoimmün hastalıklar ve kalp hastalıklarının patofizyolojilerinde de rol alır. Buna bağlı olarak, apoptozun tayini ve çalışılması hem temel hem de klinik araştırmalar açısından son derece önemlidir. Bu sebeple apoptoz tayininde kullanılacak hassas ve basit metodların geliştirilmesi gerekmektedir. Bu çalışma NAPO (apoptozda negatif) adlı, spesifik olarak apoptoz sırasında yok olan yeni bir antijenin bulunması ve karakterizasyonunu içermektedir. NAPO'ya karşı olan anti-NAPO antikoru 60 ve 70 kDa civarında yürüyen iki adet polipeptidi tanımaktadır. Bu antijen kuisens, senesens ve mitoz da dahil olmak üzere hücre siklusunun tüm safhalarında varlığını sürdürmektedir. Yani NAPO antijeninin immünoteksiyonu apoptotik olan ve olmayan hücrelerin teşhisi için kullanılabilinecek spesifik, hassas ve kolay bir methoddur.

## ACKNOWLEDGEMENTS

First, I would like to thank my supervisor Prof. Dr. Mehmet Ozturk for giving me the chance to enter the splendid world of Molecular Biology and Genetics in Turkey and particularly for letting me enter and discover this world with him, under the light of his extraordinary experience and knowledge, admirable brilliance and forethought, and amazing patience. I know, I would not be able to succeed, if I had worked with someone else. I have not only learned scientific thinking from him, but he has also influenced my scope of living.

I also would like to thank my husband Emre, for being such a perfect person and being with me in all my good and bad days. I do appreciate him for all the things we have shared in the last seven years. He is one of the very few people who has encouraged me and take me up whenever I was down, and make me smile whenever I was sad. He is not only a great spouse but also a great working partner. I truly owe him the point where I am at the moment. I thank him for all his support, motivation and love. I feel very lucky to have him in my life.

I would like to thank my father Enver Özçelik and my mother Keriman Özçelik for raising me as the person I am. I thank my father for teaching me to struggle with difficulties and to be a diligent person. He showed me that honesty, idealism, intellectuality and hard-working will always open the doors of success. His principles will always guide my life. I am deeply missing you... I also want to thank my mother for her encouragement, support, love and most importantly for being my best friend. She has always guided me with her tenderness, tolerance, deep love and understanding. I thank my sister Ayşin for being with me whenever I needed her. She will always be a support in every step I take in my life.

I also want to express my deepest gratitude to Esin and Erol Sayan, for their indispensable support and encouragement and to Eser and Korcan for their friendship.

Very special thanks to my best friends Abdullah Yalcin and Ahmet Ucar. The times I spent with them were the best times I have spent in Bilkent. They made my time here memorable and unforgettable.

I also would like to thank all the faculty of the department for their guidance and helps.

Special thanks to the members of the “Molecular Oncology Group”: Esra, Tolga, Nuri and Ozgur for their helps and friendship. Also thanks to Tuba G., Banu, Ebru, Cemaliye, Belhaj, Hani and Arzu. Biggest thanks to Tulay, for her “always good mood” and smiling face. Also to Fusun for her friendship and supply of reagents at maximum speed and I also want to thank Sevim Baran, Yavuz Ceylan and Abdullah Unlu.

## TABLE OF CONTENTS

	PAGE
ABSTRACT.....	i
ÖZET.....	ii
ACKNOWLEDGEMENT.....	iii
TABLE OF CONTENTS.....	v
LIST OF TABLES.....	xi
LIST OF FIGURES.....	xii
ABBREVIATIONS.....	xv

### CHAPTER I

#### INTRODUCTION

1-1	General Introduction.....	1
1-2	C.Elegans As The Model Organism.....	7
1-3	Caspases.....	9
	1-3.1 Structure Of Caspases.....	9
	1-3.2 Regulation Of Caspase Activation.....	13
	1-3.3 Inhibitor Of Apoptosis Proteins (IAPs).....	14
	1-3.4 Targets Of Active Caspases.....	15
1-4	The BCL-2 Family.....	16
	1-4.1 General Structure.....	16
	1-4.2 Bcl-2 Family Function In Apoptosis.....	19
	1-4.3 Regulation Of Bcl-2 Family Members.....	19
	1-4.3.1 Post-Translational Modifications.....	19
	1-4.3.2 Cellular Localization And.....	21
	Dimerization	
1-5	Death Receptor Pathway.....	22
	1-5.1 CD95/Fas/Apo-1.....	23
	1-5.2 TNF Receptors.....	25
	1-5.3 TRAIL Receptors.....	26

1-6	Mitochondria.....	27
1-6.1	General Structure.....	28
1-6.2	Cytochrome C Release From The.....	29
	Mitochondria And Apoptosis	
1-6.3	Other Factors Released From The Mitochondria.....	32
	During Apoptosis	
1-6.3.1	SMAC/DIABLO.....	32
1-6.3.2	Apoptosis Inducing Factor (AIF).....	32
1-6.3.3	Pro-Caspases.....	33
1-7	Regulation Of Apoptosis.....	33
1-8	Role Of Apoptosis In Human Disease.....	34

## CHAPTER II

### DETECTION OF APOPTOSIS IN CELLS AND TISSUES

2-1	Analysis of morphological features of apoptosis.....	40
2-2	DNA fragmentation assays.....	41
2-3	Analysis of free DNA ends.....	43
2-4	Use of Annexin V.....	44
2-5	Detection of caspase activity.....	44

## CHAPTER III

	AIM OF THE STUDY.....	46
--	-----------------------	----

## CHAPTER IV

### MATERIALS AND METHODS

4-1	Production of anti- <i>NAPO</i> antibody from hybridomas.....	48
4-1.1	Production of anti- <i>NAPO</i> antibody producing.....	48
	hybridomas	
4-1.2	Production of anti- <i>NAPO</i> ascites in Balb/c mice.....	49

4-1.3	Characterization of Ig subtype of the anti-NAPO.....	49
	antibody	
4-2	Screening of $\lambda$ TripIEx expression library with the anti-.....	50
	NAPO antibody	
4-2.1	Bacterial strains.....	50
4-2.2	Solid and liquid mediums.....	50
4-2.3	Antibiotics.....	51
4-2.4	Growth and maintenance of primary and working.....	51
	bacterial stocks	
4-2.5	Titration of $\lambda$ TripIEx expression library.....	51
4-2.6	Transfer of plaques to nitrocellulose filters.....	53
4-2.7	Immunodetection.....	54
4-2.7.1	Optimization of the secondary.....	54
	antibody concentration	
4-2.7.2	Immunodetection.....	54
4-3	Western Blotting with the anti-NAPO antibody.....	54
4-3.1	Tissue culture studies.....	54
4-3.1.1	Defrosting cells.....	55
4-3.1.2	Subculturing of cells.....	57
4-3.2	Protein extraction from cells.....	57
4-3.3	Bradford assay for protein quantitation.....	57
4-3.4	SDS-Polyacrylamide gel electrophoresis of.....	58
	proteins	
4-3.5	Transfer of proteins from SDS-polyacrylamide.....	63
	gels to solid supports	
4-3.6	Staining proteins immobilized on solid.....	65
	surfaces with Ponceau S	
4-3.7	Denaturation and renaturation of proteins on.....	65
	nitrocellulose membranes	
4-3.8	Immunological detection of immobilized.....	66
	proteins (Western Blotting)	
4-3.9	Detection of proteins immobilized on membranes.....	66
4-4	Immunoprecipitation with the anti-NAPO antibody.....	67
4-5	Immunofluorescence with the anti-NAPO antibody.....	67

4-6	Induction of apoptosis in different cell lines.....	68
4-6.1	Induction of apoptosis by serum starvation.....	68
4-6.2	Induction of apoptosis by oxidative stress and cisplatin..	69
4-6.3	Induction of apoptosis by UV-C treatment.....	69
4-6.4	Induction of apoptosis by activation of.....	69
	death-receptor mediated apoptosis	
4-6.4.1	Induction of apoptosis by TNF- $\alpha$ .....	69
	treatment	
4-6.4.2	Induction of apoptosis by anti-Fas.....	70
	antibody treatment	
4-7	p53 staining of apoptotic versus non-apoptotic Huh7 cells.....	70
4-8	TUNEL staining of apoptotic cells.....	70
4-9	Synchronization of Huh7 and MRC5 cells.....	71
4-9.1	Synchronization of MRC5 cells by serum withdrawal....	71
4-9.2	Synchronization of Huh7 cells by nocodazole treatment.	71
4-9.2.1	Optimization of nocodazole concentration	72
4-9.2.2	Mitotic shake-off.....	72
4-10	BrdU labeling and identification of S phase cells.....	72
4-11	Induction of quiescence in MRC5 cells.....	73
4-12	Senescence associated $\beta$ -Galactosidase Assay.....	73

## CHAPTER V

### RESULTS

5-1	Introduction.....	74
5-2	Production of the anti-NAPO monoclonal antibody.....	75
5-2.1	Production of anti-NAPO antibody producing.....	75
	hybridomas	
5-2.2	Characterization of Ig subtype of the anti-.....	75
	NAPO antibody	
5-3	Screening of $\lambda$ TriplEx expression library with the.....	75
	anti-NAPO antibody	

5-3.1	Titration of $\lambda$ TripIEx expression library.....	75
5-3.2	Optimization of the secondary antibody concentration...	76
5-3.3	Immunodetection.....	76
5-4	Biochemical characterization of the NAPO antigen.....	76
5-4.1	Western Blotting with the anti-NAPO antibody.....	76
5-4.2	Immunoprecipitation with the anti-NAPO antibody.....	77
5-4.3	Immunofluorescence with the anti-NAPO antibody.....	77
5-4.3.1	Staining of HCC cell lines with..... the anti-NAPO antibody	77
5-4.3.2	Species specific expression of the..... NAPO antigen	78
5-5	Identification of NAPO as an apoptotic marker.....	79
5-5.1	NAPO immunoreactivity of apoptotic..... SNU 398 and Huh7 cells	80
5-5.2	p53 immunoreactivity of apoptotic Huh7 cells....	82
5-5.3	NAPO immunostaining in cells treated with..... various apoptotic stimuli	83
5-5.3.1	NAPO immunostaining in death-..... receptor mediated apoptosis	83
5-5.3.2	NAPO immunostaining in UV-C..... irradiation induced apoptosis	84
5-5.4	NAPO immunostaining in tumorous versus non-..... tumorous cells exposed to various apoptotic stimuli	85
5-5.4.1	NAPO immunostaining in apoptotic..... tumorous cell lines versus viable counterparts	86
5-5.4.2	NAPO immunostaining in apoptotic..... non-tumorous cell lines versus viable counterparts	86
5-6	Expression of the NAPO antigen in quiescent cells.....	89
5-7	Expression of the NAPO antigen during cell cycle.....	91
5-7.1	Expression of NAPO in synchronized Huh7 cells.....	92

5-7.1.1	Synchronization of Huh7 cells by..... mitotic shake-off	92
5-7.1.2	Determination of S phase cells by..... BrdU incorporation assay	93
5-7.1.3	NAPO immunostaining at different..... phases of the cell cycle	94
5-7.2	Expression of NAPO in synchronized MRC-5 cells.....	96
5-7.2.1	Synchronization of MRC-5 cells..... by serum starvation	96
5-7.2.2	Determination of S phase cells..... by BrdU incorporation assay	96
5-7.2.3	NAPO immunostaining at different..... phases of the cell cycle	98
5-8	Expression of the NAPO antigen in senescent cells.....	100

## CHAPTER VI

DISCUSSION AND PERSPECTIVES.....	103
----------------------------------	-----

## CHAPTER VII

REFERENCES.....	112
-----------------	-----

Appendix: Publications

## LIST OF TABLES

<u>NUMBER/NAME</u>	<u>PAGE</u>
<b>Table 1-1:</b> Differences between apoptosis and necrosis.....	3
<b>Table 1-2:</b> The main sub-groups of mammalian caspases.....	9
<b>Table 1-3:</b> Dysregulation of apoptosis in some autoimmune..... diseases.	35
<b>Table 1-4:</b> Summary of the Roles of Apoptotic Initiators, ..... Regulators or Executioners in Tumorigenesis and Apoptosis	38
<b>Table 4-1:</b> Concentrations of the antibiotics used in this study.....	51
<b>Table 4-2:</b> Dilution chart of $\lambda$ TripIEx for titration.....	52
<b>Table 4-3:</b> The cell lines used for characterization of <i>NAPO</i> .....	56
<b>Table 4-4:</b> Effective range of separation of SDS-PAGE gels.....	59
<b>Table 4-5:</b> Solution of preparing resolving gels for Tris-glycine..... SDS-PAGE.	61
<b>Table 4-6:</b> Solution of preparing 5% stacking gels for..... Tris-glycine SDS-PAGE.	63
<b>Table 5-1:</b> Expression of the <i>NAPO</i> antigen in cell lines of..... different species.	79
<b>Table 5-2:</b> List of cell lines tested for loss of <i>NAPO</i> ..... immunoreactivity after induction of apoptosis by various stimuli.	80

## LIST OF FIGURES

<u>NUMBER/NAME</u>	<u>PAGE</u>
<b>Figure 1-1:</b> Schematic representation of mechanisms leading..... 2 to apoptotic cell death.	2
<b>Figure 1-2:</b> The apoptotic pathway is conserved in metazoans..... 4	4
<b>Figure 1-3:</b> Activation of death-receptor mediated apoptosis..... 5 through binding of the cognate receptor to its ligand.	5
<b>Figure 1-4:</b> Induction of apoptosis through cytochrome c..... 6 release from the mitochondria.	6
<b>Figure 1-5:</b> Activation of apoptosis machinery in the nematode..... 8 <i>C. elegans</i> .	8
<b>Figure 1-6:</b> Activation of caspases..... 11	11
<b>Figure 1-7:</b> Structure of some of the initiator and..... 12 effector caspases.	12
<b>Figure 1-8:</b> Release of inhibitory effects of IAPs on caspases..... 15 by the SMAC/DIABLO protein.	15
<b>Figure 1-9:</b> Structure of some pro- and anti-apoptotic Bcl-2..... 18 family members.	18
<b>Figure 2-1:</b> Basic morphological features of apoptosis,..... 41 differing from necrosis used in the detection of apoptosis.	41
<b>Figure 2-2:</b> Principle of DNA laddering assay and a typical..... 42 gel appearance of apoptotic cell DNA.	42
<b>Figure 2-3:</b> Labelling principle of terminal polymerase ..... 43 and terminal transferase	43
<b>Figure 2-4:</b> Use of PARP cleavage for the detection of..... 45 apoptosis by western blotting.	45

<b>Figure 5-1:</b>	Immunoprecipitation of the <i>NAPO</i> antigen from.....	77
	Huh7 cell lysate.	
<b>Figure 5-2:</b>	Nuclear localization of the <i>NAPO</i> antigen in Huh7.....	78
	and SNU 398 cell lines.	
<b>Figure 5-3:</b>	Loss of the <i>NAPO</i> antigen in serum-starved.....	81
	SNU 398 HCC cells.	
<b>Figure 5-4:</b>	<i>NAPO</i> immunoreactivity of apoptotic Huh7 cells.....	82
	in comparison with TUNEL assay	
<b>Figure 5-5:</b>	p53 staining of apoptotic Huh7 cells.....	83
<b>Figure 5-6:</b>	<i>NAPO</i> immunostaining in death receptor.....	84
	mediated apoptosis in MCF-7 and Jurkat cells.	
<b>Figure 5-7:</b>	<i>NAPO</i> staining of UV-C induced apoptotic.....	85
	MCF-7 and Jurkat cells.	
<b>Figure 5-8:</b>	Expression of <i>NAPO</i> in cells induced to undergo.....	87
	apoptosis by UV-C irradiation.	
<b>Figure 5-9:</b>	Expression of <i>NAPO</i> in non-tumorous cells.....	88
	induced to undergo apoptosis.	
<b>Figure 5-10:</b>	Brd-U incorporation test to serum starved and.....	90
	non-starved p18 MRC-5 cells.	
<b>Figure 5-11:</b>	<i>NAPO</i> immunostaining of serum starved and.....	91
	non-starved p18 MRC-5 cells.	
<b>Figure 5-12:</b>	Optimization of the most efficient nocodazole.....	93
	concentration required to arrest Huh7 cells in M phase of the cell cycle with the least cytotoxic effect.	
<b>Figure 5-13:</b>	BrdU incorporation index of M phase arrested.....	94
	Huh7 cells after mitotic shake-off.	
<b>Figure 5-14:</b>	<i>NAPO</i> immunostaining of synchronized Huh7 cells.....	95
<b>Figure 5-15:</b>	BrdU incorporation assay of synchronized.....	97
	MRC-5 cells.	
<b>Figure 5-16:</b>	BrdU incorporation index of serum starved MRC-5.....	98
	cells after release from the quiescent state.	
<b>Figure 5-17:</b>	<i>NAPO</i> immunostaining of synchronized MRC-5 cells....	99

**Figure 5-18:** SA- $\beta$  Galactosidase and *NAPO* immunostaining of..... 101  
P18 and p40 MRC-5 cells.

## ABBREVIATIONS

AIDS	Acquired Immunodeficiency Virus
AIF	Apoptosis Inducing Factor
ANT	Adenine Nucleotide Translocator
Apaf-1	Apoptotic Protease Activating Factor 1
ASK	Apoptosis Signal Regulating Kinase
ATP	Adenosine triphosphate
BH Domain	Bcl-2 Homology Domain
BIR	Baculovirus IAP Repeats
Bisacrylamide	N, N, methylene bis-acrylamide
Bp	Base Pair
BSA	Bovine Serum Albumin
<i>C. elegans</i>	<i>Caenorhabditis elegans</i>
CAD	Caspase Activated DNase
Caspase	Cysteine Aspartyl Protease
CARD	Caspase Recruitment Domain
CD	Cluster of Differentiation
ced	Cell Death Defective
CO <sub>2</sub>	Carbon Dioxide
crmA	Cytokine Response Modifier A
<i>D. melanogaster</i>	<i>Drosophila melanogaster</i>
Da	Dalton
Daxx	Death Domain Associated Protein
DcR	Decoy Receptor
DD	Death Domain
DED	Death Effector Domain
DISC	Death Inducing Signaling Complex
DMSO	Dimethyl Sulfoxide
DNA	deoxyribonucleic acid
dUTP	deoxyuridine triphosphate
EGF	Epithelial Growth Factor
ERK	Extracellular Signal-Related Kinase

EtOH	Ethanol
FADD	Fas Associated DD
FCS	Fetal Calf Serum
FIST	Fas Interacting Serine/Threonine Kinase
FLIP	Fas Associated DD like ICE Inhibitory Protein
HCC	Hepatocellular Carcinoma
HIPK3	Homeodomain Interacting Protein Kinase
HIV	Human immunodeficiency virus
HRP	Horse Redish Peroxidase
IAP	Inhibitor of Apoptosis proteins
ICAD	Inhibitor of CAD
ICE	Interleukin-1 $\beta$ Converting Enzyme
I $\kappa$ B	Inhibitor of NF- $\kappa$ B
IL	Interleukin
IPTG	isopropylthio- $\beta$ -D-galactoside
JNK/SAPK	c-Jun N-terminal Kinase/Stress-activated protein kinase
Kan	kanamycin
Kb	Kilo base
kDa	kilo daltons
LB	Luria-Bertani media
MAPK	Mitogen Activated Protein Kinase
MgSO <sub>4</sub>	Magnesium Sulfate
ml	Mililiter
mg	Miligram
MQ	MilliQ water
N-terminus	amino terminus
NaCl	Sodium Chloride
NaOH	Sodium Hydroxide
NAPO	Negative in Apoptosis
NIK	NF- $\kappa$ B Inducing Kinase
Nm	nanometer (1/10 <sup>9</sup> of a meter)
OD	Optical Density

O/N	Over Night
PAGE	polyacrylamide gel electrophoresis
PARP	Poly (ADP-ribose) polymerase
PBS	Phosphate Buffered Saline
PBS-T	Phosphate Buffered Saline with Tween-20
Pfu	Plaque Forming Unite
PKA	Protein Kinase A
PKB/Akt	Protein kinase B
PKC	Protein Kinase C
PTP	Permeability Transition Pore
RAIDD	RIP Associated ICH-1/Ced3 Homologous Protein with a Death Domain
RIP	Receptor Interacting Protein
RPM	Revolutions per minute
SDS	Sodium Dodecyl Sulfate
SDS-PAGE	SDS- Polyacrylamide Gel Electrophoresis
Ser	Serine
VDAC	Voltage dependent Anion Channel
tBid	Truncated Bid
TBS	Tris-Buffered Saline
TBS-T	Tris Buffered Saline with Tween-20
TEMED	N,N,N,N-tetramethyl-1,2 diaminoethane
Tris	tris (hydroxymethyl)-methylamine
TRADD	TNF-R-associated DD
TRAF	TNF Receptor Associated Factor
TRAIL	TNF-related Apoptosis-Inducing Ligand
TRIP	TRAF-Interacting Protein
TUNEL	TdT-mediated dUTP nick end labeling
UV	Ultraviolet
X-Gal	5-bromo-4-chloro-3-indolyl- $\beta$ -D-galactoside

# **CHAPTER I**

## **INTRODUCTION**

### **1-1 GENERAL INTRODUCTION**

Apoptosis (programmed cell death) is the most common physiological form of cell death. It is essential for the precise regulation of cellular homeostasis and development as it serves to remove unwanted (excess, damaged or infected) cells at critical and appropriate times (Vaux and Korsmeyer, 1999; Wyllie and Golstein, 2001). Apoptosis is a tightly regulated process and can be activated by various mechanisms as summarized in figure 1-1. Many morphogenetic abnormalities and diseases are linked to dysregulation of this process thus it is critical for development and survival of all metazoans (Reed, 2000; Mattson, 2000; Chervonsky, 1999; Roulston et al., 1999; Narula et al., 2000). For example in many different types of cancer, pro-apoptotic factors are inactivated and pro-survival (anti-apoptotic) factors are upregulated. This leads to accumulation of apoptosis-resistant cells and since effective chemotherapy depends on the induction of programmed cell death, these types of cancers are hard to treat (Lowe and Lin, 2000).

Apoptotic cell death is characterized by a series of morphological changes including cell shrinkage, nuclear condensation, chromatin segregation, membrane blebbing, formation of membrane-bound apoptotic bodies and internucleosomal DNA cleavage. In more detail, chromatin condenses and forms aggregates near the nuclear membrane, the nucleolus becomes enlarged and appears abnormally granular. Chromatin is then degraded first into 300-350 kb, then into 180 bp fragments by the actions of different activated endonucleases (Brown and Rose, 1992; Oberhammer et al., 1993; Wyllie AH., 1980). Then the cells shrink and

form apoptotic bodies. These apoptotic bodies are rapidly phagocytosed and digested by neighboring cells or macrophages thus inflammation does not occur during apoptosis (Saraste and Pulkki, 2000). These features of apoptosis make it a unique mechanism of cell death. In the other form of cell death, which is necrosis, cells swell and inflammation occurs. The major differences between apoptosis and necrosis are summarized in table 1-1.

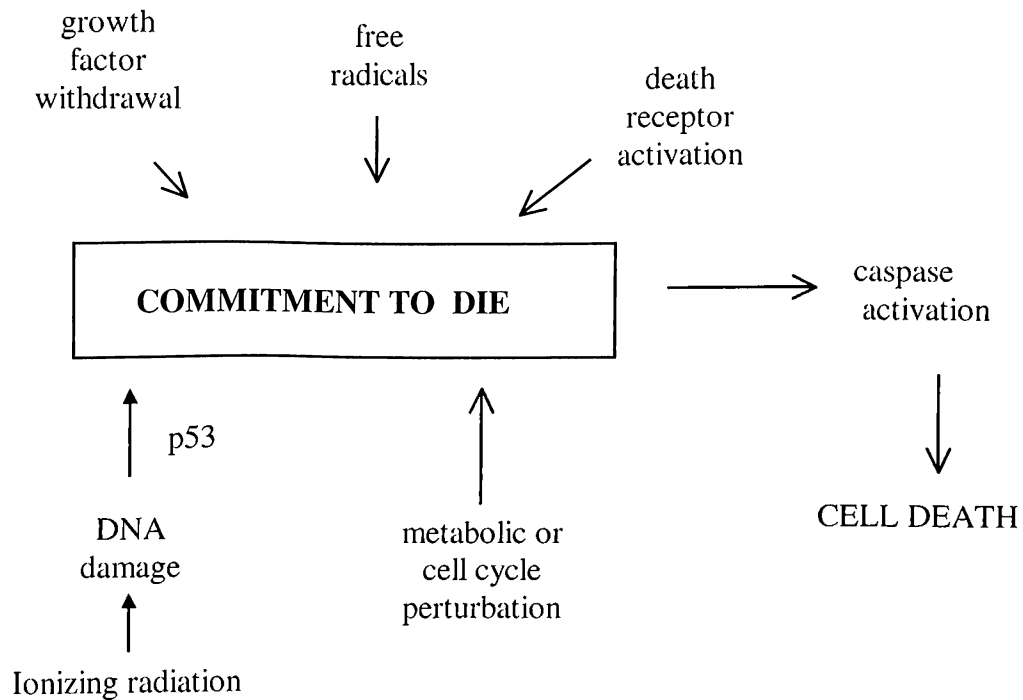


**Figure 1-1: Schematic representation of mechanisms leading to apoptotic cell death.**

**Table 1-1: Differences between apoptosis and necrosis.**

<b>Features</b>	<b>Necrosis</b>	<b>Apoptosis</b>
<b>Stimuli</b>	Toxins, severe hypoxia, massive insult and conditions of ATP depletion	Physiological and pathological conditions without ATP depletion
<b>Energy Requirement</b>	None	ATP dependent
<b>Histology</b>	Cellular swelling, disruption of organelles, death of patches of tissue	Chromatin condensation, apoptotic bodies, death of single isolated cells
<b>DNA breakdown pattern</b>	Randomly sized fragments	Ladder of fragments in internucleosomal multiples of 180 bp
<b>Plasma membrane</b>	Lysed	Intact, blebbed, with molecular alterations
<b>Phagocytosis of dead cells</b>	Immigrant phagocytes	Neighboring cells
<b>Tissue reaction</b>	Inflammation	No inflammation

Components of the apoptotic cell death mechanism are conserved in all metazoans, from nematodes to humans (figure 1-2). Thus, study of programmed cell death in the nematode “*Caenorhabditis elegans*” (*C. elegans*) has revealed both the mechanisms underlying the highly regulated apoptotic processes and the genes that are involved in the regulation of this process. As nomenclature, the genes whose protein products induce apoptosis are called “pro-apoptotic” and the ones whose protein products inhibit apoptosis are called “pro-survival” or “anti-apoptotic”.

In metazoans, apoptosis can be activated by one of the two pathways. The first is the activation of death receptors by binding of a death inducing ligand to its cognate receptor (summarized in figure 1-3). In the other pathway, apoptosis

is induced by the release of cytochrome c from the mitochondria due to activation of apoptosis inducing factors such as the pro-apoptotic members of the bcl-2 family (summarized in figure 1-4). In both cases the final outcome is the activation of the caspase cascade.

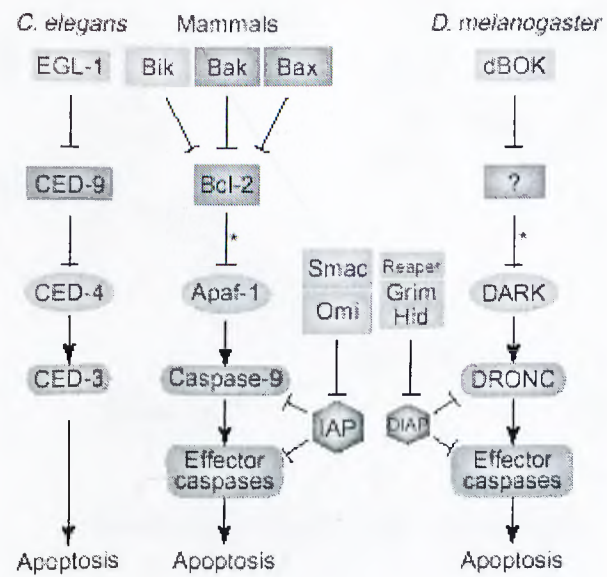
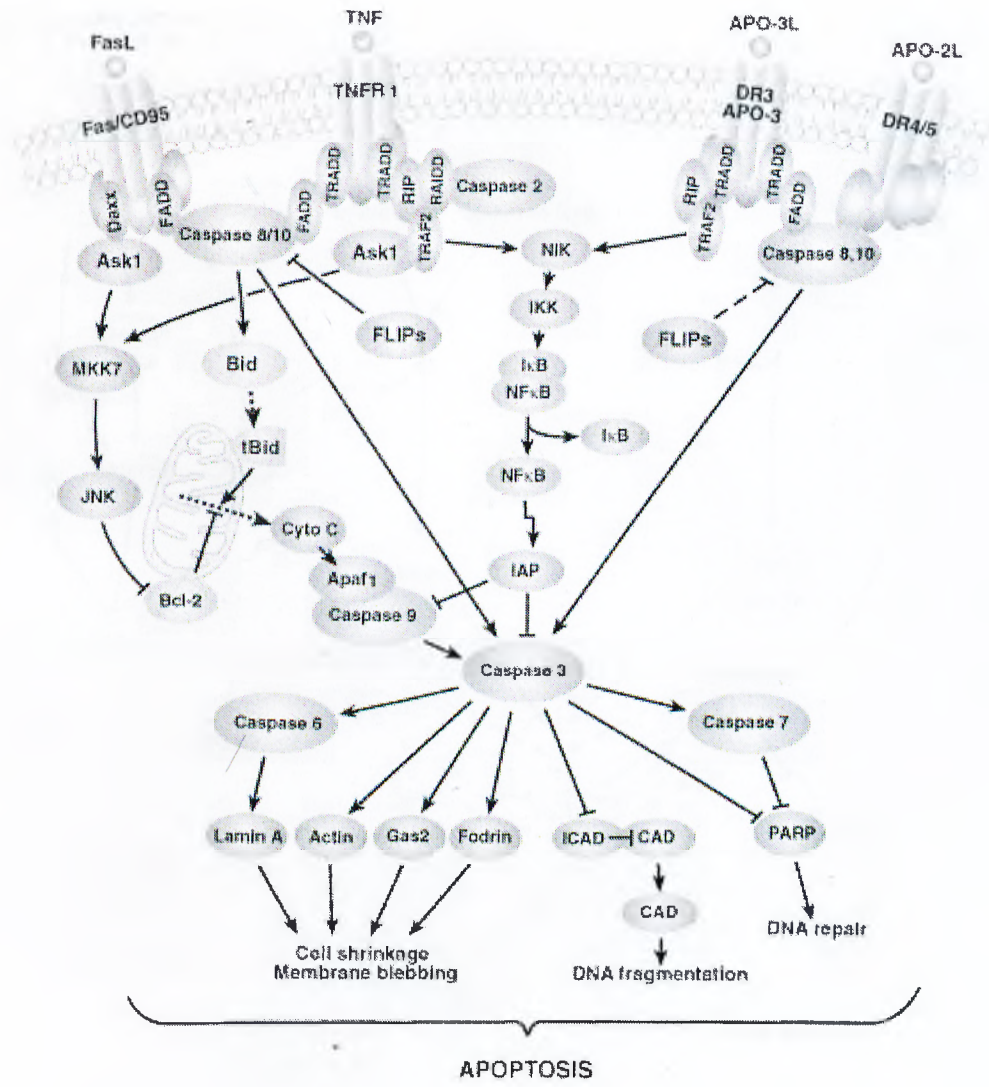
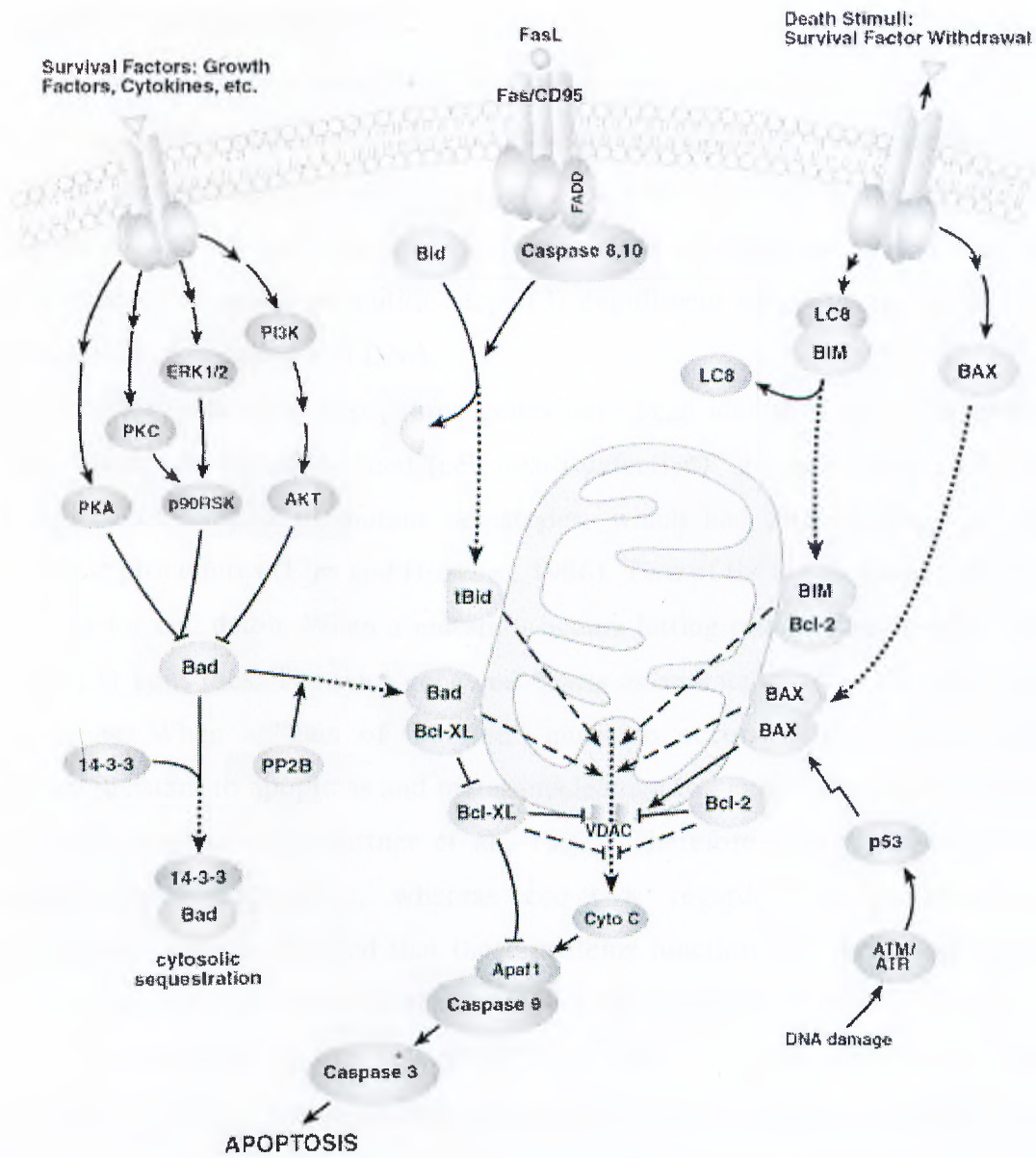


Figure 1-2: The apoptotic pathway is conserved in metazoans.



**Figure 1-3: Activation of death-receptor mediated apoptosis through binding of the cognate receptor to its ligand. (taken from cellsignaling.com)**



**Figure 1-4: Induction of apoptosis through cytochrome c release from the mitochondria.** (taken from cellsignaling.com)

## 1-2 *C.Elegans* AS THE MODEL ORGANISM

One of the organisms that have been used extensively for the study of apoptosis is the nematode *C. elegans*. During development 131 cells among 1090 cells die by apoptosis to leave a final total of 959 in the adult. The analysis of apoptosis in *C. elegans* has identified four steps in apoptosis. These are: (1) determination step, (2) execution step, (3) engulfment of apoptotic bodies, (4) degradation of engulfed cell DNA.

In the execution steps, three genes have been identified that play critical roles. These are named as “ced (cell death defective)” genes as they were first identified by analysis of mutant nematodes, which had abnormalities in their apoptotic procedures (Ellis and Horvitz., 1986). Two of these *ced-3* and *ced-4* are required for cell death. When a mutation occurs hitting one of these genes, none of the 131 cells dies. The third gene *ced-9* acts as an antagonist of the other two *ced* genes. When a “gain of function” mutation occurs in *ced-9* gene, cells become resistant to apoptosis and mutations leading to “loss of function” result in extensive apoptosis (Hengartner et al., 1992). Therefore, *ced-3* and *ced-4* are regarded as pro-apoptotic, whereas *ced-9* is regarded as anti-apoptotic. Biochemical analysis revealed that these proteins function as a ternary complex, in which activation of the protease CED-3 by the adapter protein CED-4 is normally repressed by the anti-apoptotic CED-9. In cells destined to die, expression of EGL-1 results in displacement of CED-4, activation of CED-3, and cellular demise. In more detail, the protein encoded by *ced-3*; Ced-3 is a cysteine aspartyl protease (caspase), which cleaves after aspartate residues. Caspases are synthesized as inactive pro-enzymes and upon activation their N-terminal pro-domain is cleaved resulting in the formation of an active caspase. The protein encoded by *ced-4*; Ced-4 can physically interact with both Ced-3 and Ced-9, acting as an adaptor molecule (Chinnaiyan et al., 1997). It contains a putative ATPase domain, which is required for its ability to activate Ced-3. The human homologue of Ced-4 is the Apaf-1 protein. The protein encoded by *ced-9*; Ced-9 prevents apoptosis by blocking the activation of Ced-3. It has been shown that Ced-9 utilizes two different mechanisms to inhibit Ced-3 mediated apoptotic pathways (Xue and Horvitz., 1997). It may interact directly with Ced-3 inhibiting the cleavage of pro-domain of Ced-3 or it may compete with Ced-3 and inhibit

apoptosis indirectly. For the latter mechanism first Ced-9 is cleaved by Ced-3 to form a Ced-3 like Ced-9 protein fragment. A schematic representation of the activation of apoptosis machinery in the nematode *C. elegans* is shown in figure 1-5, where egl-1 gene product acts as a pro-apoptotic protein for the inhibition of the anti-apoptotic Ced-9 protein.

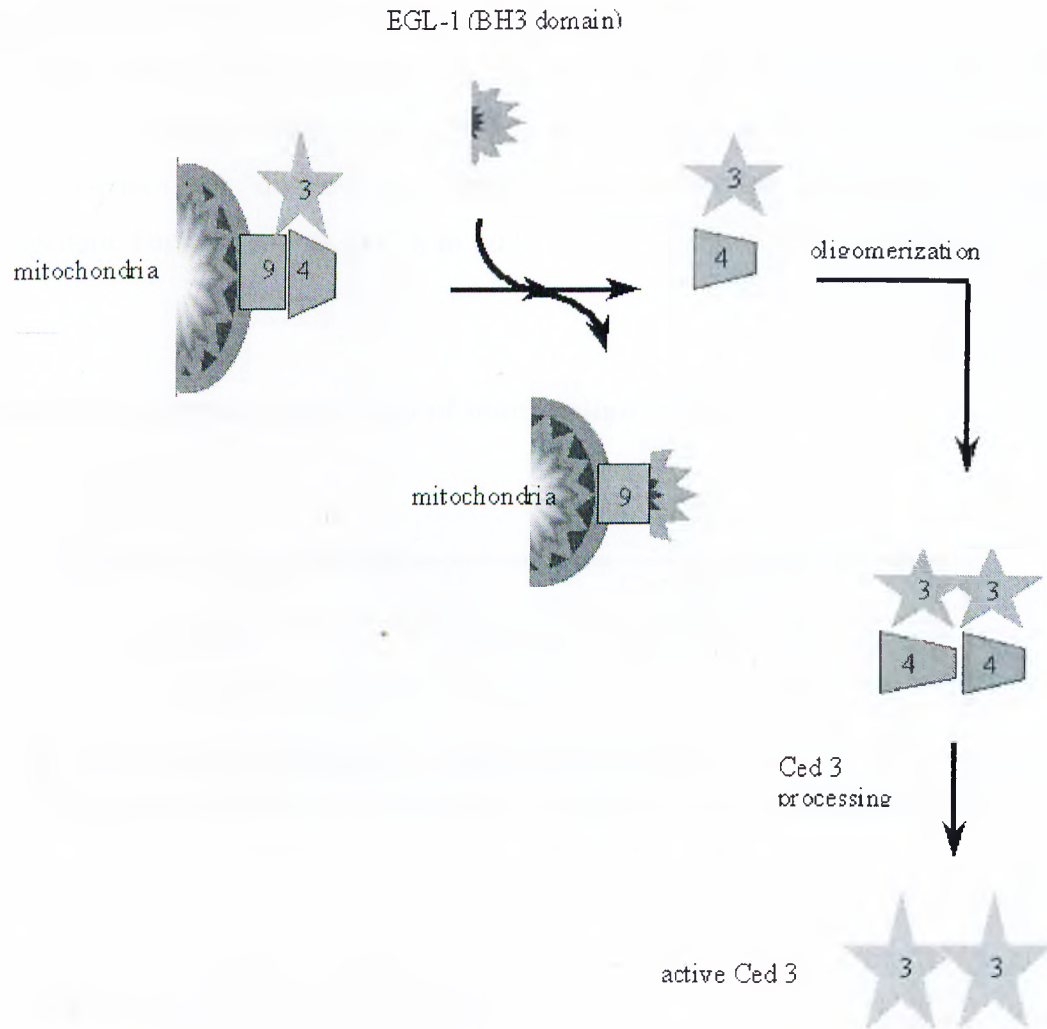


**Figure 1-5: Activation of apoptosis machinery in the nematode *C. elegans*.**

### 1-3 CASPASES

Caspases are cysteine proteases that cleave substrates after a conserved aspartate residue and are known to be the executors of apoptosis in metazoans. They are found as inactive zymogens and are activated when cleaved appropriately. The activated caspases initiate a caspase cascade by cleaving each other and the initially activated caspases are called “initiator caspases”. The caspases activated as a result of this cascade and have functions in the execution phase of apoptosis are called “effector caspases”. The first caspase; caspase-1 (ICE: Interleukin-1 $\beta$  converting enzyme) was identified in 1993 as the human homologue of ced-3 (Yuan et al., 1993). Today 14 different caspases are known. These caspases are divided into three main sub-groups according to their phylogenetic background as shown in table 1-2.

**Table 1-2: The main sub-groups of mammalian caspases**

Name	Components
ICE-subfamily	Caspase-1, -4, -5, -11, -12, -13, -14
Ced-3/ CPP32 subfamily	Caspase-3, -6, -7
ICH-1/Nedd2 subfamily	Caspase-2, -8, -9, -10

#### 1-3.1 STRUCTURE OF CASPASES

Caspases share structural and catalytic homologies. In all caspases the active site is composed of a pentapeptide sequence with the general structure QACXG (X=G, Q or R), where the cysteine in the middle, together with a distant histidine, is directly involved in the catalysis. Caspases recognize a tetrameric primary sequence in their targets, which contains an aspartic acid in the first position (Thornberry and Lazebnik, 1998).

The inactive caspases are called pro-caspases, and they contain a N-terminal prodomain, which is cleaved during activation. Caspases can be activated by one of the three mechanisms. They can cleave themselves (autoactivation), can be cleaved by previously activated caspases or they can be activated by non-caspase activators such as granzyme-B. After cleavage the cleaved subunits (large subunit and small subunit) form a heterodimer and two heterodimers form the active caspase as shown in figure 1-6.

Caspases differ in the length of their prodomains. Caspases -3, -6, -7 and -10 contain short prodomains (10-40 residues). The caspases with long prodomains contain recognizable domains in their prodomains involved in signal transduction via protein-protein interaction. Thus these prodomains play important roles in caspase regulation and function (Earnshaw et al., 1999). For example the prodomain of caspase-8 and -10 contain "death effector domain" in their prodomain, which mediate signal transduction between the death receptor and the downstream caspases through adaptor molecules. This allows death receptor-induced activation of downstream caspases in response to ligand binding to the receptor. The caspases -1, -2, -4 and -9 contain CARD domain (caspase recruitment domain) in their prodomain. CARD domain is also present in the adaptor molecule Apaf-1. The CARD domain is thought to mediate specific intermolecular interactions that regulate caspase activation. Structures of some of the caspases are shown in figure 1-7.

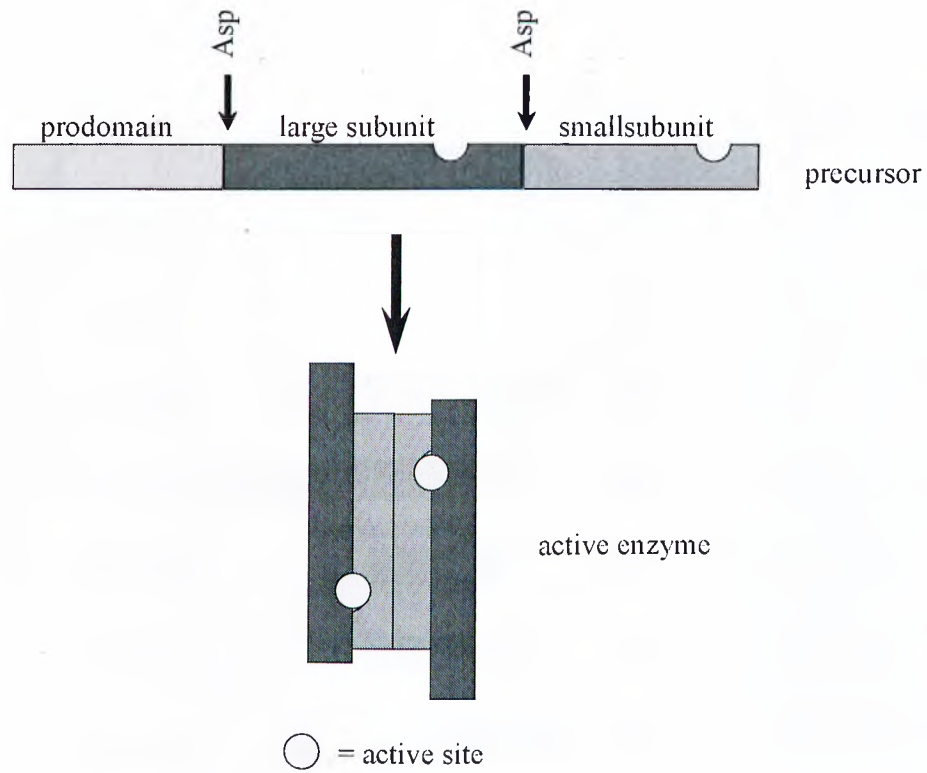


**Figure 1-6: Activation of caspases due to cleavage of the prodomain region and cleavage of the remaining part into two subunits namely small and large subunits.**

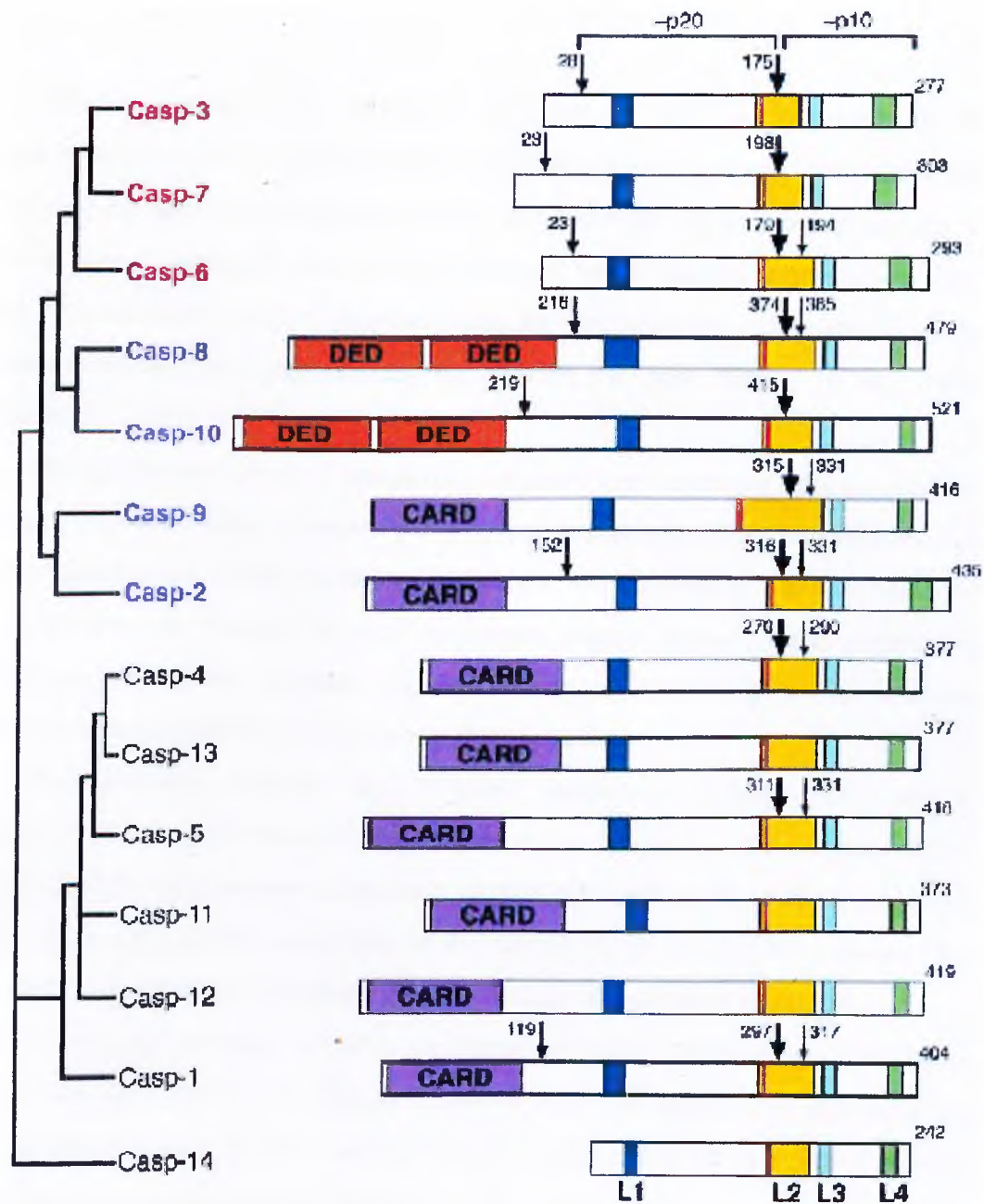


**Figure 1-7: Structure of some of the initiator and effector caspases.**

All listed caspases are of human origin except caspase-11 (mouse), -12 (mouse), and -13 (bovine). The initiator and effector caspases are labeled in purple and red, respectively. The position of the first activation cleavage (between the large and small subunits) is highlighted with a large arrow while additional sites of cleavage are represented by medium and small arrows. L1-L4 represent the regions required for the formation of the catalytic groove. The catalytic residue Cys is shown as a red line at the beginning of L2.

### 1-3.2 REGULATION OF CASPASE ACTIVATION

The availability and activation of caspases are crucial steps in the commitment of a cell to die; therefore their regulation is strictly controlled and maintained by several cellular processes. For example, caspases are subject to transcriptional regulation and posttranslational modification (Earnshaw et al., 1999). In addition, active caspases can be permanently eliminated by the ubiquitination-mediated proteasome degradation pathway (Huang et al., 2000; Suzuki et al., 2001).

Being the executors of apoptosis, caspases are targets of various caspase inhibitory proteins. This inhibition plays a very important role in pathogenesis as well as tumorigenesis. For example, as infected cells commit suicide and undergo apoptosis for the benefit of the organism, some viruses have developed mechanisms to inhibit caspase function in order to overcome the cellular apoptosis response generated due to the viral infection.

Baculoviruses express the “caspase inhibitory protein p35”, which competes with the substrates of the caspase-8 for binding to the enzyme. After binding of p35 to the caspase, caspase-8 cleaves p35 and the N-terminal fragment of p35 protein blocks the active site of the caspase in an irreversible manner (Xu et al., 2001). In mammals a homologue of p35 has not yet been identified.

A cowpox protein “crmA” (cytokine response modifier A) has been shown to be the inhibitor of caspase-1 and -8. Like the baculovirus protein p35, crmA is also cleaved by the caspase that it inhibits, but the inhibitory effects results from a conformational change in the active site of the caspase due to crmA binding (Renatus et al., 2000).

Baculoviruses also encode for another type of proteins named “IAPs” (inhibitor of apoptosis proteins). The enzymatic activity of caspases is subject to inhibition by the conserved IAP (inhibitor of apoptosis) family of proteins (Deveraux and Reed, 1999).

Some chemicals are also known to inhibit caspase activation. These are aldehydes or fluoromethyl ketone-derivatized synthetic peptide inhibitors such as (ZVAD-fmk).

### 1-3.3 INHIBITOR OF APOPTOSIS PROTEINS (IAPs)

IAPs have been identified in many different organisms from viruses to mammals due to the presence of a 65 amino acid homology domain named “BIR” (baculovirus IAP repeats). These repeats are typically found in the N-terminal region of the IAPs and mediate various types of protein-protein interactions. Certain IAPs also contain a C-terminal ring finger, which is presumed to mediate other specific protein-protein interactions. Eight distinct mammalian IAPs, including XIAP, c-IAP1, c-IAP2, and ML-IAP/Livin (Ashhab et al., 2001; Kasof and Gomes, 2001; Vucic et al., 2000), have been identified, and they target the initiator caspase, caspase-9, and the effector caspases, caspase-3 and -7 (Deveraux and Reed, 1999).

Recent structural analyses revealed that a linker segment at the N-terminal region between BIR1 and BIR2 of XIAP occupies the active site of caspases directly which results in a blockade of substrate entry. This makes IAPs unique inhibitors of caspases that function by directly binding to and inhibiting caspase function, rather than targeting the enzyme indirectly and affecting their activation. (Chai et al., 2001; Huang et al., 2001; Riedl et al., 2001). It is also noteworthy to mention that only processed caspase-9 is subject to inhibition by IAPs. It has been shown that, BIR3 of XIAP binds to the N terminus of the small subunit of caspase-9, which becomes exposed after proteolytic processing (Srinivasula et al., 2001).

However induction of apoptosis requires elimination of the caspase inhibition enforced by IAPs. Thus when apoptosis is induced, IAPs are inhibited by binding of a mitochondrial apoptosis promoting factor Smac/DIABLO to the BIR domains of IAPs (Green DR., 2000) (Figure 1-8).

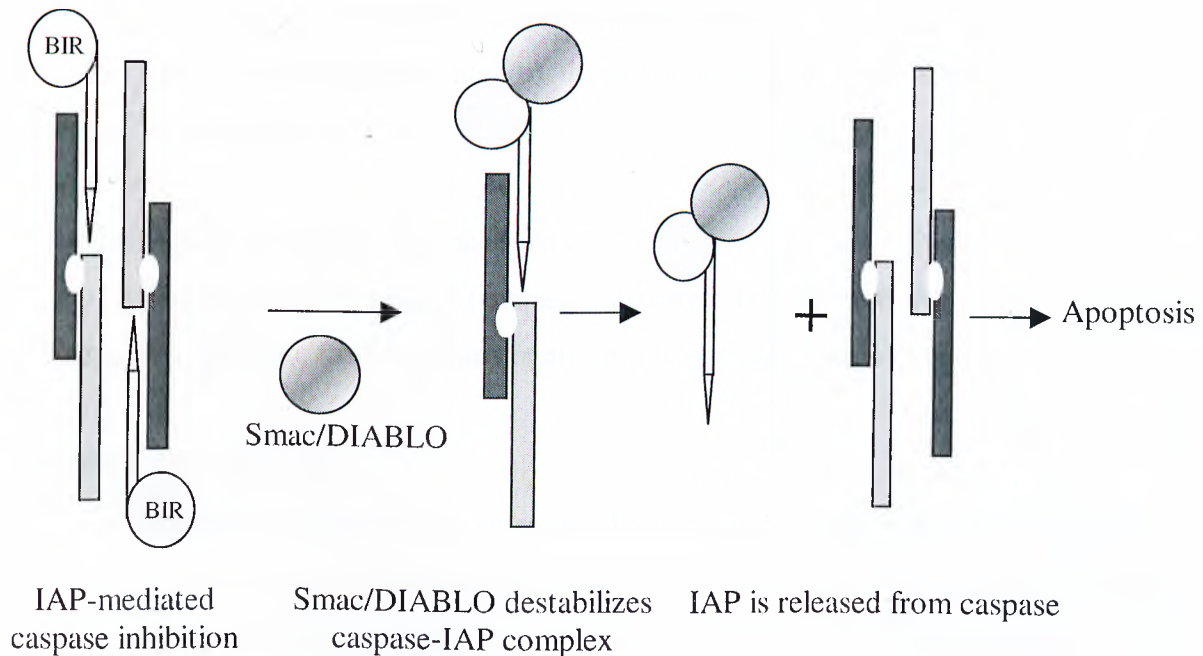


**Figure 1-8: Release of inhibitory effects of IAPs on caspases by the SMAC/DIABLO protein.**

It has been shown that deregulation of IAPs contribute to human disease. For example a single BIR domain containing IAP “Survivin” has been shown to be upregulated in many human tumours.

### 1-3.4 TARGETS OF ACTIVE CASPASES

When activated, initiator caspases activate downstream caspases and when the effector caspases are activated they cleave critical cellular protein substrates in order to advance apoptosis. (Thornberry and Lazebnik, 1998). The targets of active caspases can be grouped in 4 groups.

1- Pro- and anti-apoptotic proteins:

- a) Pro-caspases: The already activated caspases transactivate other caspases. This allows the generation of a caspase activation cascade.
- b) Anti-apoptotic proteins: Bcl-2 and bcl-XL are cleaved by caspase-3. This way the anti-apoptotic activities of these proteins are eliminated.

c) Cleavage of the pro-apoptotic protein Bid by caspase-8: The cleavage product t-Bid translocates to the mitochondria and induces the release of cytochrome c.

#### 2- Components of apoptotic machinery:

The inhibitor of CAD (caspase activated DNAase) ICAD is cleaved by caspase-3, allowing CAD to translocate to nucleus and cleave DNA.

#### 3- Structural proteins:

The structural proteins gelsolin (which regulates actin dynamics), lamins (which are the major structural proteins of nuclear envelope) and  $\beta$ -catenin (which plays important roles in cell-cell adhesion) are degraded by caspases.

#### 4- Homeostatic proteins:

Poly (ADP-ribose) polymerase (PARP) is a DNA double-break repair enzyme that is cleaved to facilitate the DNA degradation during apoptosis.

## **1-4 THE BCL-2 FAMILY**

### **1-4.1 GENERAL STRUCTURE**

Bcl-2 family proteins play a pivotal role in deciding whether a cell will die or survive. Bcl-2 was first identified as a proto-oncogene in follicular B-cell lymphoma (Tsujiimoto et al., 1985). In 1993 Oltvai et al discovered the first pro-apoptotic member of the Bcl-2 family namely Bax (Oltvai et al., 1993).

The growing Bcl-2 family consists of 'multidomain' death antagonists (e.g. Bcl-2, Bcl-XL, Bcl-w, Mcl-1, A1) and death agonists (e.g. Bax, Bak, Bok), which function primarily to protect or disrupt the integrity of mitochondrial membranes, respectively. The homology between the Bcl-2 family members is restricted to four Bcl-2 homology (BH) domains (Figure 1-9). Through these homology domains they can form homo- or heterodimers with each other. Thus the ratio of pro- versus anti-apoptotic members is very critical for making the decision of cell death. All of the anti-apoptotic members have four of the BH

domains whereas the pro-apoptotic members do not have the BH4 domain except for Bcl-Xs. There are also “BH3 only” pro-apoptotic members, which carry only the BH3 homology domain. These proteins serve as ligands to activate multidomain pro-apoptotic Bcl-2 family members or inactivate anti-apoptotic Bcl-2 family members (Huang and Strasser, 2000). BH3-only proteins include Bim, Bid, Bad, Bik/Nbk, BNIP3, Blk, Noxa, Puma, and Hrk. Another characteristic of these proteins is that they can become integral membrane proteins.

Protein crystallography and liposome reconstitution analysis with purified Bcl-2 family members suggest that, these proteins regulate the mitochondrial membrane barrier by forming channels themselves or influencing pre-existing channels in the membrane (Martinou and Green, 2001).

Alterations in expression, subcellular localization, phosphorylation status, and proteolytic processing of Bcl-2 family molecules determine whether the death program will be activated.

The anti-apoptotic members can dimerize with pro-apoptotic members to inhibit apoptosis. Among these, BH1 and BH2 are important for heterodimerization of the anti-apoptotic members Bcl-2 and Bcl-X<sub>L</sub> with Bax for the suppression of apoptosis (Borner et al., 1994). But anti-apoptotic members can perform their inhibitory effects on apoptosis without the need to bind and inactivate a pro-apoptotic member. It has been shown that a mutant form of Bcl-X<sub>L</sub>, which cannot bind the anti-apoptotic members Bax or Bad can still preserve the 70-80% of its anti-apoptotic ability (Cheng et al., 1996).

BH3 domain is the most critical domain for pro-apoptotic activity. This domain has been termed as “suicide domain” because when the BH3 domain of Bax was inserted into Bcl-2, the anti-apoptotic protein became a killer protein (Hunter et al., 1996). Also although the “BH3 only” pro-apoptotic members (Bid, Bik, Bim, Blk and Bad) carry the BH3 domain, they induce apoptosis through heterodimerizing with pro- or anti-apoptotic proteins. Crystal structure of Bcl-X<sub>L</sub> and Bid showed the presence of a region named the “flexible region” at the N-terminal of the BH3 domain, which serves as a potential phosphorylation site (Muchmore et al., 1996).

BH4 domain can be regarded as the anti-apoptotic domain, as its presence is enough to confer anti-apoptotic activity to Bcl-2 family members. Bcl-2

mutants lacking BH4 domain lose their anti-apoptotic activity and become killer proteins (Grandgirard et al., 1998). It has also been shown that during apoptosis, the BH4 domain of Bcl-2 is cleaved to accelerate the apoptotic procedure (Cheng et al., 1997, Grandgirard et al., 1998)

Another important domain found in some Bcl-2 family members is the C-terminal hydrophobic domain, which mediates the localization of these proteins to membranes.

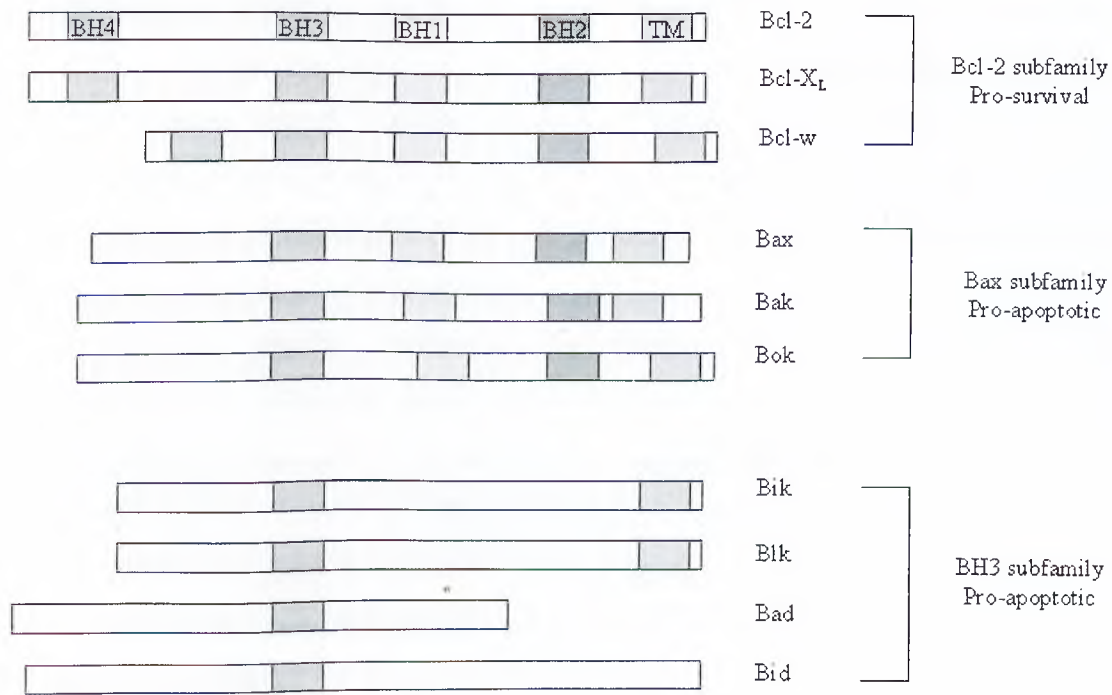


**Figure 1-9: Structure of some pro- and anti-apoptotic Bcl-2 family members.**

(TM: transmembrane domain)

## **1-4.2 BCL-2 FAMILY FUNCTION IN APOPTOSIS**

Currently, three (non-exclusive) models are used to explain Bcl-2 function. In the first model, it is proposed that Bcl-2 proteins can act as ion channels due to their structural resemblance to the diphtheria toxin and colicin (Muchmore et al., 1998). The second model suggests that Bcl-2 proteins function in the modulation of caspase activation for example by inhibition of the apical caspase-9 by Bcl-2/Bcl-xL. According to this model, Bcl-2/Bcl-xL should displace Bcl-2/Bcl-xL from the Apaf-1/ cytochrome c/caspase-9 complex and so trigger caspase-9 autoactivation just as in the case of *C. elegans* (Chinnaiyan et al., 1997). Finally, the third model proposes that these proteins act as inhibitors of cytochrome c export from mitochondria. Very recently it has been shown that Bax and Bak serve as the major mitochondrial sensors of upstream apoptosis signaling, and cells missing both factors are resistant at the mitochondrial level to killing by a wide range of stimuli (Wei et al., 2001).

Another possible mechanism by which Bcl-2 might function in the suppression of apoptosis arose from observations that Bcl-2 expression can affect intracellular  $Ca^{2+}$  homeostasis. Alterations in intracellular  $Ca^{2+}$  concentrations are known to influence apoptosis so it remains possible that Bcl-2 either directly modulates calcium channels or acts to protect lipid membranes from damage by peroxide radicals which is known to disrupt  $Ca^{2+}$  homeostasis (Pinton et al., 2002).

## **1-4.3 REGULATION OF Bcl-2 FAMILY MEMBERS**

Regulation and activity of the family members is regulated by phosphorylation, proteolysis, dimerization and by their cellular localization.

### **1-4.3.1 POST-TRANSLATIONAL MODIFICATIONS**

Members of the Bcl-2 family can be regulated by phosphorylation or proteolysis. The anti-apoptotic activity of Bcl-2 can be either inhibited or

amplified by phosphorylation. Phosphorylation of Bcl-2 at residues serine 70 and 87 and threonine 56 and 74, has been shown to inactivate its anti-apoptotic activity (Chang et al., 1997). Bcl-2 was found to be phosphorylated and thus inactivated in many tumor cell lines that are treated with chemotherapeutic agents such as taxol (Haldar et al., 1995 and 1996). One of the kinases responsible for Bcl-2 phosphorylation is a MAPK (mitogen-activated protein kinase) family member JNK/SAPK (c-Jun N-terminal Kinase/Stress-activated protein kinase) (Maundrell et al., 1997). JNK/SAPK is known to be activated by stimuli favouring apoptosis. The anti-apoptotic function of bcl-2 has been shown to be amplified by phosphorylation at serine 70 by the activation of a classic protein kinase C (PKC) isoform. This phosphorylation is required for suppression of apoptosis by Bcl-2 in murine growth factor-dependent cell lines (Ruvolo et al., 1998). Another MAPK family member ERK (extracellular signal-related kinase), is also involved in the regulation of apoptotic proteins. While JNK/SAPK functions to promote apoptosis by inhibiting Bcl-2, ERK can be activated to inhibit apoptosis (Xia et al., 1995). When activated ERK phosphorylates Bad at residues serine-112 and serine-136. Phosphorylated Bad associates with 14-3-3 protein and becomes sequestered in the cytosol (Zha et al., 1996). To inhibit this inhibitory function of Erk, during apoptosis this kinase is inactivated by the actions of caspase 3 (Widmann et al., 1998).

Similar to Bcl-2, the pro-apoptotic “BH3 only” protein Bad is a target for kinases. In the presence of survival factors BAD is phosphorylated on two serine residues (Ser-112 and Ser-136) and sequestered in the cytosol by the 14-3-3 protein (Zha et al., 1996). The kinases responsible for Bad phosphorylation are PKA (Protein kinase A) and PKB/Akt (Protein kinase B) (Harada et al., 1999, del Peso et al., 1997). PKA phosphorylates Bad at ser-112 and PKB/Act from serine-136. Thus when cells are stimulated with survival factors, Bad is phosphorylated and its anti-apoptotic activity diminishes. Following a death signal BAD is dephosphorylated and binds to the anti-apoptotic molecules Bcl-2 and Bcl-X<sub>L</sub>.

Cleavage of pro- or anti-apoptotic proteins is also an important factor, affecting the apoptotic process. By cleavage anti-apoptotic factors may become pro-apoptotic and pro-apoptotic members become more apoptotic. For example, the pro-apoptotic Bcl-2 family member Bid has been shown to be cleaved during Fas-mediated apoptosis by caspase 8 (Li et al., 1998). After activation, caspase 8

cleaves Bid, generating a C-terminal fragment of the protein that is “truncated Bid” (tBid). While full-length p22 Bid is localized in cytosol, p15 tBid translocates to mitochondria and thus transduces apoptotic signals from cytoplasmic membrane to mitochondria. Cleavage of Bcl-2 by activated caspases results in formation of a C-terminal cleavage product which has a pro-apoptotic function (Cheng et al., 1998). It has also been demonstrated that Bax is a substrate for both caspases and the calcium-activated protease calpain (Wood et al., 1998).

### **1-4.3.2 CELLULAR LOCALIZATION AND DIMERIZATION**

The Bcl-2 members have been shown to be both cytosolic and membrane associated. A considerable portion of pro-apoptotic members are localized to cytosol in the absence of an apoptotic signal in contrast to anti-apoptotic members which are localized to membranes (Hsu et al., 1997, Gross et al., 1998, Puthalakath et al., 1999). Following a death signal the pro-apoptotic members undergo a conformational change and this alteration enables them to target and integrate into membranes, especially the outer membrane of the mitochondria. Activation of Bax requires both dimerization and cellular localization.

In viable cells Bax is monomeric and localized to cytosol. Following a death stimulus Bax is translocated to mitochondria where it becomes an integral membrane protein and forms a homo or heterodimer with Bcl-2/Bcl-xL (Wolter et al., 1997, Gross et al., 1998). However in contrast to Bax, Bak is usually resides in the outer mitochondrial membrane.

The anti-apoptotic protein Bcl-2 resides in the outer mitochondrial membrane, endoplasmic reticulum and the nuclear membrane (Krajewski et al., 1993; Lithgow et al., 1994). The three dimensional structures of Bcl-X<sub>L</sub> and Bid demonstrated that they share structural homology with the pore-forming domain of certain bacterial toxins especially diphtheria toxin and colicins A and E1 (Muchmore et al., 1996). It has been shown that Bcl-X<sub>L</sub>, Bcl-2 and Bax can form channels in synthetic lipid membranes (Minn et al., 1997, Schendel et al., 1997, Antonsson et al., 1997).

Thus localization of Bcl-2 family members to mitochondria and their pore-forming activities play a very important role during apoptosis.

## **1-5 DEATH RECEPTOR PATHWAY**

Activation of a specific group of transmembrane receptors also induce activation of caspases hence apoptosis. These receptors belong to the “tumor necrosis factor (TNF)” superfamily. Mammalian TNF-R (TNF receptor) family members are type I membrane proteins with conserved extracellular cysteine-rich domains. The TNF-R superfamily members include: TNF-R1, TNF-R2, TNF-R3, CD95, LT- $\alpha$ R, LT- $\beta$ R, Ox 40, CD27, CD 28, CD 30, CD 40, 4-1 BB, p75 NGFR, GIT-R, Rank, DR6 and the TRAIL receptors. When a receptor is activated it typically forms trimeric or multimeric complexes stabilized by disulfide bonds. Some of these receptors such as CD95, TNF-R1 and TNF-R2 can also exist in soluble forms (Hughes DPM. and Crispe IN., 1995).

The ligands of these receptors also comprise a family. Some members of this family are: TNF, CD 95 ligand (FasL/CD95L), LT- $\alpha$  (lymphotoxin- $\alpha$ ), LT- $\beta$ , Ox 40L, CD27L, CD 28L, CD 30L, CD 40L and 4-1 BBL. These ligands share a characteristic 150 amino acid region at their C-terminus. This C-terminal region is responsible for specific interaction of the ligand with its cognate receptor. Although TNF and CD95L can exist as soluble proteins, others are usually found as membrane-bound trimeric or multimeric complexes.

Some members of the TNF superfamily have been shown to induce apoptosis when activated by binding of their cognate ligand and therefore are called as “death-receptors”. These include CD95, TNF-R1, DR3, DR4, DR5 and DR6. These receptors share a homology region at their cytoplasmic region, which is called “death domain”. This domain is responsible for transduction of death signals to intracellular proteins by initiating a protein-protein interaction and activation cascade.

Upon ligand binding to the receptor, intracellular adapter proteins such as FADD/MORT1, TRADD and RAIDD are recruited to the cytoplasmic regions of the receptors through homotypic death-domain (DD) interactions to form a death-inducing signaling complex (DISC) (Ashkenazi and Dixit, 1998). In turn, FADD

recruits pro-caspase- 8 via interactions between death-effector-domains (DEDs) present in both proteins, thereby stimulating caspase-8 autoproteolytic activation and initiating a caspase cascade leading to cell death. Caspase-2 can also associate with the cytoplasmic regions of death receptors, and this association requires the interaction of caspase-2 with the molecular adapter RAIDD/CRADD (Duan and Dixit, 1997; Ahmad et al., 1997)

### **1-5.1 CD95/Fas/Apo-1**

CD95 is expressed in activated lymphocytes and in all other tissues including liver, lung and heart. The ligand of the receptor CD95L is expressed in activated lymphocytes, natural killer cells, erythroblasts, immune privileged tissues and in some tumors. The main function of CD95/CD95L signaling is deletion of autoreactive lymphocytes and maintenance of peripheral tolerance.

CD95 does not have a catalytic domain. Thus in order to activate downstream signaling effector molecules it has to interact with an adaptor molecule. This interaction is mediated by a 65 amino acid intracellular domain of CD95, which is called “death domain (DD)”. Through this domain CD95 can recruit downstream effector molecules and induce apoptosis (Itoh and Nagata, 1993). These adaptor/effector molecules include FADD/MORT (Fas-associated death domain), RIP (receptor interacting protein), Daxx (death domain associated protein) and FIST/HIPK3 (Fas interacting serine/threonine kinase/Homeodomain interacting protein kinase).

One of the adaptor molecules that interact with DD of CD95 is FADD/MORT. FADD contains a DD at its C-terminus and a death effector domain at its N-terminus. Through this DED, the adaptor protein can interact with the DED of procaspase-8 leading to autocleavage and activation of caspase-8. (Boldin et al., 1996; Muzio et al., 1996). This protein complex generated upon activation of CD95 is called “DISC (death inducing signaling complex)”. Thus, recruitment of DISC to the activated receptor provides a direct link between external apoptotic signals and the basal apoptotic machinery of the cell (Kischkel et al.,1995). When caspase-8 is activated it can either directly activate downstream caspases such as caspase-3 or it can cleave the pro-apoptotic

molecule Bid to generate a Bid fragment namely t-Bid (truncated Bid). t-Bid then translocates to mitochondria where it can induce cytochrome c release (Li et al., 1998; Lluo et al., 1998).

Another receptor-associated signal transducer molecule is RIP (Stanger et al., 1995). RIP contains a DD at its C-terminal and a tyrosine kinase-like domain at its N-terminal. It has been shown that blockers of tyrosine kinase activity also inhibit the CD-95 mediated apoptotic signal transduction (Eischen et al., 1994). RIP can also activate caspase-2 through an interaction with an adaptor molecule named "RAIDD (RIPP associated ICH-1/Ced-3 homologous protein with a death domain)" (Wallach D., 1997). This DD-DD interaction recruits procaspase-2, which interacts with RAIDD through the ICH-1/Ced-3 homology region. Another molecule activated by RIP is the anti-apoptotic molecule NF- $\kappa$ B. Thus RIP can also be an intermediate for inhibition of apoptosis. Therefore caspase-8 can also cleave RIP in order to inhibit the NF- $\kappa$ B activation (Lin et al., 1999).

Daxx is an inducer of "c-Jun N-terminal kinase" JNK and has been shown to bind to DD of CD95 although it lacks a DD (Yang et al., 1997). Therefore Daxx functions as an intermediate protein that couples CD95 to activation of JNK hence apoptosis. CD95 mediated JNK activation can be inhibited by FIST/HIPK3 (Rochat-Steiner et al., 2000). FIST/HIPK3 can also interact with CD95 as well as FADD. Binding of FIST/HIPK3 to FADD induces FADD phosphorylation and inhibits CD95 mediated JNK activation.

There are two main inhibitors of CD95 mediated apoptotic signaling. One of these inhibitors is FLIPs (Fas-associated death domain like ICE inhibitory proteins) and the other is the "decoy receptors". FLIPs exert their inhibitory effect by interfering with recruitment of caspases to CD95 signaling complex. Some viruses synthesize FLIPs (v-FLIP) in order to evade host immune system (Thome et al., 1997). The cellular homologue of v-FLIP is c-FLIP and been identified by several groups in 1997 (Srinivasula et al., 1997; Irmeler et al., 1997; Goltsev et al., 1997; Shu et al., 1997; Inohara et al., 1997; Hu et al., 1997; Han et al., 1997; Rasper et al., 1998). c-FLIP shows homology to caspase-8 containing two DEDs. It also contains an inactive caspase-like domain without the conserved functional cysteine domain. Therefore c-FLIP can block caspase-8 activation at the DISC and can inhibit CD95-mediated apoptosis (Scaffidi et al., 1999).

## 1-5.2 TNF RECEPTORS

TNF is a cytokine produced by activated T-cells and macrophages that influences the proliferation, differentiation and apoptosis of cells involved in inflammation. Thus TNF plays a pivotal role in the regulation the host inflammatory response.

There are two receptors for TNF: TNF-R1 and TNF-R2. TNF- R1 is able to mediate most of the biological responses initiated by TNF, whereas TNF-R2 provides an auxiliary function in cooperating in the binding of TNF to TNF-R1 (Tartaglia et al., 1993). Although TNF-R1 alone can trigger apoptosis TNF-R2 mainly seems to promote cell survival. Nevertheless TNF-R2 was also shown to kill certain cells when over-expressed (Grell et al., 1999). Both TNF-R1 and TNF-R2 can activate the pleiotropic transcription factor NF- $\kappa$ B (Rothe et al., 1994).

Binding of the ligand to TNF-R1 activates the proteolytic caspase cascade by recruiting caspase-8 via FADD/MORT. However FADD/MORT adapter molecule cannot directly bind to TNF-R1, therefore another cytoplasmic adapter molecule with a death domain called "TRADD" (TNF-R-associated death domain) is recruited to the activated receptor. TRADD can also bind to RIP, thereby linking TNF-R1 to caspase-2 activation via RAIDD and CRADD.

Another class of signaling adapter proteins recruited to the TNF receptor is the "TRAFs" (TNFR-associated factors) of which six are currently identified (Inoue et al., 2000). TRAF proteins are signal transduction adapter proteins. All TRAFs share a conserved 230 amino acid "TRAF domain" which mediates their homo- or hetero-oligomerization with other TRAFs, their interaction with the cytoplasmic tails of members of the TNF-R superfamily, and interactions with downstream signal transducers (Lee et al., 1997). TRAFs are held in abeyance in the cytoplasm through their association in oligomeric complexes with I-TRAF [177].

TRAF-2, -5, and -6 mediate activation of SAPK/JNK or NF- $\kappa$ B (Lee et al., 1997), the latter by interaction with the downstream signaling kinase NIK. NIK, in turn, activates the I $\kappa$ B kinases, which phosphorylate and inactivate I $\kappa$ B, the endogenous cellular inhibitor of NF- $\kappa$ B (Malinin et al., 1997; Ye et al.,

1999). It is believed that TRAFs' anti-apoptotic effect is due to the activation of NF- $\kappa$ B. TRAF proteins can also interact with the death domain kinase RIP and the serine/threonine kinase IRAK. On the other hand, apoptosis signal-regulating kinase ASK-1, a TRAF-interacting kinase, was recently demonstrated to be a downstream target of TRAF-2, TRAF-5, and TRAF-6 in the JNK signaling pathway.

TRAFs can also interact with "TRIP" (TRAF-interacting protein) (Lee et al., 1997). TRIP associates with TNF receptor family members through its interaction with TRAF proteins. This binding inhibits TRAF-mediated activation of the apoptosis suppressor NF- $\kappa$ B. However TRAFs can also interact with the IAP proteins. Thus, TRAF interactions with cIAPs would suppress apoptosis whilst interactions with TRIP would promote it. The availability of TRAF interacting proteins, therefore influence the outcome of TNF-R activation.

In another report it has been shown that in the presence of RIP (required for NF- $\kappa$ B activation by TNF-R1), TNF-R2 triggers cell death in T-cells whereas in the absence of RIP, TNF-R2 activates NF- $\kappa$ B (Pimentel-Muinos and Seed, 1999). RIP is induced during interleukin (IL)-2-driven T-cell proliferation, and its inhibition reduces susceptibility to TNF-dependent apoptosis.

### **1-5.3 TRAIL RECEPTORS**

Another subfamily of TNF receptors is the "TRAIL receptors" (TNF-related apoptosis-inducing ligand receptors) (Golstein, 1997; Gura, 1997; Ashkenazi and Dixit, 1998). The ligand TRAIL (is also called as apo-2L) is synthesized as a membrane-bound protein and cleaved to generate a soluble ligand, which does not to bind either CD95 or TNF-R1.

The receptors for TRAIL are: DR4 (TRAIL-R1), DR5 (TRAIL-R2/KILLER), decoy receptor 1(DcR1/TRID/LIT/TRAIL-R3), decoy receptor 2 (DcR2/TRUNDD) and osteoprotegerin. The latter three are called "decoy receptors" because although they can bind to TRAIL they cannot transduce signals as they lack a death domain. TRAIL induces apoptosis through binding to DR4 and DR5 requiring FADD and caspase-8 (Bodmer et al., 2000).

Although many human tumor cells and tumor cell lines are sensitive to induction of apoptosis by cell surface or soluble TRAIL; normal cells are insensitive (Pitti et al., 1996). Treatment of human cancer cell lines and tumors of mice and non-human primates with TRAIL, showed some promising results such as the apoptosis induction in TRAIL treated cancer cells and regression of tumors while keeping the non-tumor tissues unharmed, respectively (Walczak et al., 1999; Chinnaiyan et al., 2000; Gibson et al., 2000; Jo et al., 2000; Nagata, 2000). This is because of the expression profile of TRAIL and its receptors (with/without death domain) in tumorous and non-tumorous tissues. Although DR4 and DR5 are expressed in most human tissues and some tumor cell lines, DcR1 and DcR2 are expressed in many tissues although not in most cancer lines examined.

## **1-6 MITOCHONDRIA**

Whereas death receptors respond to instructive signals from neighboring cells or soluble ligands, an alternative cell death pathway depends on mitochondrial dysfunction and is initiated in response to primarily cell-intrinsic cues. An array of intracellular stimuli including DNA damage, glucocorticoids, perturbations in redox balance, ceramide generation, and loss of growth factor signals can trigger permeabilization of the outer mitochondrial membrane and leakage of mitochondrial pro-apoptotic effectors into the cytosol (Kroemer and Reed, 2000; Adrain and Martin, 2001).

One such effector is cytochrome *c*, which stimulates assembly of a ternary complex, called the mitochondrial 'apoptosome', that consists of cytochrome *c*, apaf-1 and caspase-9. Cytosolic cytochrome *c* binds to Apaf1 and induces its oligomerization. Oligomerized Apaf1 recruits pro-caspase-9, which is activated auto-proteolytically and triggers activation of caspase-3.

Death-receptor apoptosis signaling is also linked with mitochondrial cytochrome *c* release. Caspase-8, which is initially activated at the death-inducing signaling complex (DISC) of cell surface death receptors, can cleave the pro-apoptotic Bcl-2 family member Bid (Li et al., 1998; Luo et al., 1998). Binding of cleaved Bid (tBid) to Bax leads to Bax oligomerization and integration into the

outer mitochondrial membrane where it triggers cytochrome c release (Eskes et al., 2000). Similarly, tBid can bind to and oligomerize to another pro-apoptotic Bcl-2 homologue, Bak, resulting in cytochrome c release (Wei et al., 2000).

### **1-6.1 GENERAL STRUCTURE**

Mitochondria are not only the power plants of the cells but they also play a key role in the regulation of gene expression and making the decisions between survival and death. Mitochondrial intermembrane space contains several proteins that are liberated through the outer membrane in order to participate in the degradation phase of apoptosis.

Mitochondria are organized into several spaces (Mannella et al., 1998). The matrix, which is surrounded by the inner membrane, is filled with enzymes of the tricarboxylic acid cycle. Cristae are structures formed by the inner membrane and are projected through the matrix space. The crista membrane contains the electron transport complexes. In the intermembrane space cytochrome c, cytochrome c reductase, cytochrome oxidase, cardiolipin, procaspase 2, 3 and 9, SMAC/DIABLO and apoptosis initiating factor (AIF) are found. Approximately 90% of cytochrome c is estimated to rest in the cristae lumen (Bernardi et al., 1999, Susin et al., 1999(a) (b)).

The inner membrane and the cristae membrane are extremely resistant to proton leakage. Due to this resistance there is approximately a  $-220$  mV membrane potential. The  $F_0F_1$  ATPase which is located to the matrix side of the cristae membrane lets the accumulated protons in the lumen of the cristae, leak back down their electrochemical gradient through the  $F_0F_1$  ATPase, which ends up in the production of ATP (Gottlieb RA., 2000). In the inner membrane there is also a protein named ANT (adenine nucleotide transporter), which forms the “permeability transition pore” (PTP) when associated with VDAC (located in the outer mitochondrial membrane) and cyclophilin D (located in mitochondrial matrix).

In the outer membrane there are voltage-dependent anion channels (VDAC), which make the outer membrane permeable to small molecules, which

are smaller than 1000 Da. The anti-apoptotic Bcl-2 family member Bcl-2 is anchored to the outer membrane of the mitochondria (Gottlieb RA., 2000).

## **1-6.2 CYTOCHROME C RELEASE FROM THE MITOCHONDRIA AND APOPTOSIS**

Cytochrome c is found in the space between the outer and inner membranes of mitochondria in association with anionic phospholipids of the inner membrane, primarily with cardiolipin, where it participates in the process of oxidative phosphorylation (Cortese et al., 1998; Gorbenko GP., 1999)

When cells are exposed to apoptotic stimuli, cytochrome c is released from mitochondria into the cytosol, where it is one of several factors implicated in the proteolytic activation of caspase-3 by caspase-9 (Slee et al., 1999). The release of cytochrome c can be induced by two different mechanisms: Ca-dependent and Ca-independent (Gogvadze et al., 2001). In the Ca<sup>2+</sup> dependent cytochrome c release pathway, mitochondrial Ca<sup>2+</sup> overload causes mitochondrial dysfunction and opening of the permeability transition pore, which results in matrix swelling and rupture of the outer mitochondrial membrane, thus release of cytochrome c. In Ca<sup>2+</sup> independent cytochrome c release pathway, the pro-apoptotic members of the Bcl-2 family such as Bax, stimulates the release.

The mitochondrial cytochrome c can be found in two distinct forms. It may be loosely or tightly bound to cardiolipin. When tightly bound it becomes a part of the mitochondrial inner membrane. Therefore for cytochrome c to be available to be released from the mitochondria, first it should be dissociated from cardiolipin. In other words, a disruption of the cytochrome c-cardiolipin interaction should occur before, or concomitantly with, permeabilization of the outer membrane in order for cytochrome c to be released from mitochondria (Ott et al., 2002).

Released cytochrome c can interact with the Ced-4 -like protein Apaf-1. Apaf-1 contains a Ced-4 homology domain flanked on one side by a region with strong homology to the CARD motif within the prodomains of Ced-3 and mammalian caspases-2 and -9 and on the other side by several WD-40 repeats believed to mediate protein-protein interactions. The CARD domains in Apaf-1

and the prodomain of caspase-9 interact and, in the presence of cytochrome c and either ATP or ADP, this induces autocatalytic activation of the caspase, which then activates the downstream caspase effector cascade involving caspases-2, -3, -6, -7, -8 and -10 (Slee et al., 1999).

As mentioned above pro-apoptotic Bcl-2 family members reside in the cytosol and translocate to the mitochondria upon apoptotic stimulus to achieve cytochrome c release by interacting with other proteins. One of the pore-forming members is Bax. Bax has been shown to interact with VDAC to form a channel.

It is speculated that cytochrome c binding to the WD repeats induces a conformational change that allows Apaf-1 to oligomerize and by promoting clustering of this caspase to activate caspase-9 (Srinivasula et al., 1998). The anti-apoptotic Bcl-2 family members Bcl-2 and Bcl-xL reside in the outer mitochondrial membrane, where they function to suppress apoptosis in both or either of two ways: blocking cytochrome c release and binding to Apaf-1 to prevent its activating caspase-9 although a direct binding of Bcl-2 or Bcl-xL to Apaf-1 has not been shown by in-vivo experiments. The mammalian pro-apoptotic Bcl-2 family members, such as Bax, Bak and Bik, may promote apoptosis by displacing Apaf-1 from Bcl-2 or Bcl-xL. The anti-apoptotic protein Aven has been shown to bind to both Bcl-xL and Apaf-1 and this molecule might link the two molecules and target the Bcl-2 family member to the apoptosome (Chau et al., 2000). It was recently demonstrated that the release of cytochrome c always precedes exposure of phosphatidylserine at the cell surface and the loss of plasma membrane integrity (Goldstein et al., 2000). This study also showed that the drop in the mitochondrial membrane potential typically seen in apoptotic cells occurs later than cytochrome c release from mitochondria and that this process is dependent on caspase activation, whereas cytochrome c release is not. These results suggest a specific permeability of the outer mitochondrial membrane without alteration of the inner mitochondrial membrane.

So far, several competing models exist to explain exactly how permeabilization of mitochondrial membranes is mediated during apoptosis (Martinou et al., 2000). All models accept the opening of a megachannel called the permeability transition pore (PTP). The adenine nucleotide translocator (ANT; located in the inner mitochondrial membrane) and the voltage-dependent anion channel (VDAC, found in the outer mitochondrial membrane) are major

components of the PTP which is proposed to span both the inner and the outer mitochondrial membranes at sites at which the two membranes are opposed.

1- PTP model proposes the presence of PTP openers, including the pro-apoptotic Bcl-2 family member Bax, which cause permeabilization of the inner membrane and mitochondrial depolarization by binding to the ANT (Marzo et al., 1998). This process allows entry of water and solutes into the matrix and leads to mitochondrial swelling.

2-VDAC closure model proposes that swelling is due to a defect in mitochondrial ATP/ADP exchange as a result of closure of the VDAC thus leading to hyperpolarization of the inner mitochondrial membrane and subsequent matrix swelling.

3- Bax channel model suggests that the outer mitochondrial membrane is not damaged but rather a pore is generated in the outer mitochondrial membrane allowing the passage of cytochrome c (and other mitochondrial proteins) into the cytosol. Bax oligomers can form large conductance channels in lipid planar bilayers (Martinou et al., 2000). Addition of Bax directly to isolated mitochondria triggers release of cytochrome c through a mechanism that is insensitive to PTP blockers and does not involve mitochondrial swelling. But it is known that some factors such as SMAC/DIABLO are too big to pass through this channel (Satio et al., 2000).

4- Another model suggests the cooperation of Bax with the VDAC to form a cytochrome c-conducting channel (Shimizu et al., 1999).

Very recently presence of a novel type of channel in the outer membrane of mitochondria is demonstrated. This “apoptotic mitochondrial channel” (MAC) is a voltage-independent channel with multiple conductance levels allowing the passage of cytochrome c and other mitochondrial proteins across outer mitochondrial membrane (Pavlov et al., 2001). Pavlov et al., demonstrated that although MAC is not equivalent to Bax channel, Bax overexpression can induce the formation of MAC and MAC formation can be inhibited by overexpression of Bcl-2.

### **1-6.3 OTHER FACTORS RELEASED FROM THE MITOCHONDRIA DURING APOPTOSIS**

Several proteins in addition to cytochrome c are released from mitochondria in cells induced to undergo apoptosis. These include Smac/Diablo, pro-caspases, and AIF.

#### **1-6.3.1 SMAC/DIABLO**

Smac/Diablo molecule can bind to, and inactivates, IAPs (Verhagen et al., 2000; Du et al., 2000). IAPs inhibit cell death by binding to procaspases and activated caspases, thereby blocking their processing and their activity. Smac/Diablo is released from the mitochondria along with cytochrome c during apoptosis and relieves inhibition of caspase-9 activation by IAP inactivation (Green, 2000).

#### **1-6.3.2 APOPTOSIS INDUCING FACTOR (AIF)**

AIF is a mitochondrial flavoprotein protein that is synthesized from a single gene locus in X chromosome and imported to the mitochondrial intermembrane space. It is ubiquitously expressed in normal tissues as well as in some cancer cell lines. When AIF is microinjected into cytoplasm of normal cells, it causes release of cytochrome c from the mitochondria, condensation of nuclear chromatin and activation of flippase in a caspase-independent manner (Daugas et al., 2000; Susin et al., 1999a). Genetic inactivation of AIF renders embryonic stem cells resistant to cell death after serum deprivation and disables PCD during cavitation of embryoid bodies in early mouse morphogenesis (Joza et al., 2001).

### **1-6.3.3 PRO-CASPASES**

Mitochondrial integrity is also important for the regulation of caspase activation (Vander Heiden and Thompson, 1999). A fraction of both caspase-9 and caspase-3 has been localized to the mitochondrial intermembrane space in some cell types, and caspase-2 has also been reported to reside in mitochondria. These caspases are released from the mitochondria to the cytosol during apoptosis induction, like cytochrome c.

## **1-7 REGULATION OF APOPTOSIS**

Several factors are implicated in the regulation of apoptosis such as activation of p53 tumor suppressor, oncoproteins, and the expression/activation/modulation of the Bcl-2 family members.

Among these p53 can be regarded as the “master regulator” of the apoptotic program, capable of coordinating the process at multiple levels via several mechanisms. Cellular stress such as DNA damage, hypoxia, and survival factor deprivation can activate apoptosis, where p53 is the critical initiator of this pathway (Lowe and Lin, 2000). p53 can be activated by DNA damage sensors such as ATM and Chk2, or by mitogenic oncogenes (Khanna and Jackson, 2001). When activated, p53 can initiate apoptosis by transcriptionally activating proapoptotic Bcl-2 family members and repressing antiapoptotic Bcl-2 and IAPs (Bartke et al., 2001; Hoffman et al., 2001; Ryan et al., 2001; Wu et al., 2001). In addition, p53 can transcriptionally activate both CD95 and TRAIL receptor 2 (TRAIL-R2/DR5), thereby sensitizing cells to death-receptor-mediated apoptosis (Herr and Debatin, 2001; Ryan et al., 2001). p53 may also have transcription-independent activities that potentiate cell death once the transcription-dependent functions initiate the process (Ryan et al., 2001). Similarly the p53 homologue p73 is shown to induce apoptosis (Stiewe and Putzer, 2001).

A number of oncoproteins induce apoptosis when overexpressed in cells. The best characterized examples are the transcription factors c-Myc, c-Jun, c-Fos, E2F1 and cyclin E. Although induction of apoptosis seems to represent the general cellular response upon oncogene overexpression, in certain cases the

reduction of c-Myc, Jun or Fos expression via an unknown mechanism leads to apoptosis. There are two hypothesis that explain how oncoproteins induce apoptosis. The first one proposes that apoptosis is induced because of the cellular conflict, that is generated through induction of cell proliferation by oncoprotein expression but in the absence of a completely activated or coordinated proliferative machinery. The other hypothesis suggests that Myc promotes proliferation and apoptosis at the same time, but in the presence of enough anti-apoptotic signals proliferation is favored and vice versa (Zornig et al., 2001). Nevertheless TRAP-1, Bax and p53 have been revealed to be activated by c-Myc (Coller et al., 2000; Mitchell et al., 2000; Zindy et al., 1998) An interaction between c-myc induced apoptosis and CD95 and CD95L has just been demonstrated such that c-Myc-induced apoptosis requires activation of the CD95 activation (Hueber et al., 1997).

As mentioned in part 1-4.3 the activities of Bcl-2 proteins can be modulated by post-translational modifications, such as phosphorylation of Bad by several prosurvival kinases, inhibiting its interaction with antiapoptotic Bcl-2 proteins, and sequestration away from the mitochondria through binding of 14-3-3 adaptor proteins (Bonni et al., 1999; Harada et al., 2001; Wang, 2001). Bcl-2 can also be phosphorylated by MAP kinases and dephosphorylated by the PP2A tumor suppressor, leading to changes in its activity (Blagosklonny, 2001).

## **1-8 ROLE OF APOPTOSIS IN HUMAN DISEASE**

Apoptosis plays a major role in the maintenance of homeostasis in adult tissues (Vaux DL. and Korsmeyer SJ., 1999; Wyllie AH. and Golstein P., 2001). Abnormalities in the apoptosis program may result in a variety of diseases such as autoimmune, neurodegenerative, infectious and heart diseases and cancer, (Reed CJ., 2000; Mattson MP., 2000; Chervonsky AV., 1999; Roulston A. et al., 1999; Narula J. et al., 2000)

Autoimmunity represents a diverse set of diseases defined clinically by the destruction of the target organ. For example in rheumatoid arthritis, T cells attack of the joints and in type I diabetes, T cell attack the insulin secreting  $\beta$  cells of pancreas. Lymphocyte development, selection and education represent

tightly controlled immune processes that normally prevent autoimmunity. Lymphocyte development requires cellular selection through apoptosis to remove potentially autoreactive cells. Dysregulated apoptosis, both interrupted as well as accentuated apoptosis, are now demonstrated as central defects in diverse human autoimmune diseases as shown in table 1-3 (Hayashi and Faustman, 2001).

**Table 1-3: Dysregulation of apoptosis in some autoimmune diseases.**

Disease	Apoptotic defect
Lupus	↓ NF-κB (p65) expression, ↑CD95 and CD95L expression, ↓ TGF-β secretion, ↓ CD95 apoptosis
Rheumatoid arthritis	↓ NF-κB
Type I diabetes	↑TNF-α apoptosis
Lymphoproliferation with autoimmunity	↓ CD95 apoptosis
Autoimmune lymphoproliferative syndrome	↓ CD95 apoptosis

Neuronal cell death due to dysregulation of apoptosis plays the major role in the formation of symptoms of many neurological disorders, including Alzheimer's disease, Parkinson's disease, Huntington's disease, stroke and amyotrophic sclerosis. Among the factors that induce apoptosis in these phenomena include oxidative stress, disturbed calcium homeostasis, mitochondrial dysfunction and activation of caspases (Mattson MP., 2000). Neurotrophins regulate neuronal apoptosis through the action of protein kinase cascades including Akt and MAPK pathways. This regulation can be

overwhelmed by the expression of abnormal protein structures in these cells such as the amyloid fibrils in Alzheimer's disease.

Apoptosis is also widely seen in infectious diseases, including AIDS. Infection with HIV-1 causes apoptosis in CD4+ T-cells which results in progressive immunodeficiency and predisposition to opportunistic infectious diseases and neoplasms. It has been demonstrated that the viral proteins activate both pro-apoptotic and pro-survival genes. For example the "tat" protein of the virus has been shown to activate caspase 8 and upregulate CD95L expression and on the other hand it also activates Akt. Nevertheless the protein encoded from the "env" gene causes the upregulation of CD95 and an increase in Bax concentration versus Bcl-2 concentration (Roshal et al., 2001).

Death of myocardial cells due to apoptosis may lead to cardiovascular disease, which is the leading cause of death worldwide. Apoptotic cell death is observed after ischemia/reperfusion injury (Freude et al., 2000) and in heart failure (Narula et al., 1999). For example in the case of ischemia/reperfusion the inhibitor of the Fas pathway, c-Flip has been shown to be degraded (Jeremias et al., 2000). Similarly overexpression of TNF- $\alpha$  and TNFR has been shown to associate with heart failure (Torre-Amione et al., 1996). Mitochondrial pathways is also involved in myocardial cell apoptosis. It has been shown that caspases 3 and 9 are activated following cytochrome c is released from the mitochondria when ischemic conditions are mimicked in cell culture system (Bialik et al., 1999).

Defects in apoptosis underpin both tumorigenesis and drug resistance, and because of these defects chemotherapy often fails. Tumorigenesis is a multistep process in which mutations in key cellular genes produce a series of acquired capabilities that allow the cancer cells to grow –even in the absence of growth signals and in the presence of growth-inhibitory signals- and evade the immune system (Hanahan and Weinberg, 2000). The p53 tumor suppressor gene is the most frequently mutated gene in human tumors, and loss of p53 function may result in the inhibition of apoptosis. Moreover, functional mutations or altered expression of p53 downstream effectors or upstream regulators occur in many human tumors. Bcl-2 family members are also altered in tumor samples. It has been shown that Bcl-2 overexpression can accelerate tumorigenesis in transgenic mice. Conversely, proapoptotic Bcl-2 proteins are inactivated in certain cancers

and disruption of these genes also promotes tumorigenesis mice. In addition, mutations or altered expression of upstream regulators of Bcl-2 proteins (such as AKT) are also associated with cancer. Alterations that disrupt apoptosis downstream of the mitochondria is also seen in cancers such as the silencing of Apaf-1 in melanomas. Inactivation of death-receptor pathway mediated apoptosis is also observed in many tumors due to mutations in CD95, TRAIL receptors, and downstream signaling pathways (Johnstone et al., 2002).

The mutations of the apoptosis pathways in tumorigenesis are summarized in table 1-4.

**Table 1-4: Summary of the Roles of Apoptotic Initiators, Regulators or Executioners in Tumorigenesis and Apoptosis**

<b>Protein</b>	<b>Role in tumorigenesis and apoptosis</b>
<b>p53</b>	Mutated or altered expression in many cancers. Initiates the intrinsic apoptotic pathway.
<b>p19<sup>ARF</sup></b>	Mutated or altered expression in many cancers. Blocks MDM2 inhibition of p53.
<b>ATM</b>	Mutated in ataxia-talangiectasia syndrome. Senses DNA double strand and stabilizes p53. Deficiencies increase risk of developing haematological malignancies and breast cancer.
<b>Chk2</b>	Mutated in Li-Fraumeni syndrome. Senses DNA double strand breaks and phosphorylates and stabilizes p53.
<b>Rb</b>	Mutated in some cancers, and functionally disrupted in many cancers. Inhibits E2F-mediated transcription. Loss of Rb function induces p53-dependent and independent apoptosis.
<b>Bax</b>	Mutated or decreased expression in some tumors. Mediates mitochondrial membrane damage.
<b>Bak</b>	Mutated or decreased expression in some tumors. Mediates mitochondrial membrane damage.
<b>PTEN</b>	Mutated or altered expression in cancers. Regulates Akt activation and subsequent phosphorylation of Bad. Loss of PTEN results in resistance to many apoptotic stimuli.
<b>Apaf-1</b>	Mutated and transcriptionally silenced in melanoma and leukemia cell lines. Necessary for activation of caspase-9 following cytochrome c release.
<b>CD-95/Fas</b>	Mutated and down-regulated in lymphoid and solid tumors. Initiates the extrinsic apoptotic pathway.

<b>TRAIL-R1/R2</b>	<p>Mutated in metastatic breast cancers.</p> <p>Initiate the extrinsic apoptotic pathway.</p> <p>Mutations lead to suppression of death receptor-mediated apoptosis.</p>
<b>Caspase-8</b>	<p>Gene silenced in neuroblastomas.</p> <p>Activates both extrinsic and intrinsic apoptotic pathways.</p>
<b>Bcl-2</b>	<p>Frequently overexpressed in many tumors.</p> <p>Antagonises Bax and/or Bak and inhibits mitochondrial membrane disruption.</p>
<b>MDM2</b>	<p>Overexpressed in some tumors.</p> <p>Negative regulator of p53.</p>
<b>IAPs</b>	<p>Frequently overexpressed in cancer.</p> <p>Down regulation of XIAP induces apoptosis in chemoresistant tumors.</p>
<b>NF-<math>\kappa</math>B</b>	<p>Deregulated activity in many cancers.</p> <p>Transcriptionally activates expression of anti-apoptotic members of the Bcl-2 and IAP families. Can inhibit both the extrinsic and intrinsic death pathways.</p>
<b>Myc</b>	<p>Deregulated expression in many cancers.</p> <p>Induces proliferation in the presence of survival factors, such as Bcl-2, and apoptosis in the absence of survival factors.</p>
<b>Akt</b>	<p>Frequently amplified in solid tumors.</p> <p>Phosphorylates Bad.</p>
<b>PI3K</b>	<p>Overexpressed or deregulated in some cancers.</p> <p>Responsible for activation of Akt and downstream phosphorylation of Bad.</p>
<b>Ras</b>	<p>Mutated or deregulated in many cancers.</p> <p>Activates PI3K and downstream pathways.</p> <p>Induces proliferation and inhibits c-myc.</p>
<b>FLIP</b>	<p>Overexpressed in some cancers.</p> <p>Prevents activation of caspase-8 and apoptosis induced by some chemotherapeutic drugs.</p>

## **CHAPTER II**

### **DETECTION OF APOPTOSIS IN CELLS AND TISSUES**

Detection of apoptosis in cells and tissues is a very important issue for both to study the molecular mechanisms of apoptosis and to study the role of apoptosis in human disease.

Several hallmarks of apoptosis, including activation of death receptors, cytochrome-c/Apaf-1 complex formation, mitochondrial potential decrease, caspase activation, phosphatidylserine exposure, DNA laddering and morphological changes, are used for the development of techniques to characterize apoptosis. Several commonly used techniques for the detection of apoptosis are summarized below.

#### **2-1 Analysis of morphological features of apoptosis**

Since the discovery of apoptosis, the morphological changes associated with apoptosis have been widely used to detect apoptotic cell death. These morphological changes include, membrane blebbing, shrinking of cytoplasm, condensation of nucleus and formation of apoptotic bodies (figure 2-1).

Although this techniques offers a simple and quantitative method to detect apoptosis, it is not possible to detect apoptosis in the early stages and these late apoptotic cells may not be easily observed under a light microscope due to their small size.

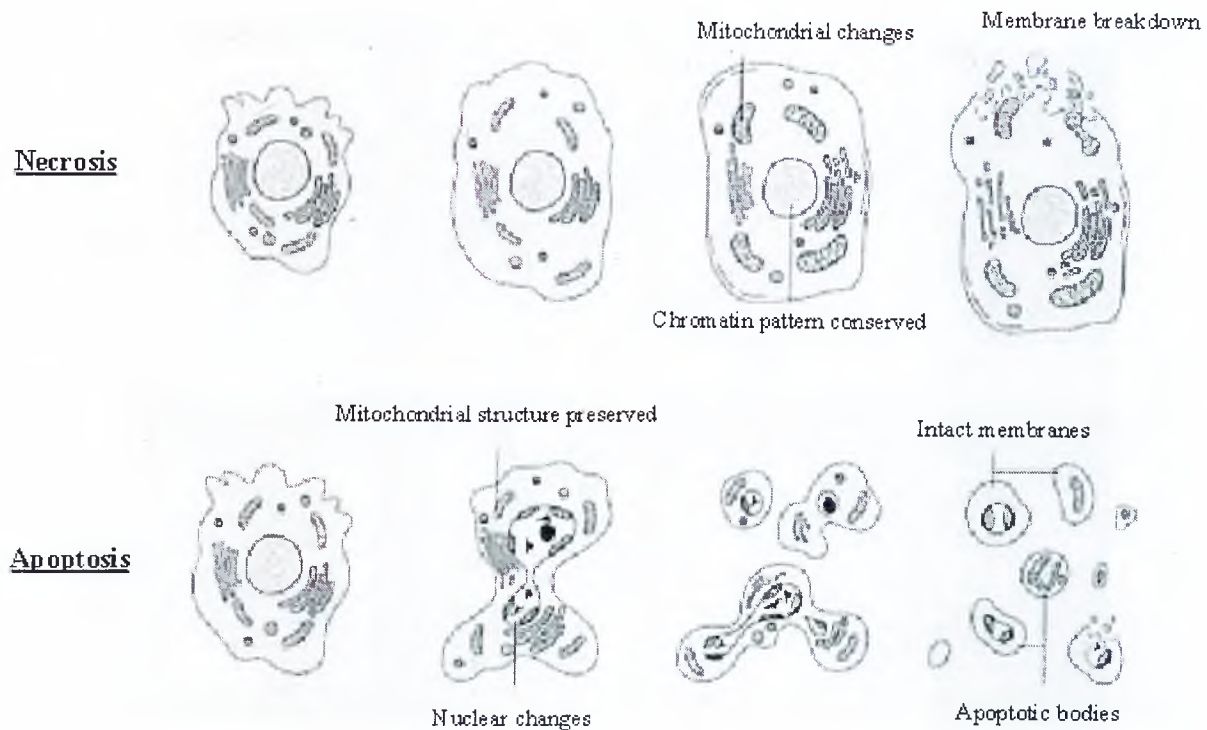


**Figure 2-1: Basic morphological features of apoptosis, differing from necrosis used in the detection of apoptosis.**

## 2-2 DNA fragmentation assays

Agarose gel electrophoresis is a commonly used technique to demonstrate the ladder pattern of DNA, which is generated by the activation of caspase dependent endonucleases during apoptosis. As described above in section 1-1, during apoptosis chromatin is first cleaved into 300-350 kb, then into 180 bp fragments, leading to generation of monomers (180 bp) and oligomers (multiples of 180 bp) of DNA as shown in figure 2-2 (Brown and Rose, 1992; Oberhammer et al., 1993; Wyllie AH., 1980).

Several drawbacks of this method is that, DNA isolation requires millions of cells and obtained results can not be quantified.

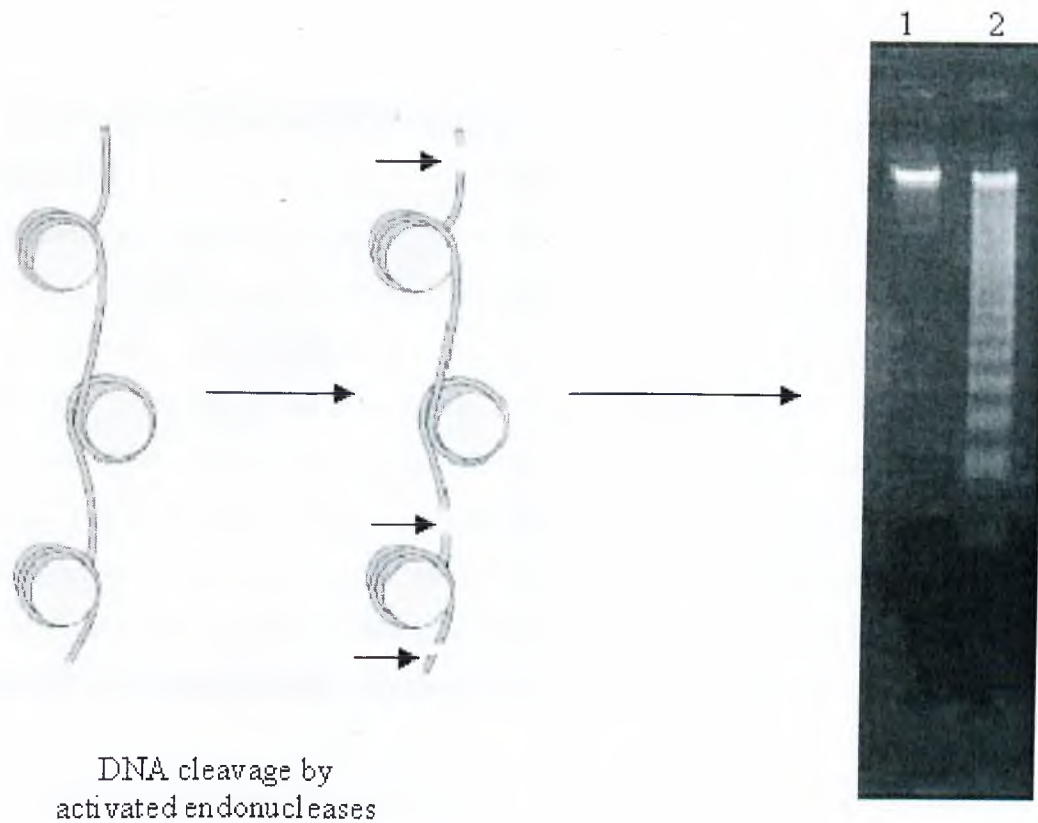


**Figure 2-2: Principle of DNA laddering assay and a typical gel appearance of apoptotic cell DNA.**

(Lane 1: nonapoptotic cells, Lane 2: apoptotic cell)

DNA fragmentation can also be detected by using the ELISA approach which allows semi-quantitative detection of apoptosis or necrosis without previous cell labeling. This method involves permeabilization of cell membrane and release of cytoplasmic nucleosome fragments, followed by utilization of an anti-histone antibody that reacts with nucleosomes.

### 2-3 Analysis of free DNA ends

Cleavage of genomic DNA during apoptosis may yield double-stranded, low molecular weight DNA fragments, as well as single strand breaks ("nicks") in high molecular weight DNA. Those DNA strand breaks can be identified by labeling free 3'-OH termini with modified nucleotides in an enzymatic reaction.

There are two methods for the labelling fragmented DNA. The first utilized the "terminal polymerase" which incorporates labelled nucleotides at nicked sites of the DNA (figure 2-3). The second method which is also known as "TUNEL" (TdT-mediated dUTP nick end labeling) uses the "terminal transferase (TdT)" enzyme. This enzyme tails labelled nucleotides at nicked DNA as well as at 3'-OH-ends of fragmented DNA in a template-independent manner (figure 2-3). TUNEL is a more sensitive method and therefore is preferred over the first method.

Although sensitive, this method is associated with a number of artifacts, as it labels DNA strand breaks occurred by any cause, in both apoptotic and nonapoptotic cells.

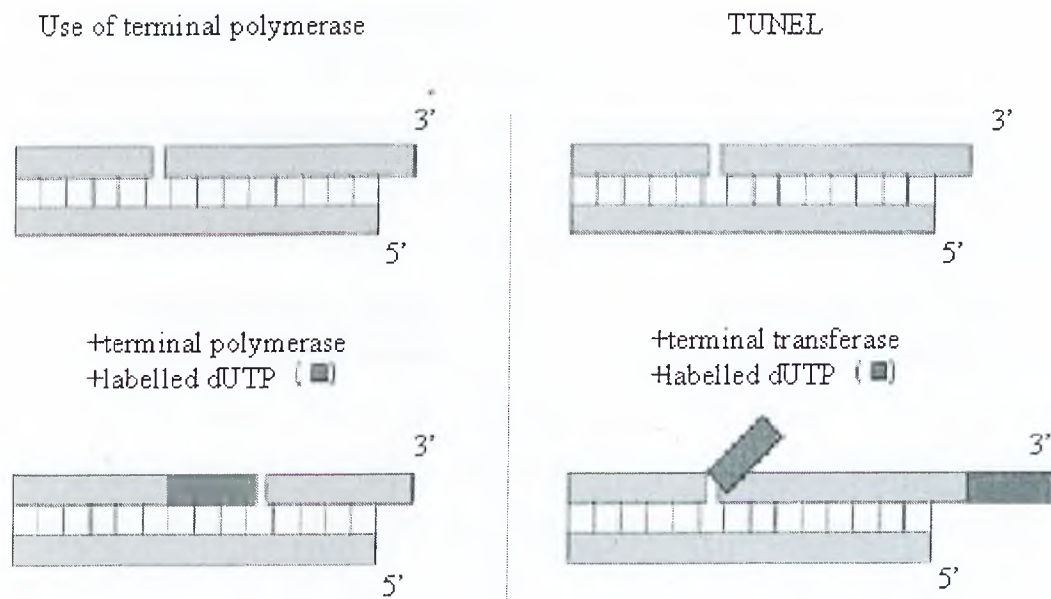


**Figure 2-3: Labelling principle of terminal polymerase and terminal transferase**

## **2-4 Use of Annexin V**

Annexin V is a commonly used method for the detection of apoptosis in unfixed cells. Annexin V is a member of a family of calcium-dependent phospholipid-binding proteins that has a strong affinity for phosphatidylserine. Phosphatidylserines in cell membrane is externalized to the surface in very early stages of apoptosis by the action of flippase.

A drawback of this method is that annexin V detects phosphatidylserines in the outer membrane that has occurred after any kind of cell membrane injury.

## **2-5 Detection of caspase activity**

Caspase activity can be assessed in cell populations as well as single cells. Measurement of apoptosis in single cells offers a sensitive, antibody based, quantitative analysis, however this requires antibodies against either active forms of caspases or caspase targets.

Detection of apoptosis in cell populations is also performed by antibodies against either active forms of caspases or caspase targets. One of the most widely used antibody is anti-PARP (Poly-(ADP-ribose)-polymerase) antibody. PARP is a zinc-dependent, eukaryotic, DNA-binding protein that specifically recognizes DNA strand breaks produced by various genotoxic agents. During apoptosis, 113 kD PARP is cleaved by Caspase-3 into 89 kD and 24 kD fragments, which could serve as an early specific marker of apoptosis as shown in figure 2-4. Another method involves usage of substrates that contain a caspase target sequence. These methods utilizes the ELISA principles, in which an anti-caspase antibody coated plate is treated with cell lysate, followed by exposure of the plate wells to a caspase substrate which in the end facilitates fluorometric analysis of apoptosis.

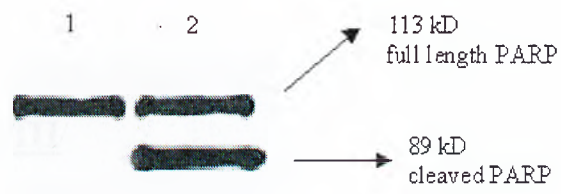


**Figure 2-4: Use of PARP cleavage for the detection of apoptosis by western blotting.**

## **CHAPTER III**

### **AIM OF THE STUDY**

Apoptosis is the target subject for understanding cellular mechanisms of many diseases, as well as for developing new drugs that interfere with either pro-apoptotic or anti-apoptotic molecular networks. A major difficulty with researching apoptosis and drugs to control it, is that a reliable marker of apoptosis has not yet been developed. Currently available techniques for apoptosis detection are based on the study of morphology of apoptotic cells (light microscopy and fluorescence microscopy coupled to nuclear staining with specific dyes, electron microscopy), DNA fragmentation detected by TUNEL and similar techniques, membrane changes detected by annexin V in vivo labelling, and on immunological assays using antibodies directed to apoptosis-related proteins such as PARP and caspases.

Therefore there is a great need for a specific, antigenic, versatile marker for the rapid detection of cell death by apoptosis, which can be used for research, diagnostics, and therapeutics. This marker must be able to distinguish between cell death by apoptosis and other known states of cells which includes quiescence, proliferation (composed of G1, S, G2 and mitosis phases), and senescence. Essential requirements for apoptosis detection techniques include high sensitivity for apoptotic cells, the ability to differentiate between apoptosis and other forms of cellular states. However, there is a relative paucity for simple techniques fulfilling these requirements, and furthermore allowing quantitative analysis. Immunological detection of apoptosis-related proteins is probably the best approach to overcome this obstacle, but there are only a few known apoptosis marker antigens.

This study is directed to the characterization of the biochemical features of anti-NAPO antibody and development of a novel method to detect and quantify apoptosis, and to distinguish apoptotic cells from quiescent, proliferating, mitotic and senescent cells by using this antibody.

## **CHAPTER IV**

### **MATERIALS AND METHODS**

#### **4-1 Production of anti-*NAPO* antibody from hybridomas**

##### **4-1.1 Production of anti-*NAPO* antibody producing hybridomas**

Anti-*NAPO* antibody producing hybridomas were previously produced by Mehmet Ozturk. Ten millions of COLO 320 cells were lysed in 2 ml PBS and 0.5 ml of lysate was injected into tail vein of Balb/c mice. One month later, mice were immunized twice more at one week intervals, hybridomas were prepared from splenic cells, and antibody-producing clones were selected as described previously (Ozturk et al., 1989). One of the antibodies named Anti-*NAPO* (negative in apoptosis) was used for further studies.

The frozen anti-*NAPO* antibody producing hybridoma stocks were cultured in RPMI medium supplemented with 20% FCS, 1% penicillin/streptomycin and 1% non-essential amino acids. Cells were grown in the incubator set to 37°C and 5% CO<sub>2</sub> and the hybridoma supernatant was collected by centrifugation of the culture at 5000 rpm for 5 minutes at 4°C. This supernatant containing the anti-*NAPO* antibody was stored at -40°C. New stocks were prepared by frosting 10 million hybridoma cells in 90% FCS and 10% DMSO.

#### 4-1.2 Production of anti-*NAPO* ascites in Balb/c mice

The balb/c mice was primed by injecting 500 µl incomplete Freund's adjuvant to the intraperitoneal region. After 7-14 days  $5 \times 10^5$  cells were washed twice in sterile PBS and centrifuged at 1500 rpm for 5 minutes. The cell pellet was resuspended in 500 µl PBS and injected to the intraperitoneal region of the mice. After 7-14 days the ascitic fluid was taken from the animal by using an injector and was incubated at 37°C for 1 hour. The ascitic fluid was then incubated at 4°C overnight and centrifuged at 3000 g for 10 minutes. The oil layer was discarded and the supernatant was stored at -70°C.

#### 4-1.3 Characterization of Ig subtype of the anti-*NAPO* antibody

The ELISA plates were coated O/N at 4°C with 150 µl Anti-*NAPO* ascitic fluid diluted as 1:100, 1:1000 and 1:10,000 in PBS. Next day following one hour saturation with 200 µl PBS containing 3% BSA, 100 µl HRP-conjugated secondary antibodies (IgG1, IgG2a, IgG2b and IgG3) which were diluted in different ratios (1:1000, 1:1500 and 1:2000) were added to the plates. After a one-hour incubation at room temperature, Lumilight (Roche- 2 015 200) substrates A and B were mixed in equal rate and was added to each well. After incubation with Lumilight substrate for 5 minutes, ELISA plates were put onto X-ray films in the dark room and the films were developed. The secondary antibodies used are listed below.

<u>Name of the antibody</u>	<u>Company-catalog number</u>
Anti-IgG1-HRP conjugated	Santa Cruz/sc-2060
Anti-IgG2a-HRP conjugated	Santa Cruz/sc-2061
Anti-IgG2b-HRP conjugated	Santa Cruz/sc-2062
Anti-IgG3-HRP conjugated	Santa Cruz/sc-2063

## **4-2 Screening of $\lambda$ TripIEx expression library with the anti-*NAPO* antibody**

### **4-2.1 Bacterial strains**

The screening bacteria XL-1 Blue was grown in media containing 15  $\mu$ g/ml tetracycline in all studies. The BM25.8 bacteria which is used for cre-lox-mediated excision of pTripIEx from  $\lambda$ TripIEx was grown in media containing 50  $\mu$ g/ml kanamycin and 34  $\mu$ g/ml chloramphenicol.

### **4-2.2 Solid and liquid mediums**

#### **LB medium:**

10g/L tryptone, 5 g/L yeast-extract, 5 g/L NaCl  
(pH was adjusted to 7.0 with 5 M NaOH)

#### **LB/MgSO<sub>4</sub>/maltose broth:**

10 mM MgSO<sub>4</sub> in LB medium. Autoclaved, cooled to 50°C, 0.2% maltose was added.

#### **LA medium:**

10g/L tryptone, 5 g/L yeast-extract, 5 g/L NaCl, 15 g/L agar  
(pH was adjusted to 7.0 with 5 M NaOH)

#### **LB/MgSO<sub>4</sub> soft agar:**

1 lt LB broth, 10 mM MgSO<sub>4</sub>, 7.2 g agar  
Supplemented with appropriate antibiotics.

### 4-2.3 Antibiotics

Kanamycin, tetracycline and chloramphenicol were used in this study (Table 4-1).

**Table 4-1: Concentrations of the antibiotics used in this study**

Name	Stock solution		working concentration
	concentration	storage	
Kanamycin	25 mg/ml in H <sub>2</sub> O	- 20°C	50 µg/ml
Tetracycline	15 mg/ml in H <sub>2</sub> O	- 20°C	15 µg /ml
Chloramphenicol	34 mg/ml in EtOH	- 20°C	34 µg /ml

### 4-2.4 Growth and maintenance of primary and working bacterial stocks

5 µl of frozen culture of XL-1 Blue was streaked on LB-agar plate and grown overnight at 37°C. A single colony from this primary plate was streaked on LB/MgSO<sub>4</sub> agar plate and grown overnight. These plates were used as a source of fresh colonies for inoculating liquid cultures and for preparing the next fresh working stocks.

### 4-2.5 Titration of λTripIEx expression library

A single colony from this plate was inoculated into 20 ml LB/MgSO<sub>4</sub> maltose broth without antibiotic. The culture was incubated at 37°C overnight shaking (140 rpm) until OD<sub>600</sub> reaches 2.0. The culture was centrifuged for 5 minutes at 5000 rpm and the pellet was dissolved in 7.5 ml 10 mM MgSO<sub>4</sub>. Meanwhile 4 LB/MgSO<sub>4</sub> agar plates were warmed to 37°C in a bacteria

incubator. 1:100 (10 µl of library lysate into 1 ml 1X lambda dilution buffer) and 1:10.000 (10 µl of 1:100 dilution into 1 ml 1X lambda dilution buffer) dilutions of the phage lysate were prepared. From the 1:10.000 dilution four different library dilutions was generated as described in table 4-2.

**Table 4-2: Dilution chart of λTripIEx for titration**

<b>Tube</b>	<b>1X lambda dil. buffer</b>	<b>O/N bacterial culture</b>	<b>1:10.000 phage dil.</b>
1	100 µl	200 µl	5 µl
2	100 µl	200 µl	10 µl
3	100 µl	200 µl	20 µl
4	100 µl	200 µl	0 µl

The tubes were incubated at 37°C water bath for 15 minutes and 3 ml melted- warmed (45°C) soft-agar was added to each tube. Mixture was vortexed briefly and the contents were poured onto pre-warmed LB/MgSO<sub>4</sub> agar plates. These plates were cooled at room temperature for 10 minutes to allow the soft-agar harden and incubated at 37°C for at least 6-7 hours until the plaques appear. The plaques were counted and the titre was calculated as follows:

$$\text{Pfu/ml} = \frac{\text{\# of plaques} \times \text{dilution factor} \times 10^3 \text{ } \mu\text{l/ml}}{\mu\text{l of diluted phage plated}}$$

**10 X lambda dilution buffer:**

1M NaCl, 0.1 M MgSO<sub>4</sub>.7H<sub>2</sub>O, 0.35 M Tris.Cl (pH 7.5)

**1 X lambda dilution buffer:**

100 ml 10 X lambda dilution buffer, 0.01 % gelatine (Volume was adjusted to 1 lt and autoclaved)

#### **4-2.6 Transfer of plaques to nitrocellulose filters**

A single colony from this plate was inoculated into 20 ml LB/MgSO<sub>4</sub> maltose broth without antibiotic. The culture was incubated at 37°C overnight shaking (140 rpm) until OD<sub>600</sub> reaches 2.0. The culture was centrifuged for 5 minutes at 5000 rpm and the pellet was dissolved in 7.5 ml 10 mM MgSO<sub>4</sub>. Appropriate dilutions of the library were prepared in 1X lambda dilution buffer so that 3x10<sup>3</sup> plaques will be formed on a 100 mm plate or 1.2x10<sup>4</sup> plaques will be formed on a 150 mm plate. Appropriate amount of the diluted phage was mixed with 200 µl concentrated XL-1 Blue O/N culture and incubated at 37°C for 15 minutes. 2.5 ml (for 100 mm plate) or 5 ml (for 150 mm) melted and warmed LB/MgSO<sub>4</sub> soft agar was added to each tube. After vortexing briefly the mixture was poured onto pre-warmed LB/MgSO<sub>4</sub> agar plates. These plates were cooled at room temperature for 10 minutes to allow the soft-agar harden and incubated at 42°C for 3-5 hours. Meanwhile nitrocellulose filters were soaked into 10 mM IPTG for 20 minutes and blot-dried. As soon as the plaques were visible the damp nitrocellulose filters were placed onto each plate. The orientation of the filters was spotted and the plates were incubated at 37°C for 3-5 hours. The plates were incubated at 4°C for 30 minutes to avoid sticking of the soft-agar to the filters. The filters were removed and washed in TBS-T 3-5 times. The plates were wrapped with parafilm and stored at 4°C.

##### **TBS Buffer:**

10 mM Tris.Cl (pH 8.0), 150 mM NaCl

##### **TBS-T Buffer:**

1X TBS buffer, 0.1% Tween-20

## **4-2.7 Immunodetection**

### **4-2.7.1 Optimization of the secondary antibody concentration**

Protein lysates from different cell lines were subjected to western blotting by using anti-p53 antibody as the primary antibody and Amersham <sup>125</sup>I labelled sheep-anti-mouse as the secondary antibody. Two different concentrations of the secondary were tested and the optimal concentration was chosen for the immunodetection studies.

### **4-2.7.2 Immunodetection**

The filters were washed 3 times with TBS-T following incubation with blocking solution for 30 minutes at room temperature. The primary antibody (anti-*NAPO* antibody) was diluted in TBS-T and the filters were incubated with the primary antibody for 1 hour at room temperature. After washing the nitrocellulose filters 3 times with TBS-T, secondary antibody (Amersham <sup>125</sup>I labelled sheep-anti-mouse) was diluted as 2.5 µCi/10 ml and incubated with the filters for 1 hour at room temperature. The filters were washed 3 times with TBS-T and exposed to autoradiograms.

## **4-3 Western Blotting with the anti-*NAPO* antibody**

### **4-3.1 Tissue culture studies**

All cells (listed in table 4-3) were grown in media supplemented with 10% fetal calf serum (FCS), 1% non-essential amino acids, 100 µg/ml penicillin/streptomycin at 37°C and 5% CO<sub>2</sub>.

#### **4-3.1.1 Defrosting cells**

One vial of the frozen cell line from the nitrogen tank was taken and immediately put into ice. The vial was left 1 minute on the bench to allow excess nitrogen to evaporate and then placed into 37°C water bath until the external part of the cell solution is thawed (takes approximately 1-2 minutes). The cells were resuspended gently using a pipette and transferred immediately into a 15 ml. sterile tube containing 10 ml cold medium. The cells were centrifuged at 1500 rpm at 4°C for 5 minutes. Supernatant was discarded and the pellet was resuspended in 10 ml 37°C culture medium to be plated into 100 mm dish. Cells were left O/N in culture. The following morning culture medium was refreshed.

**Table 4-3: The cell lines used for characterization of *NAPO* (Supp.Chem.:  
Supplementary chemical)**

NAME	SPECIES	TISSUE/ORIGIN	MEDIUM	SUPP. CHEM.
COS-7	Monkey	kidney	DMEM	-
IAR-6	Rat		DMEM	-
HC11	mouse		RPMI-1640	10 ng/ml EGF 5 µg/ml Insulin
CHOK-I	Hamster	ovary	DMEM	
Huh7	Human	Hepatocellular carcinoma	DMEM	-
Mahlavu	Human	Hepatocellular carcinoma	DMEM	-
Hep 40	Human	Hepatocellular carcinoma	DMEM	-
SNU 398	Human	Hepatocellular carcinoma	DMEM	-
MCF7	Human	Breast Cancer	DMEM	-
HeLa	Human	Cervix Cancer	DMEM	-
SW480	Human	Colon cancer	DMEM	-
LNCaP	Human	Prostate Cancer	RPMI-1640	-
U2OS	Human	Osteosarcoma	DMEM	-
A375	Human	Melanoma	DMEM	-
Jurkat	Human	Acute T-cell leukemia	RPMI-1640	-
MRC5	Human	Lung fibroblast	DMEM	-
293	Human	Kidney	DMEM	-

#### 4-3.1.2 Subculturing of cells

All cells were splitted once-per-week. Culture renewal was done every three days. For splitting, the medium was aspirated and the cells were washed with PBS pH 7.2 once. PBS was removed and trypsin was added to the plates. Plates were incubated in the incubator for 3-10 minutes until the cells are detached. Cells were plated in the desired dilution into new plates. For suspension cultures, cells were centrifuged at 1000 rpm for 3 minutes and desired number of cells was resuspended in fresh medium.

#### 4-3.2 Protein extraction from cells

Cells were grown to 70-80% confluency and washed two times with ice-cold PBS. Cells were scraped in ice-cold PBS and centrifuged at 1500 rpm for 5 minutes at 4°C. Pellet was either frozen in liquid nitrogen or lysed immediately in NP-40 lysis buffer (150 mM NaCl, 1.0% NP-40, 50 mM Tris (pH 8.0)). For lysis, the pellet was resuspended in 4-5 volume of NP-40 lysis buffer supplemented with protease inhibitors (Roche-complete protease inhibitor cocktail) and incubated in ice for 30 minutes. The lysate was centrifuged at 13.000 rpm for 30 minutes at 4°C. Supernatant was taken to a fresh tube and following protein quantitation, aliquoted and stored at -70°C.

#### 4-3.3 Bradford assay for protein quantitation

A standard curve was prepared by using BSA as described below:

Tubes nb.s	1	2	3	4	5	6	7	8
BSA (µl)	0	2.5	5	7.5	10	12.5	15	20
dH <sub>2</sub> O (µl)	100	97.5	95	92.5	90	87.5	85	80
Bradford (µl)	900	900	900	900	900	900	900	900

Protein samples were prepared as described below:

tubes nb.s	1	2	3	4	5	6
sample( $\mu$ l)	0	2	2	2	2	2
dH <sub>2</sub> O( $\mu$ l)	98	98	98	98	98	98
Bradford ( $\mu$ l)	900	900	900	900	900	900
lysis buffer ( $\mu$ l)	2	-	-	-	-	-

(1= blank in both tables)

OD<sub>595</sub> were read after samples were incubated at room temperature in dark for 5 minutes.

**Bradford Stock Solution:**

4.75ml ethanol + 250  $\mu$ l dH<sub>2</sub>O (95 % ethanol)

10 ml 85% phosphoric acid

17.5 mg Coomassie Brilliant Blue

**Bradford Working Solution:**

21.25 ml dH<sub>2</sub>O

0.75 ml 95% ethanol

1.5 ml 85% phosphoric acid

1.5 ml Bradford stock solution

**4-3.4 SDS-Polyacrylamide gel electrophoresis of proteins**

The glass plates were assembled according to the manufacturer's instructions (EC). The volume of the gel mold was determined according to the information provided by the manufacturer (EC). In an Erlenmeyer flask, the appropriate volume of solution containing the desired concentration of acrylamide for the resolving gel was prepared. Effective range of separation of

SDS-PAGE gels due to different acrylamide concentrations are summarized in table 4-4 and concentrations of components of the resolving gel at different concentrations are summarized in table 4-5.

**Table 4-4 Effective range of separation of SDS-PAGE gels:**

Acrylamide concentration (%)	Linear range of separation (kD)
15	12-43
10	16-68
7.5	36-94
5.0	57-212

Without delay, the mixture was swirled rapidly and the acrylamide solution was poured into the gap between the glass plates. Sufficient space for the stacking gel was left. The acrylamide solution was overlaid by using a pasteur pipette with 0.1 % SDS (for gels containing <8% acrylamide) or isobutanol (for gels containing >10% acrylamide). The gel was placed in a vertical position at room temperature. After polymerization was complete, the overlay was poured off and the top of the gel was washed several times with deionised water. As much fluid as possible was drained from the top of the gel. Any remaining water was removed with the edge of a paper towel.

Stacking gel was prepared in a disposable plastic tube at an appropriate volume and at desired acrylamide concentration. Concentrations of components of the stacking gel at different volumes are summarized in table 4-6. Without delay, the mixture was swirled rapidly and the stacking gel solution was poured directly onto the surface of the polymerized resolving gel. The comb was immediately inserted into the stacking gel, being careful to avoid trapping air bubbles. The gel was placed in a vertical position at room temperature.

While the stacking gel was polymerizing, the samples to be loaded were prepared by heating them to 100°C for 5 minutes in 1X SDS gel-loading buffer to denature the proteins. After polymerization was complete, the comb was

removed carefully. By using a squirt bottle, the wells were washed with deionized water to remove any unpolymerized acrylamide. The gel was mounted in the electrophoresis apparatus. Tris-glycine electrophoresis buffer was added to the top and bottom reservoirs. The bubbles that were trapped at the bottom of the gel between the glass plates were removed by a bent hypodermic needle attached to a syringe. 30-200  $\mu\text{g}$  of protein was loaded in a predetermined order into the wells.

The electrophoresis apparatus was attached to an electric power supply and the gel was run at 15-30 mA until the dye front has moved to the resolving gel, after the voltage was increased to 15 V/cm, until the bromophenol blue reaches the bottom of the resolving gel. Then the power supply was turned off. The glass plates were removed from the electrophoresis apparatus and placed on a paper towel. By using a spatula, the plates were pried apart. Cutting a corner from the bottom marked orientation of the gel.

#### **Tris-glycine electrophoresis buffer:**

25 mM Tris

250 mM glycine (electrophoresis grade)

0.1% SDS

#### **30% mix (Acrylamide and bis-acrylamide solution)**

A stock solution of 29% (w/v) acrylamide and 1% (w/v) bis-acrylamide.

Solution was stored in a dark bottle at 4°C.

#### **10% SDS**

A 10% (w/v) stock solution was prepared in deionized water

#### **APS**

A small amount of 10% stock solution was prepared in deionized water and stored at 4°C.

**5X gel loading buffer**

3.8 ml distilled water, 1.0 ml 0.5 M Tris-HCl

0.8 ml glycerol, 1.6 ml 10% SDS

0.4 ml 0.05% BPB

400  $\mu$ l 2- $\beta$ Me (added freshly)**Table 4-5 Solution of preparing resolving gels for Tris-glycine SDS-PAGE**

Solution components	Component Volumes (ml)							
	5 ml	10 ml	15 ml	20 ml	25 ml	30 ml	40 ml	50 ml
<b>6%</b>								
<b>dH<sub>2</sub>O</b>	2.6	5.3	7.9	10.6	13.2	15.9	21.2	26.5
<b>30% mix</b>	1.0	2.0	3.0	4.0	5.0	6.0	8.0	10.0
<b>1.5 M Tris (pH 8.8)</b>	1.3	2.5	3.8	5.0	6.3	7.5	10.0	12.5
<b>10% SDS</b>	0.05	0.1	0.15	0.2	0.25	0.3	0.4	0.5
<b>10% APS</b>	0.05	0.1	0.15	0.20	0.25	0.30	0.40	0.50
<b>TEMED</b>	0.004	0.008	0.012	0.016	0.020	0.024	0.032	0.040
<b>8%</b>								
<b>dH<sub>2</sub>O</b>	2.3	4.6	6.9	9.3	11.5	13.9	18.5	23.2
<b>30% mix</b>	1.3	2.7	4.0	5.3	6.7	8.0	10.7	13.3
<b>1.5 M Tris (pH 8.8)</b>	1.3	2.5	3.8	5.0	6.3	7.5	10.0	12.5
<b>10% SDS</b>	0.05	0.1	0.15	0.20	0.25	0.30	0.40	0.50
<b>10% APS</b>	0.05	0.1	0.15	0.20	0.25	0.30	0.40	0.50
<b>TEMED</b>	0.003	0.006	0.009	0.012	0.015	0.018	0.024	0.030

<b>10%</b>								
<b>dH<sub>2</sub>O</b>	1.9	4.0	5.9	7.9	9.9	11.9	15.9	19.8
<b>30% mix</b>	1.7	3.3	5.0	6.7	8.3	10.0	13.3	16.7
<b>1.5 M Tris (pH 8.8)</b>	1.3	2.5	3.8	5.0	6.3	7.5	10.0	12.5
<b>10% SDS</b>	0.05	0.1	0.15	0.20	0.25	0.30	0.40	0.50
<b>10% APS</b>	0.05	0.1	0.15	0.20	0.25	0.30	0.40	0.50
<b>TEMED</b>	0.002	0.004	0.006	0.008	0.010	0.012	0.016	0.020
<b>12%</b>								
<b>dH<sub>2</sub>O</b>	1.6	3.3	4.9	6.6	8.2	9.9	13.2	16.5
<b>30% mix</b>	2.0	4.0	6.0	8.0	10.0	12.0	16.0	20.0
<b>1.5 M Tris (pH 8.8)</b>	1.3	2.5	3.8	5.0	6.3	7.5	10.0	12.5
<b>10% SDS</b>	0.05	0.1	0.15	0.20	0.25	0.30	0.40	0.50
<b>10% APS</b>	0.05	0.1	0.15	0.20	0.25	0.30	0.40	0.50
<b>TEMED</b>	0.002	0.004	0.006	0.008	0.010	0.012	0.016	0.020
<b>15%</b>								
<b>dH<sub>2</sub>O</b>	1.1	2.3	3.4	4.6	5.7	6.9	9.2	11.5
<b>30% mix</b>	2.5	5.0	7.5	10.0	12.5	15.0	20.0	25.0
<b>1.5 M Tris (pH 8.8)</b>	1.3	2.5	3.8	5.0	6.3	7.5	10.0	12.5
<b>10% SDS</b>	0.05	0.1	0.15	0.20	0.25	0.30	0.40	0.50
<b>10% APS</b>	0.05	0.1	0.15	0.20	0.25	0.30	0.40	0.50
<b>TEMED</b>	0.002	0.004	0.006	0.008	0.010	0.012	0.016	0.020

**Table 4-6 Solution of preparing 5% stacking gels for Tris-glycine SDS-PAGE**

Solution components	Component Volumes (ml)							
	1 ml	2 ml	3 ml	4 ml	5 ml	6 ml	8 ml	10 ml
<b>5% gel</b>								
<b>dH<sub>2</sub>O</b>	0.68	1.4	2.1	2,7	3.4	4.1	5.5	6.8
<b>30% mix</b>	0.17	0.33	0.50	0.67	0.83	1.0	1.3	1.7
<b>1.0 M Tris (pH 6.8)</b>	0.13	0,25	0.38	0.50	0.63	0.75	1.0	1.25
<b>10% SDS</b>	0.01	0.02	0.03	0.04	0.05	0.06	0.08	0.1
<b>10% APS</b>	0.01	0.02	0.03	0.04	0.05	0.06	0.08	0.1
<b>TEMED</b>	0.001	0.002	0.003	0.004	0.005	0.006	0.008	0.01

#### **4-3.5 Transfer of proteins from SDS-polyacrylamide gels to solid supports**

As the SDS-polyacrylamide gel was approaching the end of its run, four pieces of Whatman 3MM paper and one piece of transfer membrane (PVDF or nitrocellulose) was cut to the exact size of the SDS-polyacrylamide gel by wearing gloves. The membrane was left in methanol for 1 minute and then washed with deionized water and soaked into transfer buffer for 15 minutes. Prior to assembly of the transfer sandwich, Whatman 3MM paper were soaked into transfer buffer.

The transfer apparatus was set as follows:

- 2 layers of Whatman 3MM paper that have been soaked in transfer buffer were put onto the plate, which will be positively charged (anode). All air bubbles were squeezed.

- The membrane was placed onto the Whatman 3MM papers. (The transfer membrane should be exactly aligned and the air bubbles trapped between it and the Whatman 3MM paper should be squeezed out.)
- The glass plates holding the SDS-polyacrylamide gel were removed from the electrophoresis tank, and the gel was transferred to a tray of deionized water.
- SDS-polyacrylamide gel was placed onto the transfer membrane. Any trapped air bubbles were squeezed out with a gloved hand.
- 2 layers of Whatman 3MM paper were placed to the top of the sandwich (this side will be negatively charged during the transfer (cathode side).)
- The upper plate of the apparatus, which will be the cathode during the transfer, was put onto the top.

The electrical leads of the apparatus were connected to the power supply and the transfer was carried out at a current of 3.5 mA/square cm of the gel for a period of 30-45 minutes. The electric current was turned off at the end of the run time and the transfer apparatus was disassembled from top downward, peeling off each layer in turn. The gel was transferred to a tray containing Coomassie Brilliant Blue and stained in order to check if the transfer is complete or not. The bottom left-hand corner of the membrane was cut as insurance against obliteration of the pencil mark.

**Transfer Buffer:**

- 2.9 g Glycine
- 5.8 g Trisma base
- 0.37 g SDS
- 200 ml methanol
- Adjust volume to 1 l with ddH<sub>2</sub>O

**Transfer Buffer for Denaturing/Renaturing Western:**

- 25 mM Tris.Cl (pH: 8.3)
- 192 mM glycine
- 0.01% SDS

#### **4-3.6 Staining proteins immobilized on solid surfaces with Ponceau S**

The membrane onto which proteins were transferred was washed with deionized water and then soaked into Ponceau S. When bands of proteins become visible, the membrane was washed in several changes of deionized water at room temperature. The positions of proteins used as molecular-weight standards were marked.

##### **Ponceau S:**

10% glacial acetic acid

5% Ponceau S

#### **4-3.7 Denaturation and renaturation of proteins on nitrocellulose membranes**

After transfer of proteins to nitrocellulose, the membrane was incubated with the denaturation buffer for 30 minutes at room temperature. Then the membrane was soaked into the renaturation buffer for 1 hour at room temperature. Blocking was performed at 4°C for 90 minutes in the DR-Blocking buffer.

##### **Denaturation Buffer:**

25 mM Hepes

25 mM NaCl

5 mM MgCl<sub>2</sub>

1 mM DTT, 6 M Guanidine (add freshly)

##### **Renaturation Buffer:**

25 mM Hepes

25 mM NaCl

5 mM MgCl<sub>2</sub>

1 mM DTT, 0.187 M Guanidine (add freshly)

**DR-Blocking Buffer:**

25 mM Hepes  
25 mM NaCl  
5 mM MgCl<sub>2</sub>  
1 mM DTT  
1% non-fat dried milk powder  
0.05% NP-40

**4-3.8 Immunological detection of immobilized proteins (Western Blotting)**

After staining the proteins immobilized on transfer membrane with Ponceau S, the membrane was washed gently with deionized water and neutralized with the blocking buffer for 5 minutes. In order to inhibit non-specific binding sites, the membrane was immersed in the blocking solution for one hour. Primary antibody (anti-*NAPO* antibody) was diluted 1:1 in blocking solution and incubated with the membrane at room temperature for one hour or at 4°C O/N on a slowly rotating platform. Afterwards the membrane was washed three times, once for 15 minutes and twice for 5 minutes, with TBS-T. Following the washes the membrane was incubated with the secondary antibody (HRP-conjugated rabbit anti-mouse Ig-DAKO) diluted as recommended by the supplier in blocking solution for 1 hour at room temperature and then washed three times with TBS-T. Finally the membrane was washed with deionized water and become ready for development.

**Blocking Solution:**

3% milk powder in 0.1% Tween 20-TBS solution

**4-3.9 Detection of proteins immobilized on membranes**

Detection of proteins immobilized on membranes were done by using the ECL Western Blotting kit (Amersham Life Science) (Catalog no: RPN 2106)

#### **4-4 Immunoprecipitation with the anti-*NAPO* antibody**

Huh7 cells grown to 70% confluency were starved in DMEM lacking methionine (Sigma) and labeled with 200  $\mu\text{Ci}$   $^{35}\text{S}$ -methionine (Amersham) per 4 ml medium for two hours. Cells were scraped in ice-cold PBS and lysed in NP-40 lysis buffer (150 mM NaCl, 1.0% NP-40, 50 mM Tris pH 8.0, protease inhibitor cocktail-Roche), and centrifuged at 13,000 rpm at 4°C for 30 minutes. The cell lysate was incubated with the anti-*NAPO* antibody for 2 hours at room temperature. Meanwhile Protein G sepharose (Pharmacia) was equilibrated with lysis buffer. Following anti-*NAPO* antibody incubation, the *NAPO* antigen was immunoprecipitated by using the equilibrated Protein G sepharose for 2 hours at 4°C. The pellet was washed three times with lysis buffer, resuspended in 2X gel loading buffer and loaded to 10% SDS-polyacrylamide gel. Then the gel was fixed for 30 minutes and incubated in the Amplify solution (Amersham) for 30 minutes at room temperature. Then the gel was dried and exposed to X-ray film.

#### **Fixative solution:**

50% dH<sub>2</sub>O

40% methanol

10% glacial acetic acid

#### **4-5 Immunofluorescence with the anti-*NAPO* antibody**

Cells were plated onto sterile cover slips and incubated in the incubator overnight to allow cells attach the cover slips. Cells were washed with PBS once and fixed either with 100% ice-cold acetone for 1 minute or with 4% paraformaldehyde for 1 hour. When paraformaldehyde was used, cells were permeabilized for 3 minutes with 0.1% Triton X-100 in ice-cold 0.1% sodium citrate. Following saturation with 3% BSA in PBS-T (0.1%) for 15 minutes, fixed cells were incubated with anti-*NAPO* antibody (diluted 1:1) for 1 hour at room temperature. FITC-conjugated goat-anti-mouse antibody (DAKO) was used as the secondary antibody and diluted as recommended by the supplier. In each immunofluorescence cells were counterstained with Hoechst 33258 (Sigma). For

this purpose Hoechst 33258 stock solution was diluted to 3 µg/ml in water and then cells were incubated with the dye for 5 minutes in dark. Cover slips were washed for 15 minutes with distilled water, mounted on glass microscopic slides in the mounting solution and examined under fluorescent microscope (Zeiss).

**Hoechst solution:**

Hoechst 33258 dye stock solution: 400 µg/ml in water

Hoechst 33258 dye final solution: 3 µg/ml

**Mounting solution:**

50% glycerol

50% ddH<sub>2</sub>O

**4-6 Induction of apoptosis in different cell lines**

Apoptotic cell death was induced by either serum starvation or treatment with H<sub>2</sub>O<sub>2</sub>, UV-C, cisplatin, anti-Fas antibody or TNF-α treatment. In each set of experiment TUNEL assay was performed in parallel to the *NAPO* staining as described in section 4-8.

**4-6.1 Induction of apoptosis by serum starvation**

Hepatocellular carcinoma-derived SNU 398 cells, which undergo apoptosis when grown under serum-free conditions were plated onto cover slips and serum starved for three days. By the end of this period the cells start to display morphological characteristics of apoptosis (cell shrinkage, nuclear condensation and fragmentation) and tested for *NAPO* antigen immunoreactivity as described in section 4-5.

#### **4-6.2 Induction of apoptosis by oxidative stress and cisplatin**

For oxidative stress-induced apoptosis, Huh7 hepatocellular carcinoma cells were incubated in a culture medium containing 0.1% FCS for 72 hours, and treated with freshly prepared 100  $\mu\text{M}$   $\text{H}_2\text{O}_2$  for at least 4 hours prior to apoptosis assay. 293 kidney cells were directly treated with 200  $\mu\text{M}$   $\text{H}_2\text{O}_2$  or 100  $\mu\text{M}$  cisplatin. After 48 hours cells were analysed for *NAPO* immunoreactivity by immunofluorescence.

#### **4-6.3 Induction of apoptosis by UV-C treatment**

MCF-7, HeLa, U2OS, A375, SW480, LNCaP, Jurkat and MRC-5 cells were treated with UV-C irradiation (60-120  $\text{mJ}/\text{cm}^2$ ) to induce apoptosis. For this purpose cells were plated onto cover slips in 35 mm tissue culture dishes and incubated over-night in the incubator. Cells were then washed twice with sterile PBS. PBS was aspirated and cells were exposed to different dosages of UV-C. After addition of fresh DMEM/RPMI, plates were put into incubators and incubated for 24-72 hours until apoptotic cells begin to appear.

#### **4-6.4 Induction of apoptosis by activation of death-receptor mediated apoptosis**

For physiologically induced apoptosis studies, TNF- $\alpha$ -treated (Boehringer Mannheim) MCF-7 and anti-fas antibody-treated (Upstate Biotechnology-clone CH11) Jurkat cells were used.

##### **4-6.4.1 Induction of apoptosis by TNF- $\alpha$ treatment**

50.000 MCF-7 breast adenocarcinoma cells were plated onto cover slips so that the confluency would be 50% and incubated in the incubator over-night

to allow cells attach the coverslips. TNF- $\alpha$  was diluted to 50 ng/ml concentration in DMEM. 80-90% of cells entered apoptosis after incubation with TNF- $\alpha$  for 72 hours and were subjected to immunofluorescence.

#### **4-6.4.2 Induction of apoptosis by anti-Fas antibody treatment**

400,000 Jurkat acute T-cell leukemia cells were plated in 500  $\mu$ l RPMI into 12 well dishes. Anti-Fas antibody was diluted to 50 ng/ml in RPMI lacking FCS and 500  $\mu$ l of this dilution was distributed to wells. Thus 25 ng/ml anti-Fas antibody was used to induce 400,000 Jurkat cells to undergo apoptosis. After 24 hours cells were centrifuged for 3 minutes at 800 rpm and washed once with PBS. For immunofluorescence cells were cytopinned (Shandon) for 3 minutes at 200 rpm.

#### **4-7 p53 staining of apoptotic versus non-apoptotic Huh7 cells**

In order to assess that the negative *NAP0* immunostaining of apoptotic cells is not a common feature of all nuclear antigens, 50,000 Huh7 cells were plated onto coverslips and induced to undergo apoptosis after they attached. These induced cells were stained with the anti-p53 antibody 6B10 (Yolcu et al., 2001) in parallel with non-apoptotic counterparts. The 6B10 antibody was diluted in the ratio of 1:1 in PBS-T.

#### **4-8 TUNEL staining of apoptotic cells**

The TUNEL (Terminal Deoxynucleotidyl Transferase Mediated dUTP Nick End Labelling) assay was performed using In Situ Cell Death Detection Kit (Roche). Cells were fixed with 4% paraformaldehyde for 1 minute and permeabilized with 0.1% Triton-X in 0.1 % sodium citrate for 2 minutes on ice. Then cells were incubated with the TUNEL mixture prepared according to

manufacturer's recommendations. After the TUNEL assay, cells were counterstained with Hoechst 33258 and examined under microscope.

#### **4-9 Synchronization of MRC5 and Huh7 cells**

In order to analyse the expression pattern of *NAPO* during cell cycle two different cell types: fibroblastic (MRC5) and epithelial (Huh7) cells were synchronized and stained with the anti-*NAPO* antibody at 4 hour intervals for 48 hours.

##### **4-9.1 Synchronization of MRC5 cells by serum withdrawal**

MRC-5 human embryonic lung fibroblast cells (passage 18) were grown to confluency in 100 mm tissue culture plates and splitted onto cover-slips in 6 well tissue culture dishes. Next morning cells were washed twice with PBS and incubated with serum free DMEM for 3 days to induce quiescence. Then cells were induced to enter cell cycle by addition of 20% FCS to culture medium. Starting from T0 (quiescent state), these cells were immunostained with the anti-*NAPO* antibody for 48 hours at 4 hour intervals. In order to observe S phase cells, Brd-U incorporation assay was also performed in parallel with *NAPO* stainings as described in section 4-10.

##### **4-9.2 Synchronization of Huh7 cells by nocodazole treatment**

In order to induce cell cycle arrest in Huh7 cells nocodazole was used. Nocodazole is a microtubule depolymerizing drug thus incubation of cells with nocodazole results in arrest of cell cycle at M phase (Zieve et al., 1980). Its effect can be reversed by incubating cells in nocodazole free medium.

#### **4-9.2.1 Optimization of nocodazole concentration**

Huh7 were plated onto cover-slips and incubated with different dosages of nocodazole for different time periods to find out minimum concentration of nocodazole required to arrest cells in M phase with minimum cytotoxic activity. For this purpose cells were incubated with 50, 100, 200 or 400 ng/ml nocodazole for 6, 12, 18 or 24 hours. By the end of each time period cells were fixed with acetone and stained with the Hoechst 33258 dye.

#### **4-9.2.2 Mitotic shake-off**

Huh7 cells were plated into 150 mm tissue culture dishes and grown to 60% confluency and incubated with 50 ng/ml nocodazole (Sigma) for 18 hours. Mitotic cells were collected by mitotic shake-off and replated onto coverslips. For mitotic shake-off medium was aspirated smoothly and 8 ml DMEM was spurted onto cells for several times until the slightly attached round-shaped mitotic cells detach from the plate. Then mitotic cells were washed once with PBS, counted and replated onto coverslips. Cells were immunostained with the anti-*NAPO* antibody at 4 hour intervals, taking the time of plating cells as T0. In order to observe S phase cells, Brd-U incorporation assay was also performed in parallel with *NAPO* stainings as described in section 4-10.

#### **4-10 BrdU labeling and identification of S phase cells:**

For BrdU incorporation, cells were incubated with 30  $\mu$ M BrdU for 1 hour prior to fixation with ice-cold 70% ethanol for 10 minutes. Following DNA denaturation in 2 N HCl for 20 minutes, cells were incubated with FITC-conjugated anti-BrdU antibody (DAKO) in the dilution as recommended by the supplier. Then cells were counterstained with Hoechst 33258 and examined as described.

#### **4-11 Induction of quiescence in MRC5 cells**

Fibroblasts are known to enter quiescence by both serum starvation and growth to confluency (Campisi et al.,1984). Thus pre-senescent MRC-5 cells (passage 18) were grown to confluency on coverslips and serum starved for 3 days. At the end of 3 days, one set of cells was tested for BrdU labeling and the other set was subjected to immunofluorescence for the expression of the *NAP0* antigen. Asynchronizely growing MRC-5 cells of the same passage were used as a control.

#### **4-12 Senescence associated $\beta$ -Galactosidase Assay**

MRC-5 cells were grown to passage 40 and subjected to senescence-associated  $\beta$ -galactosidase (SA  $\beta$ -gal) assay, as described by Dimri et al. (Dimri et al., 1995). Briefly, cells were fixed in 3% formaldehyde for 5 minutes and incubated with SA- $\beta$ -gal solution for up to 12 hours, and examined under light microscope.

##### **SA- $\beta$ -gal solution:**

40 mM citric acid/sodium phosphate buffer (pH: 6.0)

5 mM potassium ferro cyanide

5 mM potassium ferric cyanide

150 mM NaCl

2 mM MgCl<sub>2</sub>

1 mg/ml X-Gal

## **CHAPTER V**

### **RESULTS**

#### **5-1 Introduction**

Results are explained in the following order:

- Production of the anti-*NAPO* monoclonal antibody
  - Production of anti-*NAPO* antibody producing hybridomas
  - Characterization of Ig subtype of the anti-*NAPO* antibody
- Screening of  $\lambda$ TripIEx expression library with the anti-*NAPO* antibody
- Biochemical characterization of the *NAPO* antigen
  - Western Blotting with the anti-*NAPO* antibody
  - Immunoprecipitation with the anti-*NAPO* antibody
  - Immunofluorescence with the anti-*NAPO* antibody
    - Staining of HCC cell lines with the anti-*NAPO* antibody
    - Species specific expression of the *NAPO* antigen
- Identification of *NAPO* as an apoptotic marker
- Expression of the *NAPO* antigen in quiescent cells
- Expression of the *NAPO* antigen during cell cycle
- Expression of the *NAPO* antigen in senescent cells

## **5-2 Production of the anti-*NAPO* monoclonal antibody**

### **5-2.1 Production of anti-*NAPO* antibody producing hybridomas**

After the immunization of Balb/c mice with the colorectal cell line COLO 320 cells the animal was sacrificed and hybridomas were prepared from splenic cells and antibody-producing clones were selected. One of the antibodies named Anti-*NAPO* (negative in apoptosis) was used for further studies (Performed by M.Ozturk).

### **5-2.2 Characterization of Ig subtype of the anti-*NAPO* antibody**

The ELISA plates were coated O/N with Anti-*NAPO* ascitic fluid and incubated with secondary antibodies against different IgG subtypes. Incubation of the ELISA wells with Lumilight substrate and exposure to autoradiograms revealed that anti-*NAPO* antibody is of IgG1 isotype.

## **5-3 Screening of $\lambda$ TripIEx expression library with the anti-*NAPO* antibody**

### **5-3.1 Titration of $\lambda$ TripIEx expression library**

Two different phage libraries, HeLa and human liver, were subjected to titration. HeLa phage library titration was calculated to be  $4.624 \times 10^9$  pfu/ml and human liver library titration was calculated to be  $4.65 \times 10^9$  pfu/ml. HeLa phage library was chosen to be studied first.

### **5-3.2 Optimization of the secondary antibody concentration**

Total cell lysate was prepared from 3 different HCC cell lines, Huh7, MV and Hep 40, and 25 µg of protein was loaded to 10% SDS-PAGE. The anti-p53 antibody 6B10 was used for western blotting as the primary antibody in the dilution of 1:1 in TBS-T. Two different secondary antibody (<sup>125</sup>I-labelled anti-mouse antibody) concentration was tested: 5 µCi/10 ml and 2,5 µCi /10 ml. As 2.5 µCi /10 ml result were as good as that of 5 µCi /10 ml, this concentration was chosen for further studies.

### **5-3.3 Immunodetection**

Total 400.000 plaques were screened and among these, 70 plaques were subjected to secondary screening. None of these 70 candidates were found to be positive for *NAPO* immunoreactivity.

## **5-4 Biochemical characterisation of the *NAPO* antigen**

### **5-4.1 Western Blotting with the anti-*NAPO* antibody**

Total cell lysate from the Huh7, Mahlavu and Hep 40 HCC cell lines was prepared and loaded to 10% SDS-PAGE as a duplicate. Proteins were transferred to nitrocellulose membranes with appropriate transfer buffers. One set of the duplicate was subjected to western blotting with the anti-*NAPO* antibody directly whereas the other half was treated with the protein denaturing and renaturing buffers prior to western blotting.

No significant bands were observed in both types of western blotting suggesting that the anti-*NAPO* antibody cannot recognize its epitope under our experimental conditions.

### 5-4.2 Immunoprecipitation with the anti-*NAPO* antibody

Detergent-soluble proteins were prepared from metabolically labelled Huh7 cells and subjected to immunoprecipitation with the anti-*NAPO* antibody. As shown in figure 5-1, anti-*NAPO* antibody recognized two proteins migrating at approximately 60 and 70 kD, respectively.

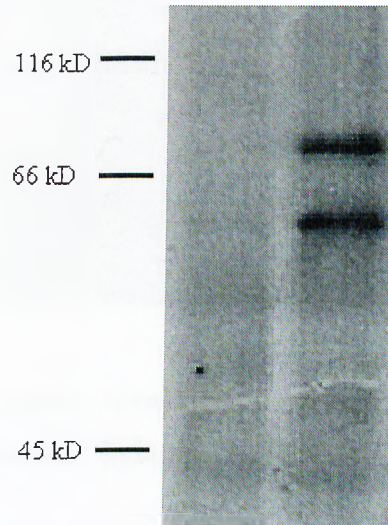


**Figure 5-1: Immunoprecipitation of the *NAPO* antigen from Huh7 cell lysate.**

(Lane 1: (-) control, Lane 2: Huh7)

### 5-4.3 Immunofluorescence with the anti-*NAPO* antibody

#### 5-4.3.1 Staining of HCC cell lines with the anti-*NAPO* antibody

SNU 398 and Huh7 HCC cells were grown on coverslips and subjected to immunofluorescence with the anti-*NAPO* antibody. Counter-staining with the Hoechst 33258 revealed that in both cell lines expression of the *NAPO* antigen was nuclear (figure 5-2).

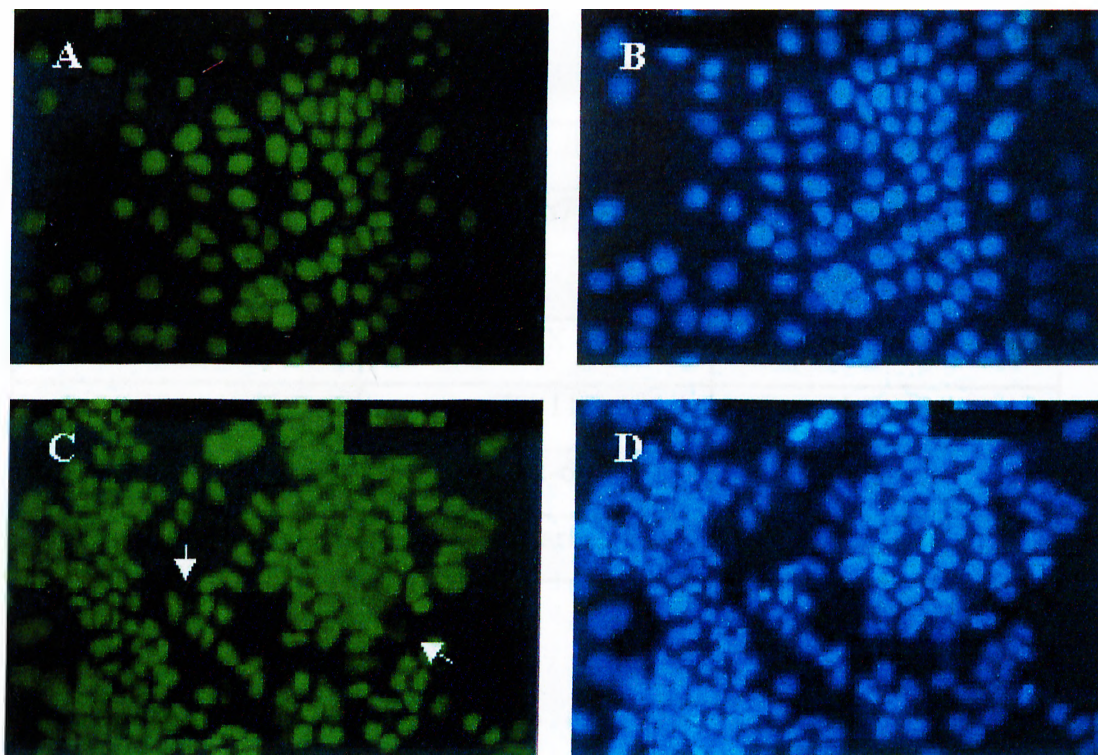


**Figure 5-2: Nuclear localization of the *NAPO* antigen in Huh7 and SNU 398 cell lines.** Arrows indicate cells that show morphologic characteristics of apoptosis.

(A: *NAPO* staining of Huh7 cells, B: Hoechst 33258 counterstaining of Huh7 cells, C: *NAPO* staining of SNU 398 cells, D: Hoechst 33258 counterstaining of SNU 398 cells)

#### 5-4.3.2 Species specific expression of the *NAPO* antigen

Mouse (HC 11), rat (IAR-6), hamster (CHOK-I), bovine (Ankara) and monkey (COS-7) cells were grown on cover-slips and immunostained with the anti-*NAPO* antibody (table 5-1). The *NAPO* antigen was absent in all of these cell lines tested except for the monkey cell line COS7.

**Table 5-1: Expression of the *NAPO* antigen in cell lines of different species.**

<b>Species</b>	<b>Cell Line</b>	<b><i>NAPO</i> staining</b>
Human	Huh7	Positive
Monkey	Cos-7	Positive
Hamster	CHOK-1	Negative
Mouse	HC-11	Negative
Rat	IAR-6	Negative
Bovine	Ankara	Negative

These results suggest that this antibody is specific for human and monkey *NAPO*, since the human cell lines tested and monkey cell line COS-7 showed positive immunostaining, but mouse (HC 11), rat (IAR-6) and hamster (CHOK-I) cell lines are negative.

### **5-5 Identification of *NAPO* as an apoptotic marker**

Although *NAPO* antigen was ubiquitously present in all human cell lines so far tested, small nuclear fragments, which are occasionally observed with some cell lines under normal culture conditions, were negative (figure 5-2, panels C and D, as an example). This suggested us that *NAPO* antigen could be lost during apoptosis. For this purpose several different cell lines originated from different tissues were induced to undergo apoptosis by exposure to different apoptotic stimuli as summarized in table 5-2.

**Table 5-2: List of cell lines tested for loss of *NAPO* immunoreactivity after induction of apoptosis by various stimuli.**

Cell line	Origin	Morphology	Apoptosis stimuli
Huh7	Hepatocellular carcinoma	Epithelial	H <sub>2</sub> O <sub>2</sub>
SNU 398	Hepatocellular carcinoma	Epithelial	Serum starvation
MCF7	Breast cancer	Epithelial	TNF- $\alpha$ , UV-C
HeLa	Cervix cancer	Epithelial	UV-C
SW480	Colon cancer	Epithelial	UV-C
LNCaP	Prostate cancer	Epithelial	UV-C
U2OS	Osteosarcoma	Epithelial	UV-C
A375	Melanoma	Epithelial	UV-C
Jurkat	Acute T-cell leukemia	Lymphoid	Anti-Fas, UV-C
MRC-5	Lung	Fibroblastic	UV-C
Hek 293	Embryonal kidney	Epithelial	Cisplatin, UV-C

### 5-5.1 *NAPO* immunoreactivity of apoptotic SNU 398 and Huh7 cells

Hepatocellular carcinoma-derived SNU 398 cells, which undergo apoptosis when grown under serum-free conditions, were serum starved for three days and tested for *NAPO* antigen immunoreactivity. Cells displaying morphological characteristics of apoptosis (cell shrinkage, nuclear condensation and fragmentation) displayed negative *NAPO* staining in contrast to positive nuclear staining of all non-apoptotic cells (figure 5-3).

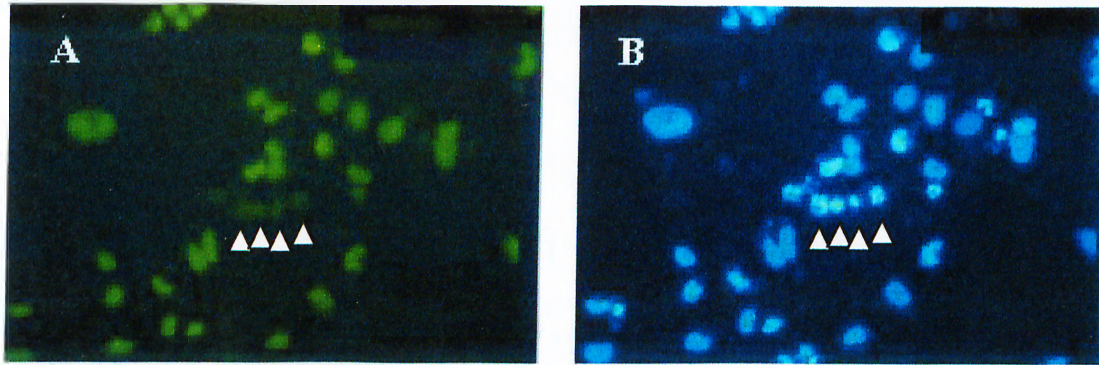


**Figure 5-3: Loss of the *NAPO* antigen in serum-starved SNU 398 HCC cells.** Arrows indicate the cells displaying morphological characteristics of apoptosis. (A: *NAPO* staining of SNU 398 cells, B: Hoechst 33258 counterstaining of SNU 398 cells)

To confirm the loss of *NAPO* antigen during apoptosis in another cellular system, hepatocellular carcinoma-derived Huh7 cells were used. Huh7 cells are known to enter apoptosis when treated with 100  $\mu\text{M}$   $\text{H}_2\text{O}_2$  under serum deficient conditions. Thus these cells were grown on cover-slips for three days in medium supplemented with 0.1% FCS and then treated with 100  $\mu\text{M}$   $\text{H}_2\text{O}_2$  for 24 hours. Our *NAPO* antigen was negative in apoptotic Huh7 cells that are identified as cells with small nuclei by Hoechst 33258 counterstaining (figure 5-4). In order to demonstrate that these small-nucleated cells are in fact apoptotic, TUNEL assay was performed in parallel with the *NAPO* immunostaining.

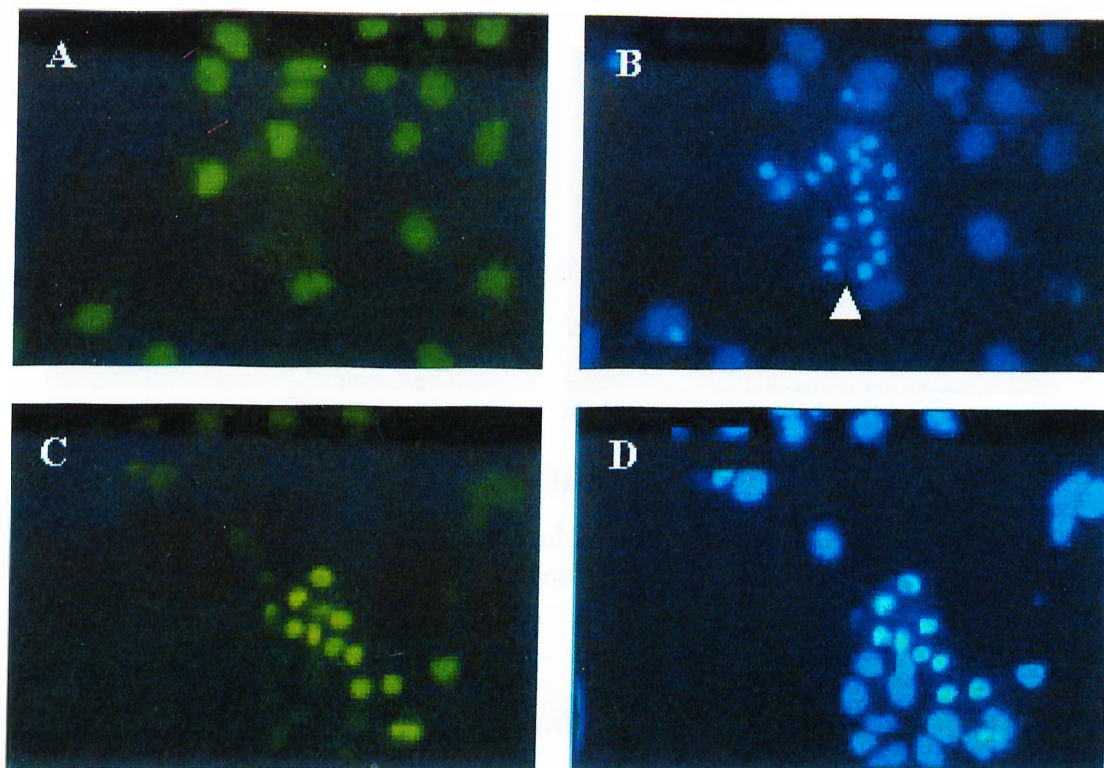


**Figure 5-4: *NAPO* immunoreactivity of apoptotic Huh7 cells in comparison with TUNEL assay.** The white arrow indicates the apoptotic cells.

(A: *NAPO* immunostaining of  $H_2O_2$  treated apoptotic Huh7 cells; B: Hoechst 33258 counterstaining of the cells shown in panel A; C: TUNEL assay of  $H_2O_2$  treated apoptotic Huh7 cells; D: Hoechst 33258 counterstaining of the cells shown in panel C)

### 5-5.2 p53 immunoreactivity of apoptotic Huh7 cells

To test whether the loss of *NAPO* expression is specific to this antigen, rather than a common feature shared by nuclear proteins, Huh7 cells were also tested for p53 protein immunoreactivity, under similar conditions. Huh7 cells express a mutant p53 protein that accumulates in their nuclei (Volkman et al., 1994). Both apoptotic and non-apoptotic Huh7 cells displayed positive staining for p53 protein. Indeed, apoptotic cells displayed stronger p53 immunoreactivity when compared to non-apoptotic cells (figure 5-5).

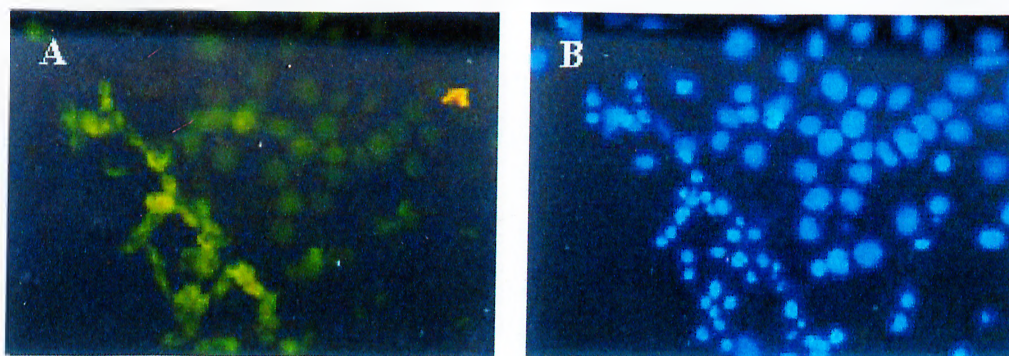


**Figure 5-5: p53 staining of apoptotic Huh7 cells.**

(A: p53 immunostaining of H<sub>2</sub>O<sub>2</sub> treated apoptotic Huh7 cells; B: Hoechst 33258 counterstaining of the cells shown in panel A.)

This indicated that the loss of *NAPO* immunoreactivity in apoptotic Huh7 cells was specific to this antigen rather than a common feature of nuclear proteins.

### **5-5.3 *NAPO* immunostaining in cells treated with various apoptotic stimuli**

For further characterization of *NAPO* as an apoptosis marker, additional studies were performed in different cell lines treated with different apoptosis stimuli. For all experiments *NAPO* tests were run in parallel with TUNEL or Annexin-V staining.

#### **5-5.3.1 *NAPO* immunostaining in death-receptor mediated apoptosis**

In order to show whether *NAPO* antigen is lost during death-receptor mediated apoptosis, MCF 7 breast cancer and Jurkat acute T-cell leukemia cells were used. To initiate apoptosis MCF7 cells were treated with TNF- $\alpha$  and Jurkat cells were treated with anti-Fas antibody. As shown in figure 5-6 *NAPO* was lost in apoptotic Jurkat and MCF-7 cells.

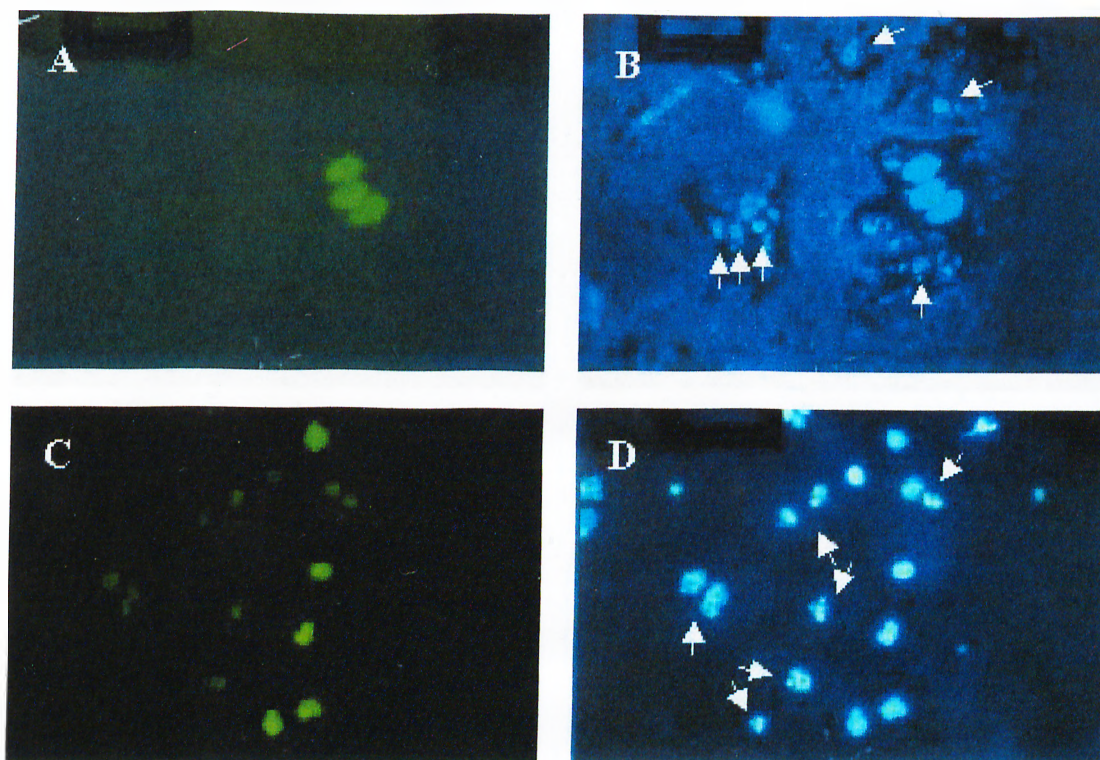


**Figure 5-6: *NAPO* immunostaining in death receptor mediated apoptosis in MCF-7 and Jurkat cells.** The white arrows indicate the apoptotic cells.

(A: *NAPO* immunostaining of TNF- $\alpha$  treated apoptotic MCF7 cells; B: Hoechst 33258 counterstaining of the cells shown in panel A; C: *NAPO* immunostaining of antagonistic anti-Fas antibody treated apoptotic Jurkat cells; D: Hoechst 33258 counterstaining of the cells shown in panel C.)

### 5-5.3.2 *NAPO* immunostaining in UV-C irradiation induced apoptosis

To demonstrate that *NAPO* antigen is lost during apoptosis induced by exposure to UV-C irradiation, MCF-7 and Jurkat cell lines were plated onto coverslips and exposed to 60-120 mJ/cm<sup>2</sup> UV-C irradiation and after 24 hours the cells were tested for *NAPO* immunoreactivity. As shown in figure 5-7, *NAPO* immunoreactivity was lost in apoptotic cells whereas the viable cells were still *NAPO* immunoreactivity positive.

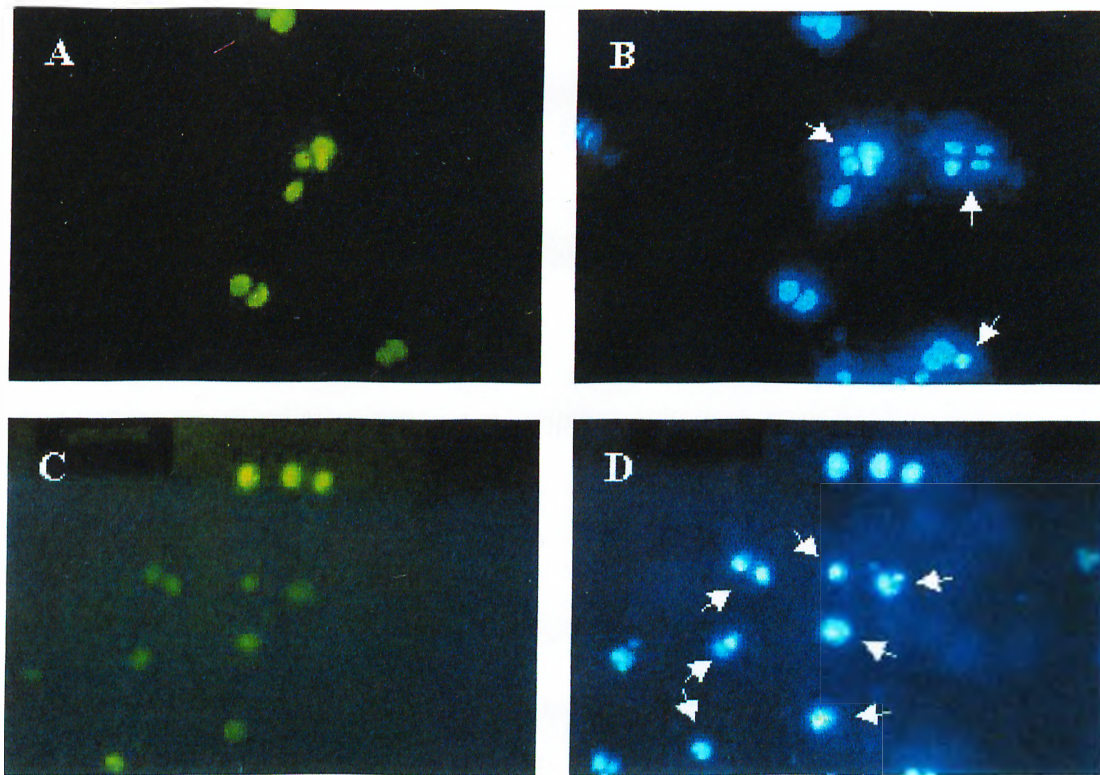


**Figure 5-7: *NAPO* staining of UV-C induced apoptotic MCF-7 and Jurkat cells.** The white arrows indicate the apoptotic cells.

(A: *NAPO* immunostaining of UV-C treated apoptotic MCF7 cells; B: Hoechst 33258 counterstaining of the cells shown in panel A; C: *NAPO* immunostaining of UV-C treated apoptotic Jurkat cells; D: Hoechst 33258 counterstaining of the cells shown in panel C.)

This result suggests that *NAPO* is also lost during UV-C mediated apoptosis in the same manner with death-receptor mediated apoptosis.

#### **5-5.4 *NAPO* immunostaining in tumorous versus non-tumorous cells exposed to various apoptotic stimuli**

To further verify that *NAPO* loss is universal among cell lines of different origin, the other cell lines summarized in table 5-2 were also induced to undergo apoptosis and subjected to *NAPO* immunostaining.

#### **5-5.4.1 *NAPO* immunostaining in apoptotic tumorous cell lines versus viable counterparts**

HeLa (cervix cancer), SW480 (colon cancer), U2OS (osteosarcoma), A375 (melanoma) and LNCaP (prostate cancer) cell lines were exposed to UV-C and tested for *NAPO* staining. It was observed that *NAPO* staining was lost in all apoptotic cells in contrast to strong nuclear staining of the non-apoptotic counterparts as shown in figure 5-8. This suggests that *NAPO* is ubiquitously expressed in cell lines originated from different tumorous tissues and is lost during apoptosis.

#### **5-5.4.2 *NAPO* immunostaining in apoptotic non-tumorous cell lines versus viable counterparts**

MRC-5 lung and Hek293 embryonic kidney cell lines were exposed to UV-C and H<sub>2</sub>O<sub>2</sub> respectively and tested for *NAPO* staining to assess the *NAPO* immunoreactivity in apoptotic normal tissue originated cell lines. As shown in figure 5-9, these cells also do not express *NAPO* when they are induced to undergo apoptosis.

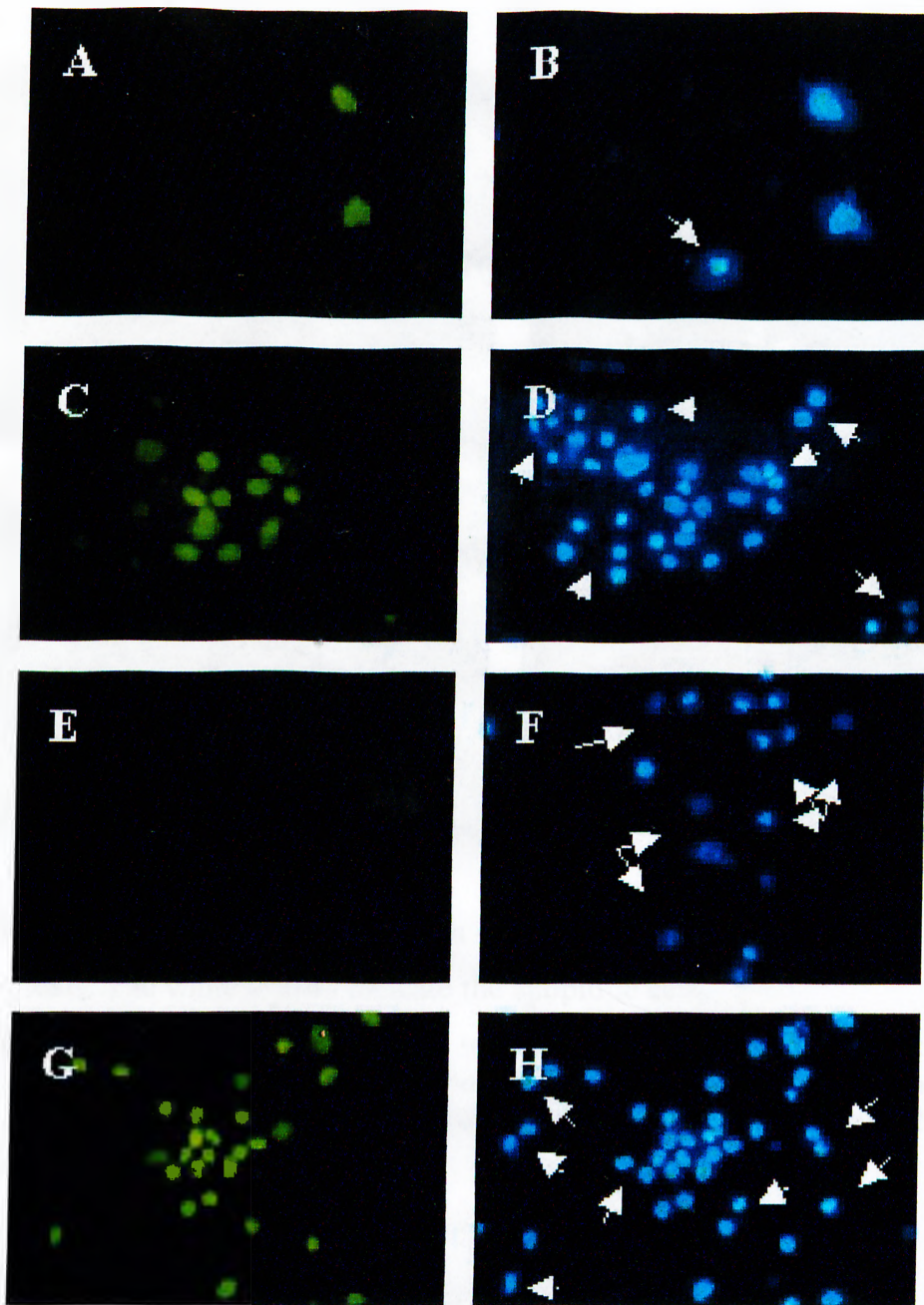


**Figure 5-8: Expression of *NAPO* in cells induced to undergo apoptosis by UV-C irradiation.** The white arrows indicate the apoptotic cells.

(A: *NAPO* immunostaining of UV-C treated apoptotic HeLa cells; B: Hoechst 33258 counterstaining of the cells shown in panel A; C: *NAPO* immunostaining of UV-C treated apoptotic SW480 cells; D: Hoechst 33258 counterstaining of the cells shown in panel C; E: *NAPO* immunostaining of UV-C treated apoptotic U2OS cells; F: Hoechst 33258 counterstaining of the cells shown in panel E; G: *NAPO* immunostaining of UV-C treated apoptotic A375 cells; H: Hoechst 33258 counterstaining of the cells shown in panel G.)

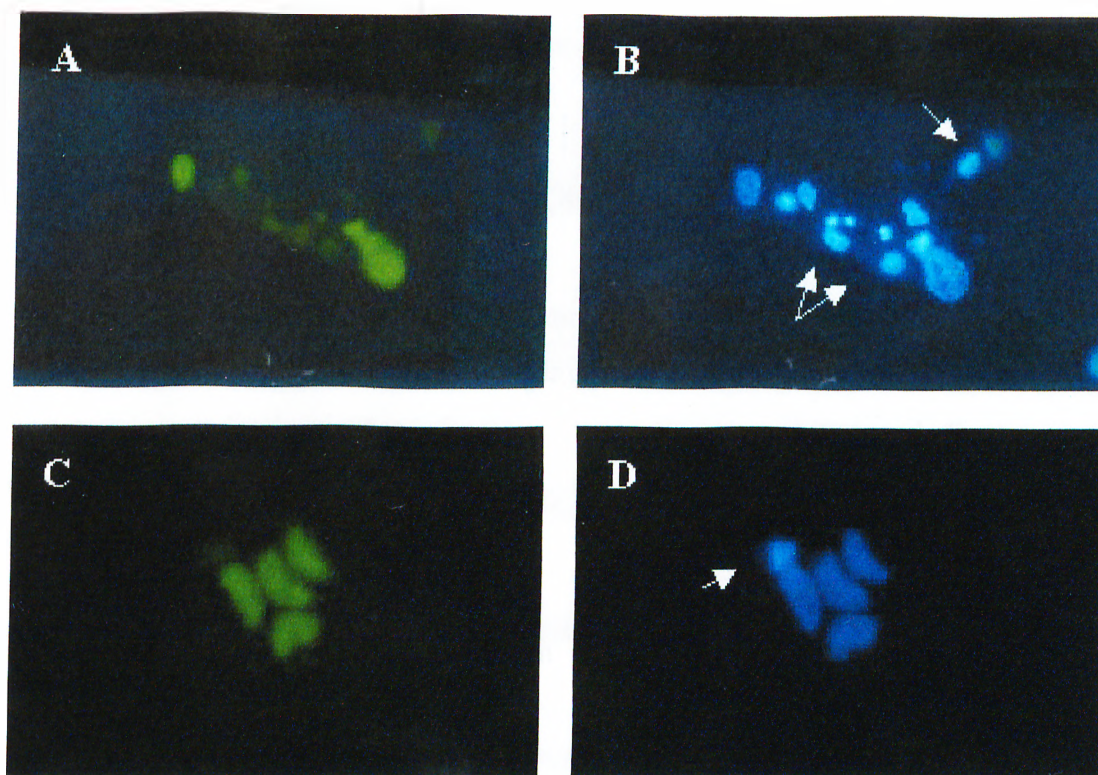


**Figure 5-9: Expression of *NAPO* in non-tumorous cells induced to undergo apoptosis.** The white arrows indicate the apoptotic cells.

(A: *NAPO* immunostaining of UV-C treated apoptotic MRC-5 cells; B: Hoechst 33258 counterstaining of the cells shown in panel A; C: *NAPO* immunostaining of H<sub>2</sub>O<sub>2</sub> treated apoptotic Hek 293 cells; D: Hoechst 33258 counterstaining of the cells shown in panel C.)

These results demonstrate that *NAPO* is ubiquitously expressed in living cells but lost during apoptosis independent of the apoptosis-activating pathway (Table 5-2).

The loss of *NAPO* during apoptosis strongly suggests that this antigen is a nuclear caspase substrate. The epitope recognized by anti-*NAPO* antibody on this antigen is probably lost as a result of caspase mediated protein cleavage. However, it is presently unclear whether any of 60 and 70 kD polypeptides of the *NAPO* antigen are known caspase substrates. Thus, *NAPO* appears to be a novel marker for apoptosis that could serve to distinguish apoptotic from non apoptotic cells. However, it was important to know whether the antigenic reactivity is

modified under different growth conditions such as quiescence, cell cycle (especially mitosis) and senescence.

#### **5-6 Expression of the *NAPO* antigen in quiescent cells**

MRC-5 human embryonic lung fibroblast cells (passage 18) were grown to confluency and serum starved for 3 days to induce quiescence. To show that these cells are indeed quiescent, BrdU incorporation was also tested. Our results indicate that approximately 15 % of asynchronously growing MRC-5 cells is positive for BrdU i.e. in S phase, whereas no BrdU labeling was observed in quiescent cells (figure 5-10).

*NAPO* immunostaining of serum starved cells versus cells grown in DMEM supplemented with 10% FCS revealed that these quiescent cells also express *NAPO* as shown in figure 5-11.

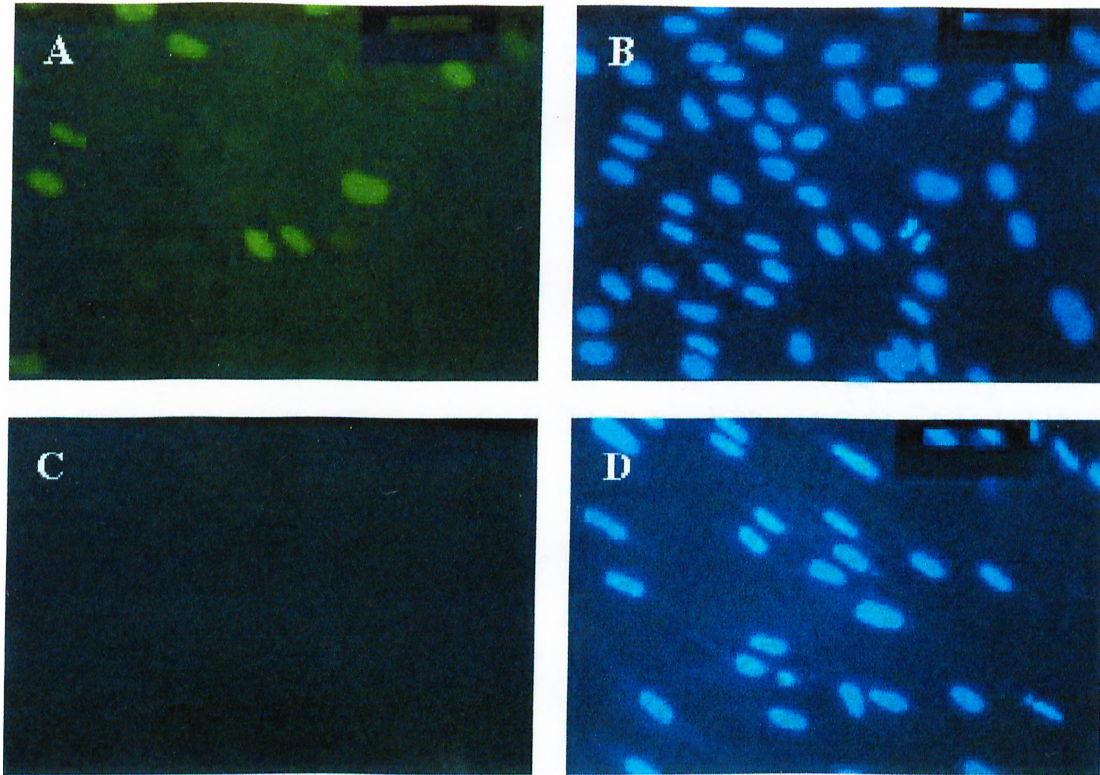


**Figure 5-10: Brd-U incorporation test to serum starved and non-starved p18 MRC-5 cells.**

(A: Brd-U incorporation test of MRC-5 cells grown in DMEM supplemented with 10% FCS; B: Hoechst 33258 counterstaining of the cells shown in panel A; C: Brd-U incorporation test of serum starved MRC-5 cells; D: Hoechst 33258 counterstaining of the cells shown in panel C.)

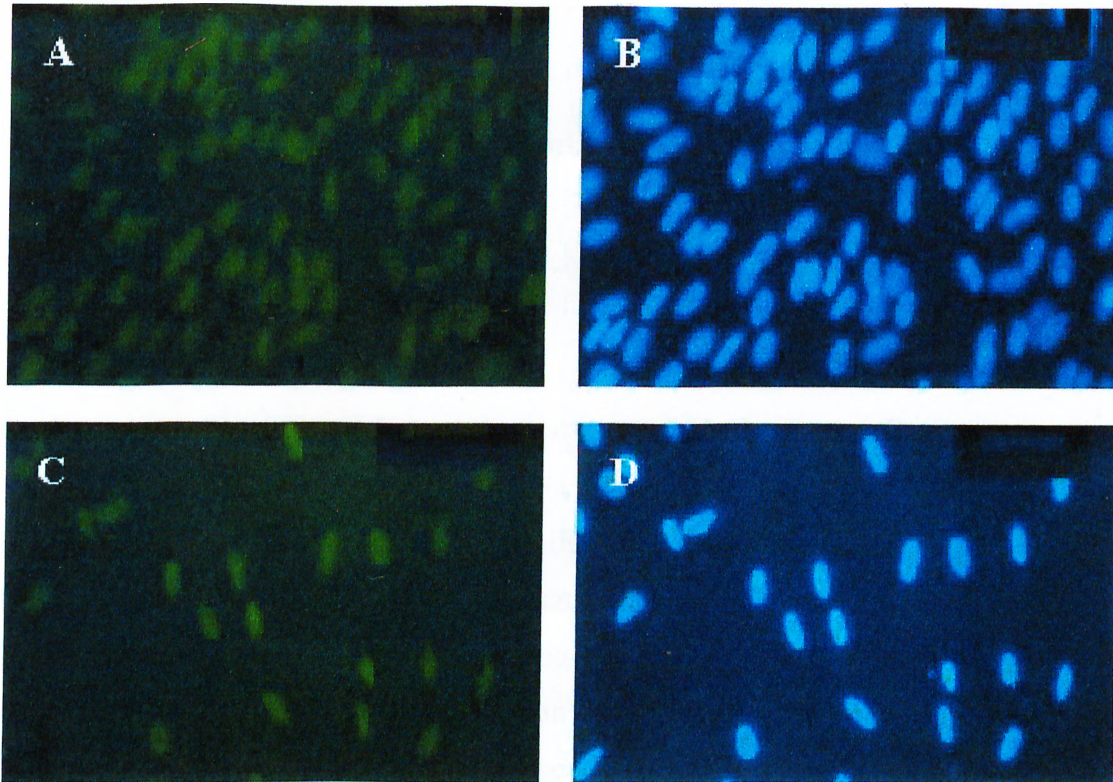


**Figure 5-11: *NAPO* immunostaining of serum starved and non-starved p18 MRC-5 cells.**

(A: *NAPO* immunostaining of MRC-5 cells grown in DMEM supplemented with 10% FCS; B: Hoechst 33258 counterstaining of the cells shown in panel A; C: *NAPO* immunostaining of serum starved MRC-5 cells; D: Hoechst 33258 counterstaining of the cells shown in panel C.)

Under both conditions, all cells displayed a similarly positive nuclear staining for *NAPO*. These observations indicated that *NAPO* expression is not lost in non-dividing quiescent cells.

### **5-7 Expression of the *NAPO* antigen during cell cycle**

In order to claim *NAPO* as a novel apoptotic marker, it was also necessary to demonstrate that the *NAPO* antigen is present in cells throughout the cell

cycle. For this purpose Huh7 and MRC5 cells were synchronized and tested for *NAPO* immunoreactivity at 4 hour intervals for 36 and 48 hours respectively.

### **5-7.1 Expression of *NAPO* in synchronized Huh7 cells**

#### **5-7.1.1 Synchronization of Huh7 cells by mitotic shake-off**

Huh7 cells were treated with different doses of the microtubule depolymerizing drug nocodazole, to arrest cells at the M phase of the cell cycle. Cells exit M phase when incubated in nocodazole free medium. A high dose of nocodazole is known to have cytotoxic effects on cells. Therefore first cells were incubated in different doses of nocodazole for different periods of time, to optimize the required least cytotoxic drug amount required to arrest cells in M phase. As shown in figure 5-12, incubation of cells in 50 ng/ml nocodazole for 18 hours resulted in a highly efficient M phase arrest with the least cytotoxic effect.

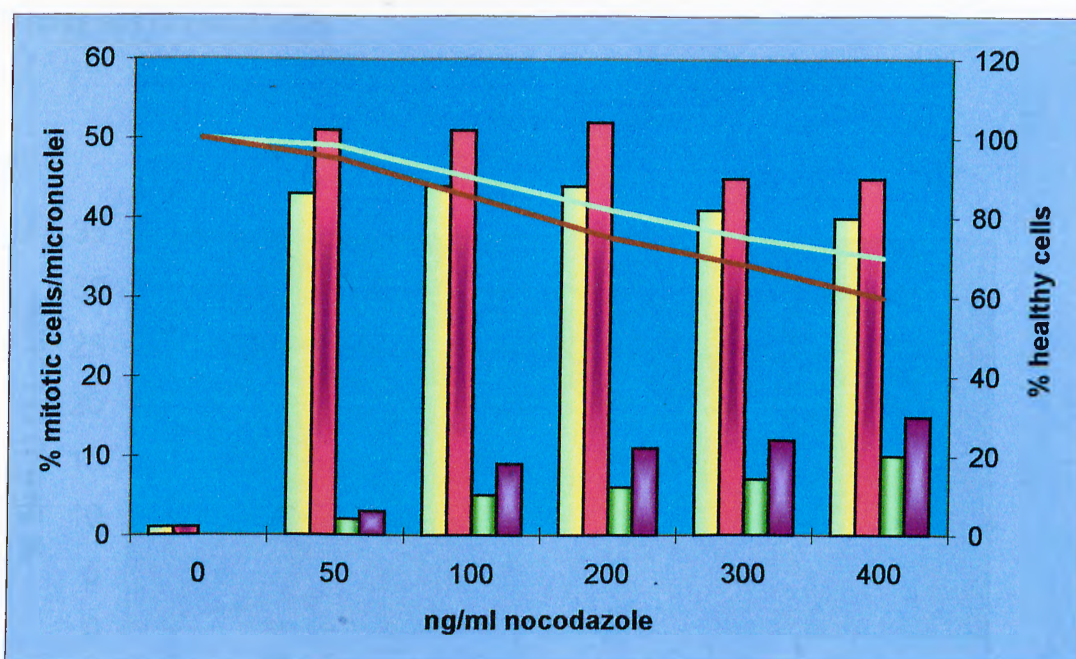


**Figure 5-12: Optimization of the most efficient nocodazole concentration required to arrest Huh7 cells in M phase of the cell cycle with the least cytotoxic effect.**

(Columns represent % mitotic cells or % of micronuclei, lines represent % healthy cells; yellow bars represent % mitotic cells at 18 hour and pink bars represent 24 hour incubation with nocodazole; green bars represent % micronuclei at 18 hour incubation and purple bars represent % micronuclei at 24 hour incubation; white line represents % healthy cells at 18 hour incubation and brown line represents % healthy cells at 24 hour incubation.)

#### 5-7.1.2 Determination of S phase cells by BrdU incorporation assay

After nocodazole treatment, cells were collected by mitotic shake-off and mitotic cells were plated onto coverslips. Synchronized Huh7 cells were tested every 4 hours for 36 hours of culture for both BrdU incorporation and *NAPO* staining. BrdU incorporation was minimal until 16 hour after the release from mitotic arrest with a maximum of BrdU incorporation at 24 hour, followed by a significant decrease at 36 hour (figure 5-13). According to BrdU incorporation index, cells at time points before 16 hour were evaluated as G1 phase cells, cells

between time points 20 hour and 32 hour as S phase cells, and those at time point 36 hour as G2 phase cells.

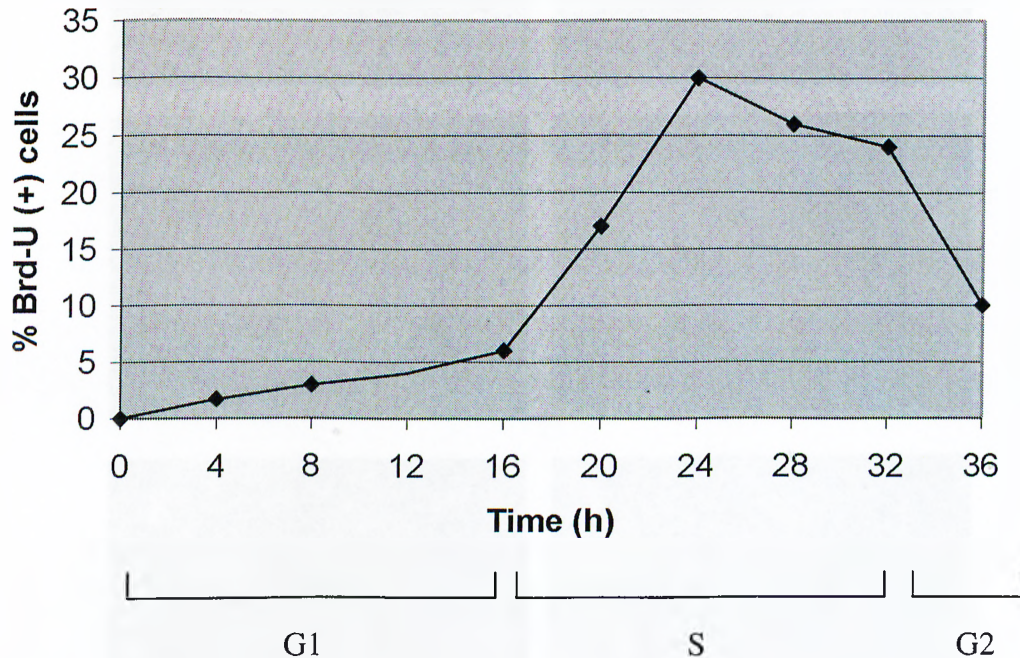


**Figure 5-13: BrdU incorporation index of M phase arrested Huh7 cells after mitotic shake-off.**

(Time points before 16 hour were evaluated as G1 phase cells, cells between time points 20 hour and 32 hour as S phase cells, and those at time point 36 hour as G2 phase cells.)

### 5-7.1.3 *NAPO* immunostaining at different phases of the cell cycle

Staining of these cells with the anti-*NAPO* antibody demonstrated that, mitotically arrested cells showed a diffusely positive (nuclear and cytoplasmic) *NAPO* staining (figure 5-14). *NAPO* staining pattern was nuclear throughout the cell cycle, at all time points (time points 8 h, 24 h and 36 h are shown in figure 5-14).

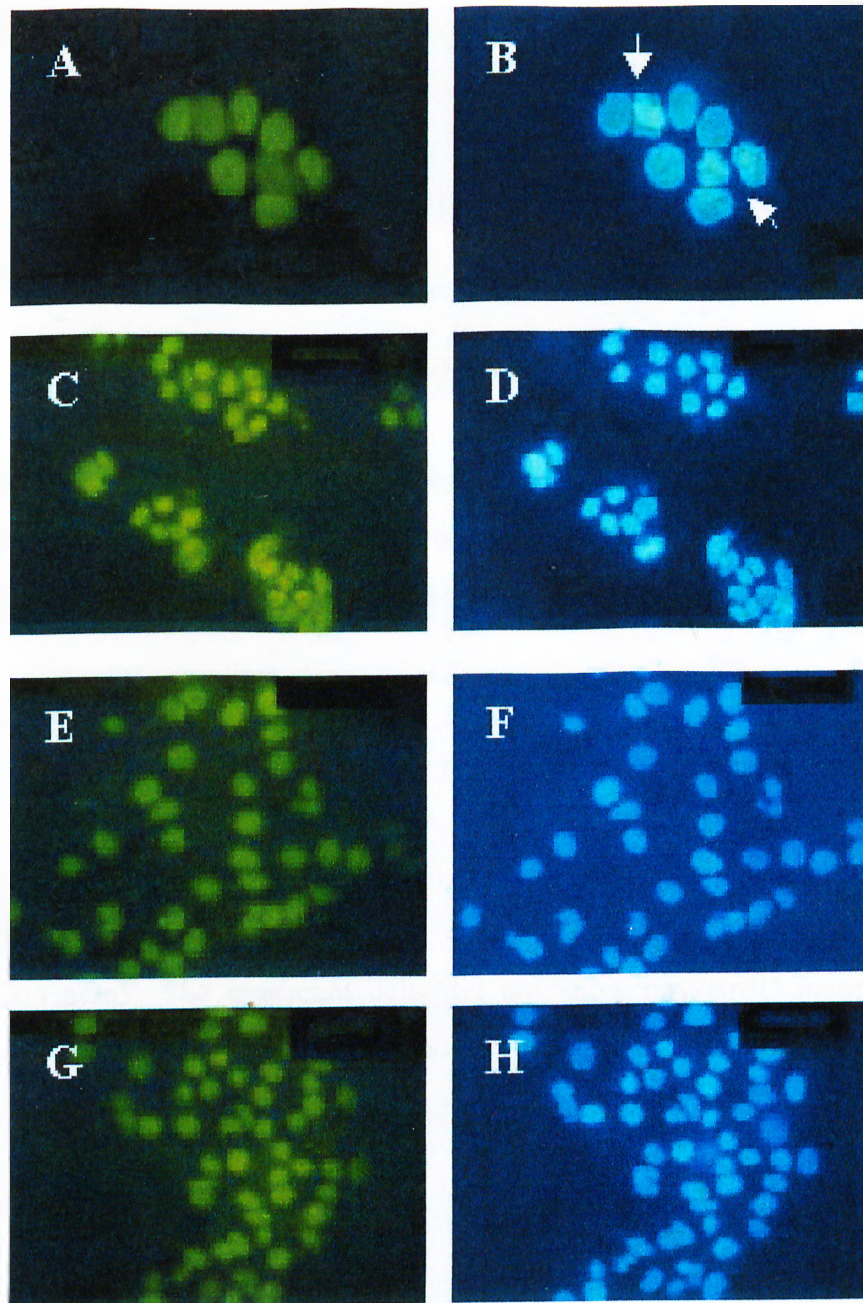


**Figure 5-14: NAPO immunostaining of synchronized Huh7 cells.** Arrows indicate mitotic cells

(A: NAPO staining of Huh7 cells arrested in M phase of the cell cycle; B: Hoechst 33258 counterstaining of the cells shown in panel A; C: NAPO immunostaining of Huh7 cells 8 hours after mitotic shake-off; D: Hoechst 33258 counterstaining of the cells shown in panel C; E: NAPO immunostaining of Huh7 cells 16 hours after mitotic shake-off; F: Hoechst 33258 counterstaining of the cells shown in panel E; G: NAPO immunostaining of Huh7 cells 36 hours after mitotic shake-off; H: Hoechst 33258 counterstaining of the cells shown in panel G.)

These results demonstrated that, *NAPO* staining was always positive during the cell cycle, the only noticeable change being a diffuse staining during mitosis, in contrast to strictly nuclear staining in other phases of the cell cycle.

## **5-7.2 Expression of *NAPO* in synchronized MRC-5 cells**

### **5-7.2.1 Synchronization of MRC-5 cells by serum starvation**

MRC-5 human embryonic lung fibroblast cells (passage 18) were grown to confluency and serum starved for 72 hours to induce quiescence. Then cells were induced to enter cell cycle by addition of 20% FCS to culture medium.

### **5-7.2.2 Determination of S phase cells by BrdU incorporation assay**

Starting from T0 (quiescent state), these cells were immunostained with the anti-*NAPO* antibody for 48 hours at 4 hour intervals in parallel with BrdU incorporation assay. The quiescent cells did not show any BrdU incorporation whereas cells at different time points showed BrdU incorporation as shown in figure 5-15.

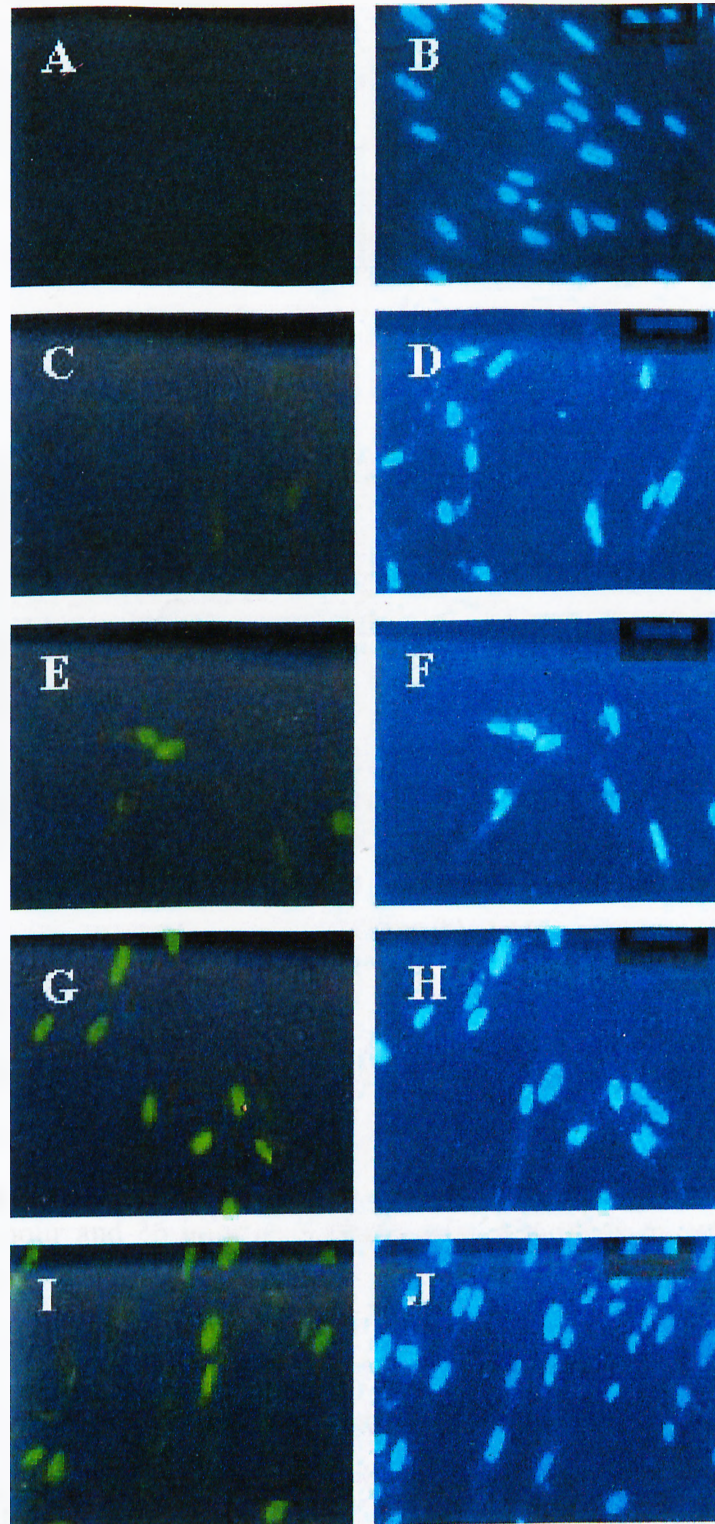


**Figure 5-15: BrdU incorporation assay of synchronized MRC-5 cells.**

(A: T0-quiescent cells; B: Hoechst 33258 counterstaining of the cells shown in panel A; C: T16 cells; D: Hoechst 33258 counterstaining of the cells shown in panel C; E: T24 cells; F: Hoechst 33258 counterstaining of the cells shown in panel E; G: T28 cells; H: Hoechst 33258 counterstaining of the cells shown in panel G; I: T36 cells; J: Hoechst 33258 counterstaining of the cells shown in panel I.)

According to the BrdU incorporation assay a graph representing the estimated cell cycle phases of synchronized MRC-5 cells were drawn as shown in figure 5-16. Due to this curve cells at time points before 20 hour were evaluated as G1 phase cells, cells between time points 24 hour and 36 hour as S phase cells, and those at time point 40 hour as G2 phase cells.

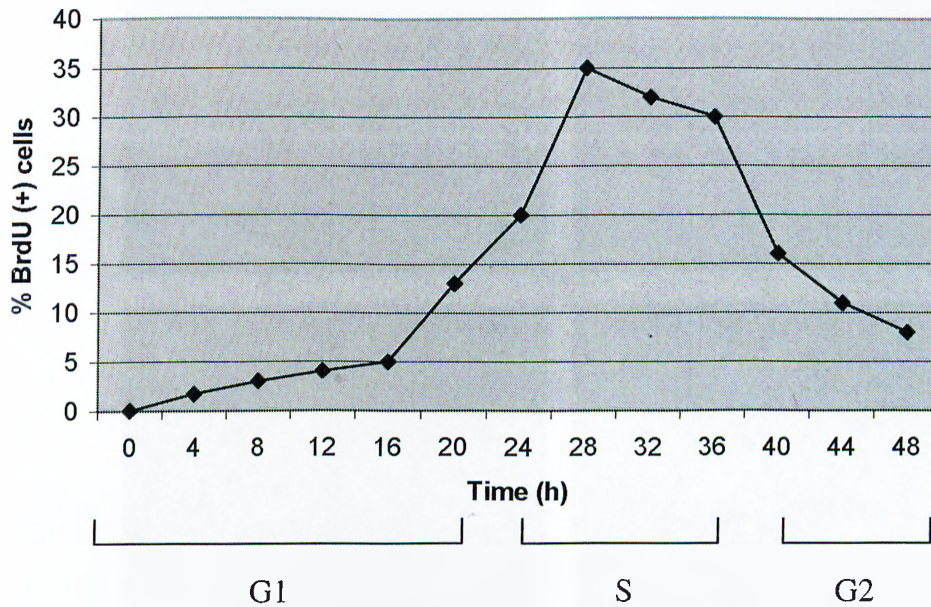


**Figure 5-16: BrdU incorporation index of serum starved MRC-5 cells after release from the quiescent state.**

(Time points before 20 hour were evaluated as G1 phase cells, cells between time points 24 hour and 36 hour as S phase cells, and those at time point 40 hour as G2 phase cells.)

### 5-7.2.3 *NAPO* immunostaining at different phases of the cell cycle

Staining of these cells with the anti-*NAPO* antibody demonstrated that, *NAPO* staining pattern was nuclear throughout the cell cycle as shown in figure 5-17.

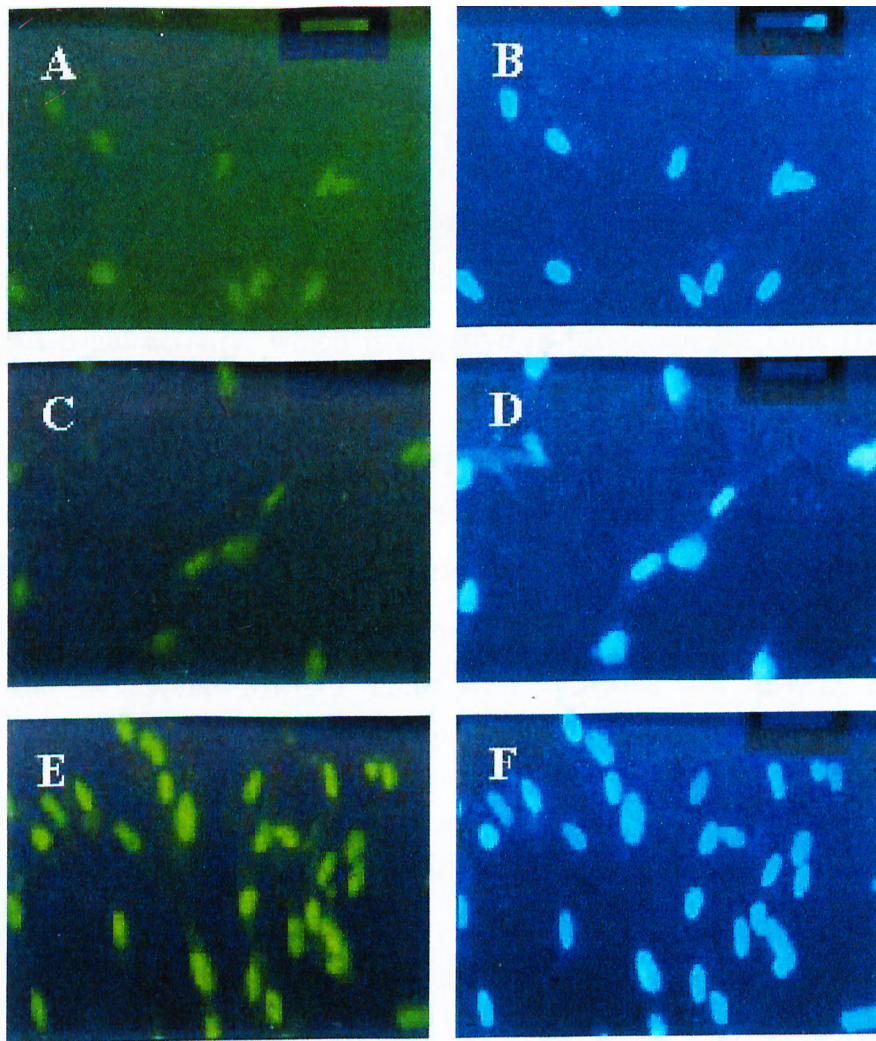


**Figure 5-17: *NAPO* immunostaining of synchronized MRC-5 cells.**

(A: *NAPO* staining of T4 MRC-5 cells; B: Hoechst 33258 counterstaining of the cells shown in panel A; C: *NAPO* immunostaining of T28 MRC-5; D: Hoechst 33258 counterstaining of the cells shown in panel C; E: *NAPO* immunostaining of T40 MRC-5 cells; F: Hoechst 33258 counterstaining of the cells shown in panel E.)

These results showed that *NAPO* is present in all phases of the cell cycle as demonstrated in two different cell lines, synchronized by two different approaches. The only exception was the M phase in which *NAPO* was still positive but showed cytoplasmic and nuclear diffused staining.

## 5-8 Expression of the *NAPO* antigen in senescent cells

To test whether *NAPO* antigen expression is modified during senescence, MRC-5 cells were grown until passage 40 at which point they remain alive and attached to cell plate, but they stop dividing, a characteristic feature of senescence (Fulder and Holliday, 1975). The senescence is often accompanied by a positive SA- $\beta$ -gal activity, which is negative in pre-senescent cells (Dimri et al., 1995).

In figure 5-18, panels A, C and E represent the pre-senescent MRC-5 cells and panels B, D and F represent the senescent MRC-5 cells. In contrast to pre-senescent MRC-5 cells at passage 18, senescent MRC-5 cells at passage 40 were positive for SA- $\beta$ -gal activity. Immunofluorescence data indicated that both pre-senescent and senescent MRC-5 cells were positive for *NAPO* antigen immunoreactivity, demonstrating that *NAPO* expression is not lost in senescent cells.

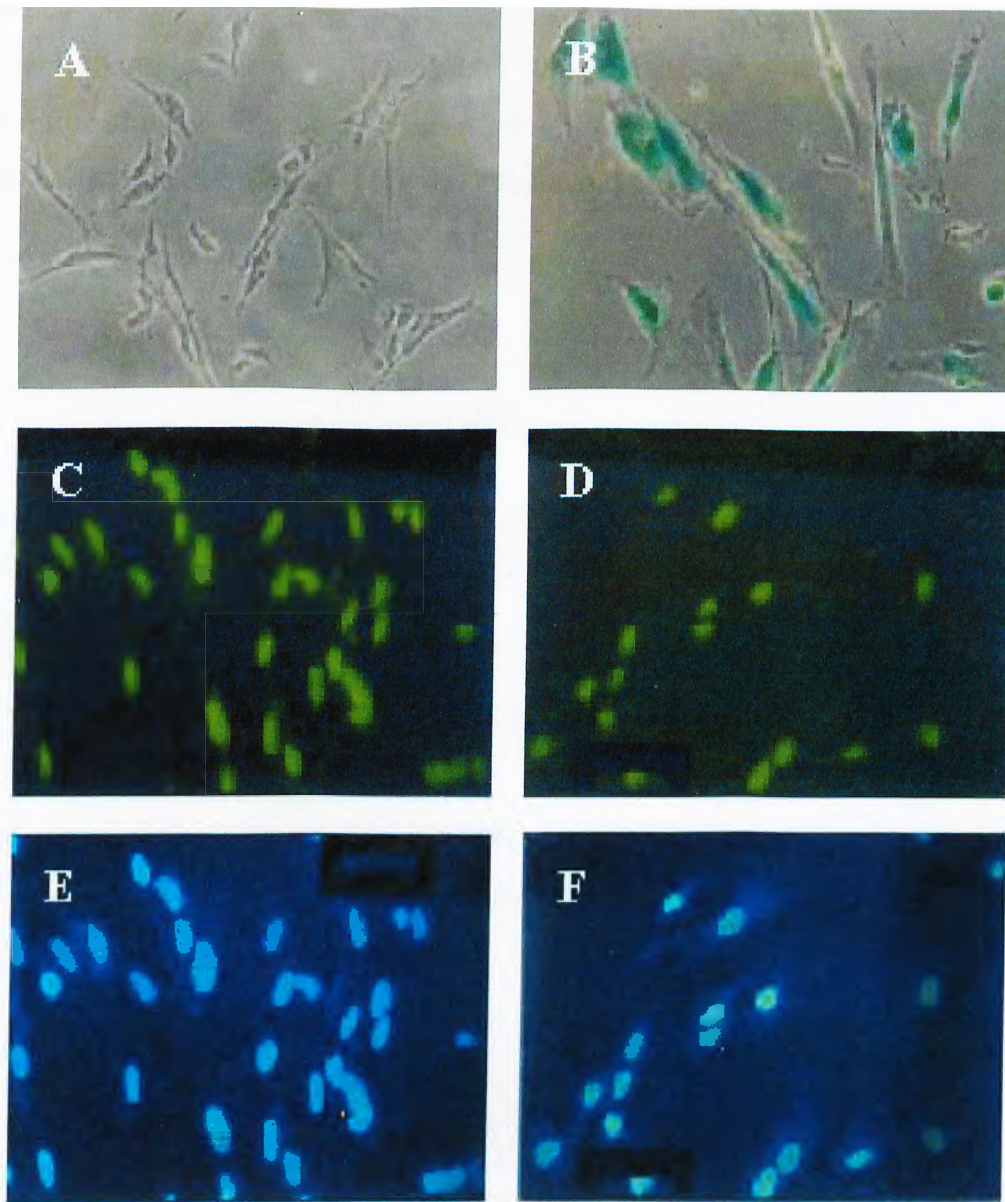


**Figure 5-18: SA- $\beta$  Galactosidase and *NAPO* immunostaining of P18 and p40 MRC-5 cells.**

(A: SA- $\beta$  Galactosidase assay of p18 MRC-5 cells; B: SA- $\beta$  Galactosidase assay of p40 MRC-5 cells; C: *NAPO* immunostaining of p18 MRC-5 cells; D: *NAPO* immunostaining of p40 MRC-5 cells; E: Hoechst 33258 counterstaining of the cells shown in panel C; F: Hoechst 33258 counterstaining of the cells shown in panel D.)

Together these data demonstrate that, *NAPO* is a nuclear antigen composed of two polypeptides, that is present in all human cell lines so far tested. The unique feature of this antigen is that it gets lost in apoptotic cells

independent of the mechanism of apoptosis induction. Furthermore this antigen is present throughout the cell cycle and also during quiescence and senescence. Therefore the mouse monoclonal anti-*NAPO* antibody would serve as a perfect tool for the detection of apoptosis in human and monkey cells.

## **CHAPTER V**

### **DISCUSSION AND PERSPECTIVES**

*NAPO* is a monoclonal antibody-defined nuclear antigen, which is lost specifically in apoptotic cells, while it is ubiquitously expressed in living cells independent of cell cycle, quiescence and senescence. The immunoreactivity of *NAPO* in living cells is strong enough to easily distinguish apoptotic from non apoptotic cells. Immunoprecipitation experiments indicate that the anti-*NAPO* monoclonal antibody captures specifically two different polypeptides of 60 and 70 kD. Our attempts to detect these antigens by western blotting, and expression cloning of their coding cDNAs were so far unsuccessful. Thus, it is presently unclear whether anti-*NAPO* antibody recognizes an epitope, which is common to or shared by these two polypeptides. Alternatively, these two proteins could be a heterodimer and the antibody recognizes either one of them under our experimental conditions.

The loss of *NAPO* during apoptosis strongly suggests that this antigen is a nuclear caspase substrate. The epitope recognized by anti-*NAPO* antibody on this antigen is probably lost as a result of caspase mediated protein cleavage. However, it is presently unclear whether any of 60 and 70 kD polypeptides of the *NAPO* antigen are known caspase substrates. To our knowledge, proteins with similar molecular weight have not been described previously as apoptosis-associated proteins. Thus, *NAPO* appears to be a novel marker for apoptosis. When compared to other available apoptosis detection systems, *NAPO* antigen offers the simplicity of antibody-based assays. The anti-*NAPO* antibody can be used for detection of apoptotic cells under different conditions such as in situ staining of cells and tissue sections, and for flow cytometry. TUNEL assay (Gavrieli et al., 1992) is widely used for the identification of apoptotic cells, even

though it requires several cumbersome experimental steps. As *NAPO* and TUNEL assays provide exclusive nuclear staining of alive and apoptotic cells, respectively, both assays may be combined for better identification of apoptosis. Moreover, *NAPO* assay may detect apoptotic cells prior to DNA fragmentation and it does not require special pre-treatment of assay samples. *NAPO* may also be used in combination with Annexin V staining (Martin et al., 1995). *NAPO* differs from previously identified and antibody-defined apoptosis markers (Grand et al., 1995; Hammond et al., 1998; Srinivasan et al., 1998; Leers et al., 1999; Zhang et al., 1996) by its exclusive loss in apoptotic cells, but not in quiescent, proliferating, senescent or even mitotic cells. We believe that this antibody will be very helpful for development of simple and easy immunoassays for measurement of apoptosis in both cell lines and tissue samples.

A eukaryotic cell can be in proliferation, quiescence, senescence and apoptosis states, depending on its internal program that can be regulated by external effectors. When it is proliferating, a cell passes through different stages of the cell cycle (G1, S, G2 and M). Quiescence is the non-proliferating state of cells and can be reversible. Senescence defines a physiologically irreversible state in which cells are no longer able to reenter the cell cycle, unless the senescence program is overwritten by a process called immortalization as seen in most cancer cells (Nurse, 2000; Sherr CJ. and DePinho RA., 2000; Murray A. and Hunt T., 1993)

Apoptosis is programmed cell death, a naturally occurring process involved in both the development and aging of cells. It is the process where the body can rid itself of unwanted, old, or damaged cells. Apoptosis is the physiological counterpart of cell proliferation. It is essential for both biological processes such as normal tissue turnover, embryonic development, and maturation of the immune system, including pathological processes, such as hormone deprivation, thermal stress and metabolic stress. Programmed cell death is required for proper embryonic development as well as for the maintenance of homeostasis in adult tissues (Vaux DL. and Korsmeyer SJ., 1999; Wyllie AH. and Golstein P., 2001). Moreover, apoptosis is involved in the etiology and pathophysiology of a variety of diseases such as cancer, neurodegenerative, autoimmune, infectious and heart diseases (Reed CJ., 2000; Mattson MP., 2000; Chervonsky AV., 1999; Roulston A. et al., 1999; Narula J. et al., 2000)

Apoptosis is characterized by a decrease in cell volume, condensation of chromatin, cellular budding, and the fragmentation of DNA into a ladder of 180 base pair (bp) oligomers with 3'-OH free ends, a hallmark of apoptosis. Cell membranes maintain their integrity through the process, and lysosomes remain intact (Saraste A., and Pulkki K., 2000). There is no inflammatory response from apoptosis. Affected cells undergo phagocytosis by adjacent normal cells and by some macrophages.

Morphological changes observed in apoptotic cells result from a series of genetically programmed biochemical changes initiated by either the activation of death receptors or by intracellular stress conditions such as DNA damage. These pro-apoptotic signals are conveyed to mitochondria to cause the release of caspase-activating factors from this organelle, followed by a cascade of caspase activation, which leads to cell death (Earnshaw WC. et al., 1999; Gottlieb RA., 2000).

Apoptosis can be activated by a number of intrinsic or extrinsic signals. These signals include mild physical signals, such as ionization radiation, ultraviolet radiation, or hyperthermia, low to medium doses of toxic compounds, such as azides or hydrogen peroxides; chemotherapeutic drugs, such as etoposides and cis-platinum, death receptor activators such as tumor necrosis factor- $\alpha$ , fas ligand and its agonists. Apoptosis can also be activated when cells are deprived from their survival factors that maintain them in a viable condition (Zornig M. et al., 2001).

Unregulated apoptosis is involved in diseases such as cancer, heart disease, neurodegenerative disorders, autoimmune disorders, and viral and bacterial infections. Cancer, for example, not only triggers cells to proliferate but also blocks apoptosis. Cancer is partly a failure of apoptosis: the orders for the cells to kill themselves by apoptosis are blocked (Huang P and Oliff A., 2001). Disease and shock can cause cardiac cells to induce apoptosis. For example, cells deprived of oxygen after a heart attack release signals that induce apoptosis in cells in the heart (Haunstetter A and Izumo S, 2000; Hajjar RJ. et al., 2000). Apoptosis may also be involved in the destruction of neurons in people afflicted by strokes or neurodegenerative diseases such as Alzheimer's disease and Parkinson's disease. There is evidence suggesting that ischemia can kill neurons by inducing apoptosis. Thus, inhibition of apoptosis may be a therapeutic

strategy for the treatment of neurodegenerative disorders such as stroke (Deigner H. et al., 2000; Irizarry MC. and Hyman BT., 2001). A failure of apoptosis in the immune system can lead to autoimmune diseases. T-cells differentiate between self and nonself (foreign) cells in the body. Autoimmune diseases such as rheumatoid arthritis, diabetes, and multiple sclerosis, result when a small percentage of T-cells attack the body's own tissue (Vaux DL. and Flavell RA., 2000). There is also evidence suggesting that AIDS develops when the human immunodeficiency virus (HIV) sets off unregulated and untimely apoptosis in CD-4 and CD-8 cells, the defenders of the immune system. Inhibition of HIV-induced apoptosis is a target field for treatment of AIDS (Gougeon ML. and Montagnier L., 1999).

There is an enormous therapeutic potential in controlling apoptosis in these diseases. Therefore, apoptosis is a target subject for understanding cellular mechanisms of many diseases, as well as for developing new drugs that interfere with either pro-apoptotic or anti-apoptotic molecular networks. Much research is now focusing on developing drugs that can either inhibit or induce apoptosis depending on the targeted disease.

A major difficulty with researching apoptosis and drugs to control it is that a reliable marker of apoptosis has not yet been developed. Therefore, it has become important to develop reliable assays to measure cell death. A marker is also needed in order to determine whether cells are dying or have been killed by apoptosis in the diagnosis of these diseases. For example, a marker for apoptosis could be used to determine the extent of neuronal damage caused by a stroke. Apoptosis drugs are being used in therapy, and a reliable marker is needed in order to evaluate the progress of the therapy. For example, a major goal of some cancer chemotherapies has become to kill cancer cells by inducing apoptosis in these cells. It is estimated, however, that almost 50 percent of cancer drug treatments fail. It would be useful to have a method to assess the performance of new treatments in a reliable and effective manner.

Currently available techniques for apoptosis detection are based on the study of morphology of apoptotic cells (light microscopy and fluorescence microscopy coupled to nuclear staining with specific dyes, electron microscopy), DNA fragmentation detected by terminal transferase-mediated dUTP nick-end labelling (TUNEL) and similar techniques, membrane changes detected by

annexin V in vivo labelling, and on immunological assays using antibodies directed to apoptosis-related proteins (Stadelmann C. and Lassmann H., 2000).

Currently, the most commonly used marker to detect apoptosis is TUNEL labelling of the 3'-OH free end of DNA fragments produced during apoptosis (Gavrieli Y. et al., 1992). The TUNEL method consists of catalytically adding a nucleotide, which has been conjugated to a chromogen system or to a fluorescent tag, to the 3'-OH end of DNA fragments as indicative of apoptosis. However this method involves a number of limitations. Early detection of apoptosis is not possible with this method as the DNA fragmentation is an end-point in the apoptosis pathway. False positives are often obtained when using the TUNEL method as a result of DNA damage that generates DNA fragments that have 3'-OH ends. In most TUNEL applications, mitotic cells can give false positive results. False negatives can also occur in certain cell types or situations where apoptosis does not lead to DNA laddering. Furthermore, the method is not quantitative since the amount of DNA fragments per cell is dependent upon the stage of apoptosis of the cell. In addition, this method is tedious, requires many steps and basic skills of molecular biology.

Another marker that is currently available is Annexin-V. During apoptosis, due to activation of the enzyme flippase, a cell membrane's phospholipid asymmetry changes such that the phospholipids of the inner membrane are exposed on the outer membrane (Fadok et al., 1992). Annexins are a homologous group of proteins that bind these phospholipids in the presence of calcium. This marker, however, suffers from a number of problems. Annexin-based tests have a strong potential for a lack of specificity due to the fact that the binding reaction is not as specific as antigen-antibody binding reactions. As well, its use is often limited to cells grown in suspension, however, most cells are adherent and are grown on a matrix. The method also requires the use of live or unpreserved cells.

There is therefore a great need for a specific, antigenic, versatile marker for the rapid detection of cell death by apoptosis, which can be used for research, diagnostics, and therapeutics. This marker must be able to distinguish between cell death by apoptosis and other known states of cells, which includes quiescence, proliferation (composed of G1, S, G2 and mitosis phases), and senescence. Essential requirements for apoptosis detection techniques include

high sensitivity for apoptotic cells, the ability to differentiate between apoptosis and other forms of cellular states. However, there is a relative paucity for simple techniques fulfilling these requirements, and furthermore allowing quantitative analysis (van Heerde WL. et al., 2000). Immunological detection of apoptosis-related proteins is probably the best approach to overcome this obstacle, but there are only a few known apoptosis marker antigens (Stadelmann C. and Lassmann H., 2000).

The anti-NAPO antibody recognizes the nuclear antigen “NAPO” that comprises two proteins of about 60 kD and 70 kD. As analyzed by indirect immunofluorescence microscopy, this antigen is present in all normal and cancerous human cell types tested including epithelial, lymphoid and fibroblastic cells as well as in all different states of a cell namely quiescence, proliferation (composed of G1, S, G2 and mitosis phases) and senescence. In contrast, the antibody fails to label cells undergoing apoptosis regardless the apoptosis-inducing stimuli.

The use of anti-NAPO antibody to detect apoptosis has numerous advantages over other methods that are currently commercially available. First of all usage of the anti-NAPO antibody offers the specificity of the antibody-antigen interaction. Furthermore the use of anti-NAPO antibody can distinguish cells that are dead or dying by apoptosis, from those that are viable, quiescent, proliferating, mitotic or senescent; thus provide reliable results. Most cell death kits currently available on the market are based on markers present in apoptotic, but absent in viable cells. NAPO is a marker with opposite features meaning that it is a marker present in viable, but absent in apoptotic cells. It can easily be used in combination with currently available kits to increase test specificity and for confirmation.

Furthermore the protocols used by current products are time consuming and require sophisticated laboratory equipment and expertise. A further advantage of use of the anti-NAPO antibody is that it can be used with a choice of qualitative and quantitative protocols adaptable to various laboratory equipment and expertise. For example, it can be applied using common laboratory techniques such as ELISA and immunochemistry where no specialized laboratory equipment is required. It can also be applied using specialized equipment such as a flow cytometer.

Therefore the mouse monoclonal anti-NAPO antibody can be used in the detection and quantification of cell apoptosis as well as to distinguish apoptotic cells from quiescent, proliferating, mitotic and senescent cells. This antibody can also be used as a valuable diagnostic tool in research relating to diseases in which apoptosis is involved to test the ability of cells to undergo apoptosis upon treatment with a selected agent and for testing the ability of a drug to induce or to inhibit apoptosis. Thus it can serve both to determine the mechanisms of the diseases and method of treatment.

For example, anti-NAPO antibody could be used in cancer research, where a potential chemotherapeutic drug could be tested for its ability to induce apoptosis. This could be done by exposing a cell sample to different concentrations of the test drug. The cells would then be analyzed for the presence of NAPO using the anti-NAPO antibody. The ability of the chemotherapeutic test drug to induce apoptosis could be determined and compared to the apoptosis induction of well-known drugs. Additionally, anti-NAPO antibody could be used as markers to assess the dose response of cells to chemotherapeutic drugs in order to determine ideal dosages for treatment.

The anti-NAPO antibody could also be used in the basic research and drug development for neurodegenerative disorders such as Alzheimer's disease and Parkinson's disease, including neuronal post-ischemic damage in stroke. For example, cells could be treated with an apoptosis inhibitor test drug at different concentrations and at different times post-apoptosis induction. Cells would then be collected at chosen times after the introduction of the test drug. The anti-NAPO antibody would provide a method of assessing the drug's apoptosis inhibitory potency. It would also allow determination of the stage of apoptosis at which the test drug has an inhibitory effect and the stage at which the drug is no longer effective.

The high specificity of the anti-NAPO antibody in recognition of apoptosis enables the usage of the antibody in identification of the extent of damage caused by a particular disease such as diseases caused by apoptosis due to post-ischemic neuronal damage. The TUNEL method has proven to be an inadequate marker for estimation of neuronal damage by necrosis versus apoptosis within in vivo and in vitro models. With the anti-NAPO antibody, however, it would be possible not only to quantify the severity of the damage

caused by ischemia but also the proportion of cell death that was caused by apoptosis at various time points. This knowledge is important for designing and monitoring apoptosis inhibitor drug therapies, especially in terms of effectiveness, doses, and treatment schedule of the drugs. The same strategy could also be applied to neurodegenerative diseases.

As a summary the anti-NAPO antibody can be used for the detection and quantification of apoptosis as well as to test the ability of drugs to modulate apoptosis in cell culture systems.

The anti-NAPO antibody can also be used in combination with other apoptotic markers such as TUNEL or Annexin-V staining for better definition of apoptotic cells in the same sample. Following staining with Annexin V, cells can be fixed and permeabilized and stained with anti-NAPO antibody. Cells in which a decrease or loss of NAPO immunoreactivity is observed combined with a positive Annexin V staining indicates apoptotic cells; cells in which NAPO levels are not decreased/not lost in combination with a negative Annexin V reading indicates viable cell.

However the anti-NAPO antibody based apoptosis detection system should also be tested in tissue sections by immunohistochemistry. As the NAPO system stains living cells but not apoptotic cells, utilization of this system in tissue sections, in combination with another apoptosis marker that stains apoptotic cells but not living cells, will provide more accurate and reliable data about the rate of apoptosis in that particular tissue section.

Although the nature of the epitope/antigen recognized by the anti-NAPO antibody is still unknown, determination of the stage of apoptosis, where the NAPO immunoreactivity is lost, would provide valuable information about the nature of the antigen recognized by the anti-NAPO antibody. For this purpose after cells are induced to undergo apoptosis the decline in NAPO expression can be assessed by FACS analysis. Usage of caspase inhibitors followed by NAPO staining would also provide data about the stage of NAPO immunoreactivity loss as well as data about the effect of caspase cascade activation on the NAPO epitope loss.

The effect of NAPO expression/loss on apoptosis can also be identified by inhibiting the NAPO antigen activity, by microinjecting the anti-NAPO antibody to cells. Following microinjection if apoptosis is induced this would mean that

the NAPO antigen is a protein involved in the prevention of apoptosis (acts like a pro-survival factor) and its loss promotes apoptosis. This experiment would provide an evidence about the importance of NAPO loss during apoptosis.

Furthermore the NAPO antigen recognized by the anti-NAPO antibody could be tried to be purified and identified by using affinity-chromatography, followed by micro-sequencing or mass spectrophotometry. The collected data would be analysed *in-silico* on the protein databases and the candidate proteins would be evaluated.

## **CHAPTER VII**

### **REFERENCES**

- Adrain C. and Martin SJ., **“The mitochondrial apoptosome: A killer unleashed by the cytochrome seas.”**  
Trends Biochem. Sci., vol:26, pp:390–397, 2001.
- Ahmad M., Srinivasula SM., Wang L., Talanian RV., Litwack G., Fernandes-Alnemri T. and Alnemri ES., **“CRADD, a novel human apoptotic adaptor molecule for caspase-2, and FasL/tumor necrosis factor receptor-interacting protein RIP.”**  
Cancer Research, vol:57, pp:615–619, 1997.
- Antonsson B, Conti F, Ciavatta A, Montessuit S, Lewis S, Martinou I, Bernasconi L, Bernard A, Mermoud JJ, Mazzei G, Maundrell K, Gambale F, Sadoul R and Martinou JC., **“Inhibition of Bax channel-forming activity by Bcl-2.”**  
Science, vol:277, pp:370-372, 1997.
- Ashhab Y., Alian A., Polliack A., Panet A., and Yehuda, DB., **“Two splicing variants of a new inhibitor of apoptosis gene with different biological properties and tissue distribution pattern.”**  
FEBS Lett., vol:495, pp:56–60, 2001.
- Ashkenazi A. and Dixit VM., **“Death receptors: Signaling and modulation.”**  
Science, vol:281, pp:1305–1308, 1998.
- Bartke T., Siegmund D., Peters N., Reichwein M., Henkler F., Scheurich P., and Wajant H., **“p53 upregulates cFLIP, inhibits transcription of NF- $\kappa$ B-regulated genes and induces caspase-8- independent cell death in DLD-1 cells.”**  
Oncogene, vol:20, pp:571–580, 2001.
- Bernardi P., Scorrano L., Colonna R, Petronilli V, Di Lisa F., **“Mitochondria and cell death. Mechanistic aspects and methodological issues.”**  
Eur. J. Biochem., vol:264, pp:687-701, 1999.

- Bialik S., Cryns VL., Drincic A., Miyata S., Wollowick AL., Srinivasan A. and Kitsis RN., **“The mitochondrial apoptotic pathway is activated by serum and glucose deprivation in cardiac myocytes.”**  
Circ. Res., vol:85, pp:403-414, 1999.
- Blagosklonny MV., **“Unwinding the loop of Bcl-2 phosphorylation.”**  
Leukemia, vol:15, pp:869–874, 2001.
- Bodmer JL., Holler N., Reynard S., Vinciguerra P., Schneider P., Juo P., Blenis J. and Tschopp J., **“TRAIL receptor-2 signals apoptosis through FADD and caspase-8.”**  
Nature Cell Biol., vol:2, pp:241-243, 2000.
- Boldin M., Goncharov T., Golstev Y. and Wallach D., **“Involvement of MACH, a novel MORT1/FADD-interacting protease, in Fas/APO-1- and TNF receptor-induced cell death.”**  
Cell, vol:85, pp: 803-815, 1996.
- Bonni A., Brunet A., West AE., Datta SR., Takasu MA., and Greenberg ME., **“Cell survival promoted by the Ras-MAPK signaling pathway by transcription-dependent and –independent mechanisms.”**  
Science, vol:286, pp:1358–1362, 1999.
- Borner C, Martinou I, Mattmann C, Irmeler M, Schaerer E, Martinou JC and Tschopp J., **“The protein bcl-2 alpha does not require membrane attachment, but two conserved domains to suppress apoptosis.”**  
J. Cell Biol., vol:126, pp:1059-1068, 1994.
- Brown DA. and Rose JK., **“Sorting of GPI-anchored proteins to glycolipid-enriched membrane subdomains during transport to the apical cell surface.”**  
Cell, vol:68, pp:533-544, 1992.
- Campisi J., Morreo G. and Pardee AB., **“Kinetics of G1 transit following brief starvation for serum factors.”**  
Exp. Cell Res., vol:152, pp:459-466, 1984.
- Chai J., Shiozaki E., Srinivasula SM., Wu Q., Datta P., Alnemri ES., and Shi Y., **“Structural basis of caspase-7 inhibition by XIAP.”**  
Cell, vol:104, pp:769–780, 2001.
- Chau BN., Cheng EH., Kerr DA. and Hardwick JM., **“Aven, a novel inhibitor of caspase activation, binds Bcl-XL and Apaf-1.”**  
Mol.Cell, vol:6, pp:31-40, 2000.
- Chang BS, Minn AJ, Muchmore SW, Fesik SW and Thompson CB., **“Identification of a novel regulatory domain in Bcl-X(L) and Bcl-2.”**  
EMBO J., vol:16, pp:968-977, 1997.

- Cheng EH, Levine B, Boise LH, Thompson CB and Hardwick JM., **“Bax-independent inhibition of apoptosis by Bcl-XL.”**  
Nature, vol:379, pp:554-556, 1998.
- Cheng EH, Kirsch DG, Clem RJ, Ravi R, Kastan MB, Bedi A, Ueno K and Hardwick JM., **“Conversion of Bcl-2 to a Bax-like death effector by caspases.”**  
Science, vol:278, pp:1966-1968, 1997.
- Chervonsky AV., **“Apoptotic and effector pathways in autoimmunity.”**  
Curr. Opin. Immunol., vol:11, pp:684-688, 1999.
- Chinnaiyan AM., O'Rourke K., Lane BR. and Dixit VM., **“Interaction of CED-4 with CED-3 and CED-9: a molecular framework for cell death.”**  
Science, vol:275, pp:1122-1126, 1997.
- Chinnaiyan AM., Prasad U., Shankar S., Hamstra DA., Shanaiah M., Chenevert TL., Ross BD., Rehemtulla A., **“Combined effect of tumor necrosis factor-related apoptosis-inducing ligand and ionizing radiation in breast cancer therapy.”**  
Proc. Natl. Acad. Sci. USA, vol:97, pp:1754-1759, 2000.
- Coller HA., Grandori C., Tamayo P., Colbert T., Lander ES., Eisenman RN. and Golub TR., **“Expression analysis with oligonucleotide microarrays reveals that MYC regulates genes involved in growth, cell cycle, signaling, and adhesion.”**  
Proc. Natl. Acad. Sci. USA, vol:97, pp:3260-3265, 2000.
- Cortese JD., Voglino AL. and Hackenbrock CR., **“Multiple conformations of physiological membrane-bound cytochrome c.”**  
Biochemistry, vol:37, pp:6402-6409, 1998.
- Daugas E., Nochy D., Ravagnan L., Loeffler M., Susin SA., Zamzami N. and Kroemer G., **“Apoptosis-inducing factor (AIF): a ubiquitous mitochondrial oxidoreductase involved in apoptosis.”**  
Febs Letters, vol: 476, pp:118-123, 2000.
- Deigner HP, Haberkorn U, Kinscherf R., **“Apoptosis modulators in the therapy of neurodegenerative diseases.”**  
Expert Opin. Investig. Drugs, vol:9, pp:747-764, 2000.
- del Peso L., Gonzalez-Garcia M., Page C., Herrera R. and Nunez G., **“Interleukin-3-induced phosphorylation of BAD through the protein kinase Akt.”**  
Science, vol:278, pp:687-689, 1997.
- Deveraux, QL., and Reed, JC., **“IAP family proteins-suppressors of apoptosis.”**  
Genes Dev., vol:13, pp:239-252, 1999.

- Dimri GP., Lee X., Basile G., Acosta M., Scott G., Roskelley C., Medrano EE., Linskens M., Rubelj I., Pereira-Smith O., Peacocke M. and Campisi J., **“A biomarker that identifies senescent human cells in culture and in aging skin in vivo.”**  
Proc. Natl. Acad. Sci. USA, vol:92, pp:9363-9367, 1995.
- Du C., Fang M., Li Y., Li L. and Wang X., **“Smac, a mitochondrial protein that promotes cytochrome c-dependent caspase activation by eliminating IAP inhibition.”**  
Cell, vol:102, pp:33-42, 2000.
- Duan, H. and Dixit, VM., **“RAIDD is a new ‘death’ adaptor molecule.”**  
Nature, vol:385, pp:86–89, 1997.
- Earnshaw, WC., Martins, LM., and Kaufmann, SH., **“Mammalian caspases: structure, activation, substrates, and functions during apoptosis.”**  
Annu. Rev. Biochem., vol:68, pp:383–424, 1999.
- Eischen CM., Dick CJ. and Leibson PJ., **“Tyrosine kinase activation provides an early and requisite signal for Fas-induced apoptosis.”**  
J. Immunol., vol:153, pp:1947-1954, 1994.
- Ellis HM. and Horvitz HR., **“Genetic control of programmed cell death in the nematode *C. elegans*.”**  
Cell, vol:44, pp:817-829, 1986.
- Eskes R., Desagher S., Antonsson B. and Martinou JC., **“Bid induces the oligomerization and insertion of Bax into the outer mitochondrial membrane.”**  
Mol.Cell. Biol., vol:20, pp:929-935, 2000.
- Fadok VA., Savill JS., Haslett C., Bratton DL., Doherty DE., Campbell PA. and Henson PM., **“Different populations of macrophages use either the vitronectin receptor or the phosphatidylserine receptor to recognize and remove apoptotic cells.”**  
J. Immunol., vol:149, pp:4029-4035, 1992.
- Freude B., Masters TN., Robicsek F., Fokin A., Kostin S., Zimmermann R., Ullmann C., Lorenz-Meyer S. and Schaper J., **“Apoptosis is initiated by myocardial ischemia and executed during reperfusion.”**  
J. Mol. Cell Cardiol., vol:32, pp:197-208, 2000.
- Fulder SJ. and Holliday RA., **“Rapid rise in cell variants during the senescence of populations of human fibroblasts.”**  
Cell, vol:6, pp:67-73, 1975.
- Gougeon ML. and Montagnier L., **“Programmed cell death as a mechanism of CD4 and CD8 T cell deletion in AIDS. Molecular control and effect of highly active anti-retroviral therapy.”**  
Ann. NY Acad. Sci., vol:887, pp:199-212, 1999.

- Gavrieli Y., Sherman Y. and Ben-Sasson SA., **“Identification of programmed cell death in situ via specific labelling of nuclear DNA fragmentation.”**  
J. Cell Biol., vol:119, pp: 493-501, 1992.
- Gibson SB., Oyer R., Spalding AC., Anderson SM. and Johnson GL., **“Increased expression of death receptors 4 and 5 synergizes the apoptosis response to combined treatment with etoposide and TRAIL.”**  
Mol. Cell. Biol., vol:20, pp:205-212, 2000.
- Gogvadze V., Robertson JD., Zhivotovsky B. and Orrenius S., **“Cytochrome c release occurs via Ca<sup>2+</sup>-dependent and Ca<sup>2+</sup>-independent mechanisms that are regulated by Bax.”**  
J. Biol. Chem., vol:276, pp:19066-19701, 2001.
- Goldstein JC., Waterhouse NJ., Juin P., Evan GI. and Green DR., **“The coordinate release of cytochrome c during apoptosis is rapid, complete and kinetically invariant.”**  
Nature Cell Biol., vol:2, pp:156-162, 2000.
- Golstein P., **“Cell death: TRAIL and its receptors.”**  
Curr. Biol., vol:7, pp:R750-R753, 1997.
- Goltsev YV., Kovalenko AV., Arnold E., Varfolomeev EE., Brodianskii VM. and Wallach D., **“CASH, a novel caspase homologue with death effector domains.”**  
J. Biol. Chem., vol:272, pp:19641-19644, 1997.
- Gorbenko GP., **“Structure of cytochrome c complexes with phospholipids as revealed by resonance energy transfer.”**  
Biochim. Biophys. Acta., vol:1420, pp:1-13, 1999.
- Gottlieb R.A., **“Mitochondria: execution central.”**  
FEBS Letters, vol:482, pp:6-12, 2000.
- Grand RJ., Milner AE., Mustoe T., Johnson GD., Owen D., Grant ML. and Gregory CD., **“A novel protein expressed in mammalian cells undergoing apoptosis.”**  
Exp. Cell Res., vol: 218, pp:439-451, 1995.
- Grandgirard D, Studer E, Monney L, Belser T, Fellay I, Borner C and Michel MR., **“Alphaviruses induce apoptosis in Bcl-2-overexpressing cells: evidence for a caspase-mediated, proteolytic inactivation of Bcl-2.”**  
EMBO J., vol:17, pp:1268-1278, 1998.
- Green DR., **“Apoptotic pathways: paper wraps stone blunts scissors.”**  
Cell, vol:102, pp:1-4, 2000.

- Grell M., Zimmermann G., Gottfried E., Chen CM., Grunwald U., Huang DC., Wu Lee YH., Durkop H., Engelmann H., Scheurich P, Wajant H. and Strasser A., **“Induction of cell death by tumour necrosis factor (TNF) receptor 2, CD40 and CD30: a role for TNF-R1 activation by endogenous membrane-anchored TNF.”**  
EMBO J., vol:18, pp:3034-3043, 1999.
- Gross A., Jockel J., Wei MC. and Korsmeyer SJ., **“Enforced dimerization of BAX results in its translocation, mitochondrial dysfunction and apoptosis.”**  
EMBO J., vol:17, pp:3878-3885, 1998.
- Gura T., **“How TRAIL kills cancer cells, but not normal cells.”**  
Science, vol:277, pp:768, 1997.
- Hajjar RJ, del Monte F., Matsui T. and Rosenzweig A., **“Prospects for gene therapy for heart failure.”**  
Circulation Research., vol:86, pp:616-621, 2000.
- Haldar S, Jena N and Croce CM., **“Inactivation of Bcl-2 by phosphorylation.”**  
Proc. Natl. Acad. Sci. U S A, vol:92, pp:4507-4511, 1995.
- Haldar S, Chintapalli J and Croce CM., **“Taxol induces bcl-2 phosphorylation and death of prostate cancer cells.”**  
Cancer Res., vol:56, pp:1253-1255, 1996.
- Hammond EM., Brunet CL., Johnson GD., Parkhill J., Milner AE., Brady G., Gregory CD. and Grand RJ., **“Homology between a human apoptosis specific protein and the product of APG5, a gene involved in autophagy in yeast.”**  
FEBS Lett., vol:425, pp:391-395, 1998.
- Han DK., Chaudhary PM., Wright ME., Friedman C., Trask BJ., Riedel RT., Baskin DG., Schwartz SM. and Hood L., **“MRIT, a novel death-effector domain containing protein, interacts with caspases and BclXL and initiates cell death.”**  
Proc. Natl. Acad. Sci. USA, vol:94, pp:11333-11338, 1997.
- Hanahan D., and Weinberg RA., **“The hallmarks of cancer.”**  
Cell, vol:100, pp:57–70, 2000.
- Harada H, Backnell B, Wilm M, Mann M, Huang L.J., Taylor S.S. and Korsmeyer S.J., **“Phosphorylation and inactivation of BAD by mitochondrial-anchored protein kinase-A.”**  
Mol. Cell, vol:3, pp:413-422, 1999.
- Harada H., Andersen JS., Mann M., Terada N. and Korsmeyer SJ., **“p70S6 kinase signals cell survival as well as growth, inactivating the pro-apoptotic molecule BAD.”**  
Proc. Natl. Acad. Sci. USA, vol:98, pp:9666–9670, 2001.

- Haunstetter A and Izumo S., **“Future perspectives and potential implications of cardiac myocyte apoptosis.”**  
Cardiovasc. Res., vol:45, pp:795-801, 2000.
- Hayashi T. and Faustman D L., **“Implications of altered apoptosis in diabetes mellitus and autoimmune disease.”**  
Apoptosis, vol:6, pp:31–45, 2001.
- Hengartner MO., Ellis RE. and Horvitz HR., **“Caenorhabditis elegans gene ced-9 protects cells from programmed cell death.”**  
Nature, vol:356, pp:494-499, 1992.
- Herr I., and Debatin KM., **“Cellular stress response and apoptosis in cancer therapy.”**  
Blood, vol:98, pp:2603–2614, 2001.
- Hoffman WH., Biade S., Zilfou JT., Chen J. and Murphy, M., **“Transcriptional repression of the anti-apoptotic survivin gene by wild type p53.”**  
J. Biol. Chem., vol:19, pp:19, 2001.
- Hsu YT., Wolter KG. and Youle RJ., **“Cytosol-to-membrane redistribution of Bax and Bcl-X(L) during apoptosis.”**  
Proc. Natl. Acad. Sci. U S A, vol:94, pp: 3668-3672, 1997.
- Hu S., Vincenz C., Ni J., Gentz R. and Dixit VM., **“I-FLICE, a novel inhibitor of tumor necrosis factor receptor-1- and CD-95-induced apoptosis.”**  
J. Biol. Chem., vol:272, pp:17255-17257, 1997.
- Huang, DC. and Strasser, A., **“BH3-Only proteins-essential initiators of apoptotic cell death.”**  
Cell, vol: 103, pp: 839–842, 2000.
- Huang HK., Joazeiro CAP., Bonfoco E., Kamada S., Levenson JD., and Hunter T. **“The inhibitor of apoptosis, cIAP2, functions as a ubiquitin-protein ligase and promotes in vitro monoubiquitination of caspase 3 and 7.”**  
J. Biol. Chem., vol:275, pp:26661–26664, 2000.
- Huang Y., Park YC., Rich RL., Segal D., Myszka DG., and Wu H., **“Structural basis of caspase inhibition by XIAP: differential roles of the Linker versus the BIR domain.”**  
Cell, vol:104, pp:781–790, 2001.
- Huang P and Oliff A., **“Signaling pathways in apoptosis as potential targets for cancer therapy.”**  
Trends Cell Biol., vol:11, pp:343-348, 2001.
- Hueber AO., Zornig M., Lyon D., Suda T., Nagata S., and Evan GI., **“Requirement for the CD95 receptor-ligand pathway in c-myc induced apoptosis.”**  
Science, vol:278, pp:1305-1308, 1997.

- Hughes DP. and Crispe IN., **“A naturally occurring soluble isoform of murine Fas generated by alternative splicing.”**  
Exp. Med., vol:182, pp:1395-1401, 1995.
- Hunter JJ and Parslow TG., **“A peptide sequence from Bax that converts Bcl-2 into an activator of apoptosis.”**  
J Biol Chem., vol: 271, pp: 8521-8524, 1996.
- Inohara N., Koseki T., Hu Y., Chen S. and Nunez G., **“CLARP, a death effector domain-containing protein interacts with caspase-8 and regulates apoptosis.”**  
Proc. Natl. Acad. Sci. USA, vol:94, pp:10717-10722, 1997.
- Inoue J., Ishida T., Tsukamoto N., Kobayashi N., Naito A., Azuma S. and Yamamoto T., **“Tumor necrosis factor receptor-associated factor (TRAF) family: adapter proteins that mediate cytokine signaling.”**  
Exp. Cell Res., vol:254, pp:14-24, 2000.
- Irizarry MC. and Hyman BT., **“Alzheimer disease therapeutics.”**  
J Neuropathol Exp Neurol., vol:60, pp:923-928, 2001.
- Irmeler M., Thome M., Hahne M., Schneider P., Hofman K., Steiner V., Bodmer JL., Schroter M., Burns K., Mattmann C., Rimoldi D., French LE. and Tschopp J., **“Inhibition of death receptor signals by cellular FLIP.”**  
Nature, vol:388, pp:190-195, 1997.
- Itoh N. and Nagata S., **“A novel protein domain required for apoptosis. Mutational analysis of human Fas antigen.”**  
J. Biol. Chem., vol:268, pp: 10932-10937, 1993.
- Jeremias I., Kupatt C., Martin-Villalba A., Habazettl H., Schenkel J., Boekstegers P. and Debatin KM., **“Involvement of CD95/Apo1/Fas in cell death after myocardial ischemia.”**  
Circulation, vol:102, pp:915-920, 2000.
- Jo M., Kim TH., Seol DW., Esplen JE., Dorko K., Billiar TR. and Strom SC., **“Apoptosis induced in normal human hepatocytes by tumor necrosis factor-related apoptosis-inducing ligand.”**  
Nature Med., vol:6, pp:564-567, 2000.
- Johnstone RW., Ruefli AA. and Lowe SW., **“Apoptosis: A Link between Cancer Genetics and Chemotherapy.”**  
Cell, vol:108, pp:153-164, 2002.
- Joza N., Susin SA., Daugas E., Stanford WL., Cho SK., Li CY., Sasaki T., Elia AJ., Cheng HY., Ravagnan L., Ferri KF., Zamzami N., Wakeham A., Hakem R., Yoshida H., Kong YY., Mak TW., Zuniga-Pflucker JC., Kroemer G. and Penninger JM., **“Essential role of the mitochondrial apoptosis-inducing factor in programmed cell death.”**  
Nature, vol:410, pp:549-554, 2001.

- Kasof GM. and Gomes BC., **“Livin, a novel inhibitor of apoptosis protein family member.”**  
J. Biol. Chem., vol:276, pp:3238–3246, 2001.
- Khanna KK., and Jackson SP., **“DNA double-strand breaks: signaling, repair and the cancer connection.”**  
Nat. Genet., vol:27, pp:247–254, 2001.
- Kischkel FC., Hellbardt S., Behrmann I., Germer M., Pawlita M., Krammer PH. and Peter ME., **“Cytotoxicity-dependent APO-1 (Fas/CD95)-associated proteins form a death-inducing signalling complex (DISC) with the receptor.”**  
EMBO J., vol:14, pp: 5579-5588, 1995.
- Krajewski, S., Tanaka, S., Takayama, S., Schibler, M. J., Fenton, W., and Reed, J. C., **“Investigation of the subcellular distribution of the bcl-2 oncoprotein: residence in nuclear envelope, endoplasmic reticulum, and outer mitochondrial membranes.”**  
Cancer Res., vol:53, pp:4701–4714, 1993.
- Kroemer G. and Reed JC., **“Mitochondrial control of cell death.”**  
Nat. Med., vol:6, pp:513–519, 2000.
- Lee SY., Lee SY. and Choi Y., **“TRAF-interacting protein (TRIP): a novel component of the tumor necrosis factor receptor (TNFR)- and CD30-TRAF signaling complexes that inhibits TRAF2-mediated NF-kappa B activation.”**  
J. Exp. Med., vol:185, pp:1275-1285, 1997.
- Leers MP., Kolgen W., Bjorklund V., Bergman T., Tribbick G., Persson B., Bjorklund P., Ramaekers FC., Bjorklund B., Nap M., Jornvall H. and Schutte B., **“Immunocytochemical detection and mapping of a cytokeratin 18 neo-epitope exposed during early apoptosis.”**  
J. Pathol., vol:187, pp:567-572, 1999.
- Li H., Zhu H., Xu CJ. and Yuan J., **“Cleavage of BID by caspase 8 mediates the mitochondrial damage in the Fas pathway of apoptosis.”**  
Cell, vol:94, pp:491-501, 1998.
- Lin Y., Devin A., Rodriguez Y. and Liu ZG., **“Cleavage of the death domain kinase RIP by caspase-8 prompts TNF-induced apoptosis.”**  
Genes Dev., vol:13, pp:2514-2526, 1999.
- Lithgow, T., van Driel, R., Bertram, JF., and Strasser, A., **“The protein product of the oncogene bcl-2 is a component of the nuclear envelope, the endoplasmic reticulum, and the outer mitochondrial membrane.”**  
Cell Growth Diff., vol:5, pp:411–417, 1994.
- Lowe S.W. and Lin A.W., **“Apoptosis in cancer.”**  
Carcinogenesis, vol:21, pp:485-495, 2000.

- Luo X., Budihardjo I., Zou H., Slaughter C. and Wang X., **“Bid, a Bcl2 interacting protein, mediates cytochrome c release from mitochondria in response to activation of cell surface death receptors.”**  
Cell, vol:94, pp:481-490, 1998.
- Malinin NL., Boldin MP., Kovalenko AV. and Wallach D., **“MAP3K-related kinase involved in NF-kappa B induction by TNF, CD95 and IL-1.”**  
Nature, vol:385, pp:540-544, 1997.
- Martin, SJ., Reutelingsperger CP., McGahon AJ., Rader JA., van Schie RC., LaFace DM. and Green DR., **“Early redistribution of plasma membrane phosphatidylserine is a general feature of apoptosis regardless of the initiating stimulus: inhibition by overexpression of Bcl-2 and Abl.”**  
J. Exp. Med., vol:182, pp:1545-1556, 1995.
- Mannella CA, Buttle K, Rath BK and Marko M., **“Electron microscopic tomography of rat-liver mitochondria and their interaction with the endoplasmic reticulum.”**  
Biofactors, vol: 8, pp: 225-228, 1998.
- Martinou JC., Desagher S. and Antonsson B., **“Cytochrome c release from mitochondria: all or nothing.”**  
Nature Cell Biol., vol:2, pp:E41-E43, 2000.
- Martinou JC. and Green DR., **“Breaking the mitochondrial barrier.”**  
Nat. Rev. Mol. Cell Biol., vol:2, pp: 63–67, 2001.
- Marzo I., Brenner C., Zamzami N., Jurgensmeier JM., Susin SA., Vieira HL., Prevost MC., Xie Z., Matsuyama S., Reed JC. and Kroemer G., **“Bax and adenine nucleotide translocator cooperate in the mitochondrial control of apoptosis.”**  
Science, vol:281, pp:2027-2031, 1998.
- Mattson MP., **“Apoptosis in neurodegenerative disorders.”**  
Nat. Rev. Mol. Cell Biol., vol:1, pp:120-129, 2000.
- Maundrell K, Antonsson B, Magnenat E, Camps M, Muda M, Chabert C, Gillieron C, Boschert U, Vial-Knecht E, Martinou JC, Arkinstall S., **“Bcl-2 undergoes phosphorylation by c-Jun N-terminal kinase/stress-activated protein kinases in the presence of the constitutively active GTP-binding protein Rac1.”**  
J Biol Chem., vol:272, pp:25238-25242, 1997.
- Minn AJ, Velez P, Schendel SL, Liang H, Muchmore SW, Fesik SW, Fill M, and Thompson CB., **“Bcl-x(L) forms an ion channel in synthetic lipid membranes.”**  
Nature, vol:385, pp:353-357, 1997.

- Mitchell KO., Ricci MS., Miyashita T., Dicker DT., Jin Z., Reed JC. and El-Deiry WS., **“Bax is a transcriptional target and mediator of c-myc induced apoptosis.”**  
Cancer Res., vol:60, pp:6318-6325, 2000.
- Muchmore S.W., Sattler M., Liang H., Meadows R.P., Harlan J.E., Yoon H.S., Nettesheim D., Chang B.S., Thompson C.B., Wong S.L., Ng S.L. and Fesik S.W., **“X-ray and NMR structure of human Bcl-XL, an inhibitor of programmed cell death.”**  
Nature, vol:381, pp:335-341, 1996.
- Murray A. and Hunt T., **“Cell Cycle”**, W.H. Freeman and Comp.1<sup>st</sup> ed.,1993..
- Muzio M., Chinnaiyan A., Kischel FC., O'Rourke K., Shevchenko A., Ni J., Scaffidi C., Bretz JD., Zhang M., Gentz R., Mann M., Krammer P., Peter M. and Dixit V., **“FLICE, a novel FADD-homologous ICE/CED-3-like protease, is recruited to the CD95 (Fas/APO-1) death-inducing signaling complex.”**  
Cell, vol:85, pp:817-827, 1996.
- Nagata S., **“Steering anti-cancer drugs away from the TRAIL.”**  
Nature Med., vol:6, pp:502-503, 2000.
- Narula J., Pandey P., Arbustini E., Haider N., Narula N., Kolodgie F.D., Dal Bello B., Semigran MJ., Bielsa-Masdeu A., Dec GW., Israels S., Ballester M., Virmani R., Saxena S. and Kharbanda S., **“Apoptosis in heart failure: release of cytochrome c from mitochondria and activation of caspase-3 in human cardiomyopathy.”**  
Proc. Natl. Acad. Sci. USA, vol:96, pp:8144-819, 1999.
- Narula, J., Kolodgie F.D. and Virmani R., **“Apoptosis and cardiomyopathy.”**  
Curr. Opin. Cardiol., vol:15, pp:183-188, 2000.
- Nurse P., **“A Long Twentieth Century of the Cell Cycle and Beyond.”**  
Cell, vol:100, pp: 71–78, 2000.
- Oberhammer F., Wilson J., Dive C., Morris I., Hickman J., Wakeling A., Walker P. and Sikorska M., **“Apoptotic death in epithelial cells: cleavage of DNA to 300 and/or 50 kb fragments prior to or in the absence of internucleosomal fragmentation.”**  
EMBO J., vol:12, pp:3679-3684, 1993.
- Oltvai ZN., Milliman CL. and Korsmeyer SJ., **“Bcl-2 heterodimerizes in vivo with a conserved homolog, Bax, that accelerates programmed cell death.”**  
Cell, vol:74, pp:609-619, 1993.
- Ott M., Robertson JD., Gogvadze V., Zhivotovsky B. and Orrenius S., **“Cytochrome c release from mitochondria proceeds by a two step process.”**  
Proc. Natl. Acad. Sci. USA, vol:99, pp:1259-1263, 2002.

- Ozturk M., Motte P., Takahashi H., Frohlich M., Wilson B., Hill L., Bressac B. and Wands J.R., **“Identification and characterization of a Mr 50,000 adrenal protein in human hepatocellular carcinoma.”**  
Cancer Res., vol: 49, pp:6764-6773, 1989.
- Pavlov EV., Priault M., Pietkiewicz D., Cheng EH-Y., Antonsson B., Manon S., Korsmeyer SJ., Mannella CA. and Kinnally KW., **“A novel, high conductance channel of mitochondria linked to apoptosis in mammalian cells and Bax expression in yeast.”**  
J. Cell Biol., vol:155, pp:719-724, 2001.
- Pimentel-Muinos FX. and Seed B., **“Regulated commitment of TNF receptor signaling: a molecular switch for death or activation.”**  
Immunity, vol:11, pp:783-793, 1999.
- Pinton P., Ferrari D., Rapizzi E., Di Virgilio F., Pozzan T. and Rizzuto R., **“A role for calcium in Bcl-2 action?”**  
Biochimie, vol:84, pp:195-201, 2002.
- Pitti RM., Marsters SA., Ruppert S., Donahue CJ., Moore A. and Ashkenazi A., **“Induction of apoptosis by Apo-2 ligand, a new member of the tumor necrosis factor cytokine family.”**  
J. Biol. Chem., vol:271, pp:12687-12690, 1996.
- Puthalakath H., Huang DC., O'Reilly LA., King SM. and Strasser A., **“The proapoptotic activity of the Bcl-2 family member Bim is regulated by interaction with the dynein motor complex.”**  
Mol Cell, vol:3, pp:287-296, 1999.
- Rasper DM., Vaillancourt JP., Hadano S., Houtzager VM., Seiden I., Keen SL., Tawa P., Xanthoudakis S., Nasir J., Martindale D., Koop BF., Peterson EP., Thornberry NA., Huang J., MacPherson DP., Black SC., Hornung F., Lenardo MJ., Hayden MR., Roy S. and Nicholson DW., **“Cell death attenuation by 'Usurpin', a mammalian DED-caspase homologue that precludes caspase-8 recruitment and activation by the CD-95 (Fas, APO-1) receptor complex.”**  
Cell Death Differ., vol:5, pp:271-288, 1998.
- Reed CJ., **“Apoptosis and cancer: strategies for integrating programmed cell death.”**  
Semin. Hematol., vol:37, pp:9-16, 2000.
- Renatus M., Zhou Q., Stennicke HR., Snipas SJ., Turk D., Bankston LA., Liddington RC. and Salvesen GS., **“Crystal structure of the apoptotic suppressor CrmA in its cleaved form.”**  
Structure Fold Des., vol:8, pp:789-97, 2000.

- Riedl SJ., Renatus M., Schwarzenbacher R., Zhou Q., Sun C., Fesik SW., Liddington RC., and Salvesen GS., **“Structural basis for the inhibition of caspase-3 by XIAP.”**  
Cell, vol:104, pp:791–800, 2001.
- Rochat-Steiner V., Becker K., Micheau O., Schneider P., Burns K. and Tschopp J., **“FIST/HIPK3: a Fas/FADD-interacting serine/threonine kinase that induces FADD phosphorylation and inhibits fas-mediated Jun NH(2)-terminal kinase activation.”**  
J. Exp. Med., vol:192, pp:1165-1174, 2000.
- Roshal M., Zhu Y. and Planelles V., **“Apoptosis in AIDS.”**  
Apoptosis, vol: 6, pp:103-116, 2001.
- Rothe M., Wong SC., Henzel WJ. and Goeddel DV., **“A novel family of putative signal transducers associated with the cytoplasmic domain of the 75 kDa tumor necrosis factor receptor.”**  
Cell, vol:78, pp:681-692, 1994.
- Roulston, A., Marcellus R.C. and Branton P.E., **“Viruses and apoptosis.”**  
Annu Rev Microbiol., vol:53, pp:577-628, 1999.
- Ruvolo PP., Deng X., Carr BK. and May WS., **“A functional role for mitochondrial protein kinase C-alpha in Bcl2 phosphorylation and suppression of apoptosis.”**  
J Biol Chem., vol:273, pp:25436-25442, 1998.
- Ryan KM., Phillips AC. and Vousden KH., **“Regulation and function of p53 tumor suppressor protein.”**  
Curr. Opin. Cell Biol., vol:13, pp:332–337, 2001.
- Saraste A. and Pulkki K., **“Morphologic and biochemical hallmarks of apoptosis.”**  
Cardiovasc. Res., vol:45, pp:528-537, 2000.
- Satio M., Korsmeyer SJ. And Schlesinger PH., **“Bax-dependent transport of cytochrome c reconstituted in pure liposomes.”**  
Nat. Cell Biol., vol:2, pp:553-555, 2000.
- Scaffidi C., Schmitz I., Krammer PH. and Peter ME., **“The role of c-FLIP in modulation of CD95-induced apoptosis.”**  
J. Biol.Chem., vol:274, pp:1541-1548, 1999.
- Schendel SL, Xie Z, Montal MO, Matsuyama S, Montal M and Reed JC., **“Channel formation by antiapoptotic protein Bcl-2.”**  
Proc. Natl. Acad. Sci. U S A., vol: 94, pp: 5113-5118, 1997.
- Sherr CJ. and DePinho RA., **“Cellular senescence: mitotic clock or culture shock?”**  
Cell, vol:102, pp:407-410, 2000.

- Shimizu S., Narita M. and Tsujimoto Y., **“Bcl-2 family proteins regulate the release of apoptogenic cytochrome c by the mitochondrial channel VDAC.”**  
Nature, vol:399, pp:483-487, 1999.
- Shu HB., Halpin DR. and Goeddel DV., **“Casper is a FADD- and caspase-related inducer of apoptosis.”**  
Immunity, vol:6, pp:751-763, 1997.
- Slee EA., Harte MT., Kluck RM., Wolf BB., Casiano CA., Newmeyer DD., Wang HG., Reed JC., Nicholson DW., Alnemri ES., Green DR. and Martin SJ., **“Ordering the cytochrome c-initiated caspase cascade: hierarchical activation of caspases-2, -3, -6, -7, -8, and -10 in a caspase-9-dependent manner.”**  
J. Cell. Biol., vol:144, pp:281-292, 1999.
- Srinivasan A., Roth KA., Sayers RO., Shindler KS., Wong AM., Fritz LC. and Tomaselli KJ., **“In situ immunodetection of activated caspase-3 in apoptotic neurons in the developing nervous system.”**  
Cell Death Differ., vol:5, pp:1004-1016, 1998.
- Srinivasula SM., Ahmad M., Otilie S., Bullrich F., Banks S., Wang Y., Fernandes-Alnemri T., Croce CM., Litwack G., Tomaselli KJ., Armstrong RC. and Alnemri ES., **“FLAME-1, a novel FADD-like anti-apoptotic molecule that regulates Fas/TNFR1-induced apoptosis.”**  
J. Biol. Chem., vol:272, pp:18542-18545, 1997.
- Srinivasula SM., Ahmad M., Fernandes-Alnemri T. and Alnemri E.S., **“Autoactivation of procaspase-9 by Apaf-1-mediated oligomerization.”**  
Mol. Cell, vol:1, pp:949-957, 1998.
- Srinivasula SM., Saleh A., Hedge R., Datta P., Shiozaki E., Chai J., Robbins PD., Fernandes-Alnemri T., Shi Y. and Alnemri ES., **“A conserved XIAP-interaction motif in caspase-9 and Smac/DIABLO mediates opposing effects on caspase activity and apoptosis.”**  
Nature, vol:409, pp: 112–116, 2001.
- Stadelmann C. and Lassmann H., **“Detection of apoptosis in tissue sections.”**  
Cell Tissue Res., vol:301, pp:19-31, 2000.
- Stanger BZ., Leder P., Lee TH., Kim E. and Seed B., **“RIP: a novel protein containing a death domain that interacts with Fas/APO-1 (CD95) in yeast and causes cell death.”**  
Cell, vol:81, pp:513-523, 1995.
- Stiewe T. and Putzer BM., **“p73 in apoptosis.”**  
Apoptosis, vol:6, pp:447–452, 2001.

- Susin SA, Lorenzo HK, Zamzami N, Marzo I, Snow BE, Brothers GM, Mangion J, Jacotot E, Costantini P, Loeffler M, Larochette N, Goodlett DR, Aebersold R, Siderovski DP, Penninger JM and Kroemer G., **“Molecular characterization of mitochondrial apoptosis-inducing factor.”**  
Nature, vol: 397, pp: 441-446, 1999(a).
- Susin SA, Lorenzo HK, Zamzami N, Marzo I, Brenner C, Larochette N, Prevost MC, Alzari PM. and Kroemer G., **“Mitochondrial release of caspase-2 and -9 during the apoptotic process.”**  
J. Exp. Med., vol:189, pp:381-394, 1999(b).
- Suzuki Y., Nakabayashi Y. and Takahashi, R., **“Ubiquitin protein ligase activity of X-linked inhibitor of apoptosis protein promotes proteasomal degradation of caspase-3 and enhances its anti-apoptotic effect in Fas-induced cell death.”**  
Proc. Natl. Acad. Sci. USA, vol: 98, pp:8662–8667, 2001.
- Tartaglia LA., Pennica D. and Goeddel DV, **“Ligand passing: the 75-kDa tumor necrosis factor (TNF) receptor recruits TNF for signaling by the 55-kDa TNF receptor.”**  
J. Biol. Chem., vol:268, pp:18542-18548, 1993.
- Thome M., Schneider P., Hofmann K., Fickenscher H., Meinel E., Neipel F., Mattmann C., Burns K., Bodmer JL., Schroter M., Scaffidi C., Krammer PH., Peter ME. and Tschopp J., **“Viral FLICE-inhibitory proteins (FLIPs) prevent apoptosis induced by death receptors.”**  
Nature, vol:386, pp:517-521, 1997.
- Thornberry NA., Lazebnik Y., **“Caspase: enemies within.”**  
Science, vol:281, pp:1312-1316, 1998.
- Torre-Amione G., Kapadia S., Lee J., Durand JB., Bies RD., Young JB. and Mann DL., **“Tumor necrosis factor alpha and tumor necrosis factor receptors in the failing human heart.”**  
Circulation, vol:93, pp:704-711, 1996.
- Tsujimoto Y, Cossman J, Jaffe E and Croce CM., **“Involvement of the bcl-2 gene in human follicular lymphoma.”**  
Science, vol:228, pp:1440-1443, 1985.
- van Heerde WL., Robert-Offerman S., Dumont E., Hofstra L., Doevendans PA., Smits JF., Daemen MJ. and Reutelingsperger CP. **“Markers of apoptosis in cardiovascular tissues: focus on Annexin V.”**  
Cardiovasc. Res., vol:45, pp:549-559, 2000.
- Vander Heiden MG. and Thompson CB., **“Bcl-2 proteins: regulators of apoptosis or of mitochondrial homeostasis?”**  
Nature Cell Biol., vol:1, pp:E209-E216, 1999.

- Vaux DL. and Korsmeyer SJ., **“Cell death in development.”**  
Cell, vol:96, pp:245-254, 1999.
- Vaux DL. and Flavell RA., **“Apoptosis genes and autoimmunity.”**  
Curr Opin Immunol, vol:12, pp:719-724, 2000.
- Verhagen AM., Ekert PG., Pakusch M., Silke J., Connolly LM., Reid GE., Moritz RL., Simpson RJ. and Vaux DL., **“Identification of DIABLO, a mammalian protein that promotes apoptosis by binding to and antagonizing IAP proteins.”**  
Cell, vol:102, pp:43-53, 2000.
- Volkman M., Hofmann WJ., Muller M., Rath U., Otto G., Zentgraf H. and Galle PR., **“p53 overexpression is frequent in European hepatocellular carcinoma and largely independent of the codon 249 hot spot mutation.”**  
Oncogene, vol:9, pp:195-204, 1994.
- Vucic D., Stennicke HR., Pisabarro MT., Salvesen GS. and Dixit VM., **“ML-IAP, a novel inhibitor of apoptosis that is preferentially expressed in human melanomas.”**  
Curr. Biol., vol:10, pp:1359–1366, 2000.
- Walczak H., Miller RE., Ariail K., Gliniak B., Griffith TS., Kubin M., Chin W., Jones J., Woodward A., Le T., Smith C., Smolak P., Goodwin RG., Rauch CT., Schuh JC. and Lynch DH., **“Tumoricidal activity of tumor necrosis factor-related apoptosis-inducing ligand in vivo.”**  
Nature Med., vol:5, pp:157-163, 1999.
- Wallach D., **“Cell death induction by TNF: a matter of self control.”**  
Trends Biochem. Sci., vol:1997, pp:107-109, 1997.
- Wang X., **“The expanding role of mitochondria in apoptosis.”**  
Genes Dev., vol:15, pp:2922–2933, 2001.
- Wei MC., Lindsten T., Mootha VK., Weiler S., Gross A., Ashiya M., Thompson CB. and Korsmeyer SJ., **“tBID, a membrane-targeted death ligand, oligomerizes BAK to release cytochrome c.”**  
Genes Dev., vol:14, pp:2060-2071, 2000.
- Wei MC., Zong WX., Cheng EH., Lindsten T., Panoutsakopoulou V., Ross AJ., Roth KA., MacGregor GR., Thompson CB, and Korsmeyer SJ., **“Pro-apoptotic Bax and Bak: a requisite gateway to mitochondrial dysfunction and death.”**  
Science, vol:292, pp:727-730, 2001.
- Widmann C., Gibson S. and Johnson G.L., **“Caspase-dependent cleavage of signaling proteins during apoptosis. A turn-off mechanism for anti-apoptotic signals.”**  
J Biol Chem., vol:273, pp:7141-7147, 1998.

- Wolter KG., Hsu YT., Smith CL., Nechushtan A., Xi XG., Youle RJ., **“Movement of Bax from the cytosol to mitochondria during apoptosis.”**  
J Cell Biol., vol:139, pp:1281-1292, 1997.
- Wu Y., Mehew JW., Heckman CA., Arcinas M. and Boxer LM., **“Negative regulation of bcl-2 expression by p53 in hematopoietic cells.”**  
Oncogene, vol:20, pp:240–251, 2001.
- Wyllie AH., **“Glucocorticoid-induced thymocyte apoptosis is associated with endogenous endonuclease activation.”**  
Nature, vol:284, pp:555-556, 1980.
- Wyllie AH. and Golstein P., **“More than one way to go.”**  
Proc. Natl. Acad. Sci. USA, vol: 98, pp:11-13, 2001.
- Wood DE., Thomas A., Devi LA., Berman Y., Beavis RC., Reed JC. and Newcomb EW., **“Bax cleavage is mediated by calpain during drug-induced apoptosis.”**  
Oncogene, vol:17, pp:1069–1078, 1998.
- Xia Z., Dickens M., Raingeaud J., Davis R.J. and Greenberg ME., **“Opposing effects of ERK and JNK-p38 MAP kinases on apoptosis.”**  
Science, vol:270, pp:1326-1331, 1995.
- Xu G., Cirilli M., Huang Y., Rich RL., Myszka DG. and Wu, H., **“Covalent inhibition revealed by the crystal structure of the caspase-8/p35 complex.”**  
Nature, vol:410, pp:494–497, 2001.
- Xue D. and Horvitz HR., **“Caenorhabditis elegans CED-9 protein is a bifunctional cell-death inhibitor.”**  
Nature, vol:390, pp: 305-308, 1997.
- Yang X., Khosravi-Far R., Chang H. and Baltimore D., **“Daxx, a novel Fas-binding protein that activates JNK and apoptosis.”**  
Cell, vol:89, pp:1067-1076, 1997.
- Ye X., Mehlen P., Rabizadeh S., VanArsdale T., Zhang H., Shin H., Wang JJ., Leo E., Zapata J., Hauser CA., Reed JC. and Bredesen DE., **“TRAF family proteins interact with the common neurotrophin receptor and modulate apoptosis induction.”**  
J. Biol. Chem., vol:274, pp:30202-30208, 1999.
- Yolcu E., Sayan BS., Yagci T., Cetin-Atalay R., Soussi T., Yurdusev N. and Ozturk M., **“A monoclonal antibody against DNA binding helix of p53 protein.”**  
Oncogene, vol:20, pp:1398-1401, 2001.

- Yuan J., Shaham S., Ledoux S., Ellis H. and Horvitz H., **“The C. elegans cell death gene ced-3 encodes a protein similar to mammalian interleukin-1 beta-converting enzyme.”**  
Cell, vol:75, pp:641-652, 1993.
- Zhang C., Ao Z., Seth A. and Schlossman SF., **“A mitochondrial membrane protein defined by a novel monoclonal antibody is preferentially detected in apoptotic cells.”**  
J. Immunol., vol:157, pp:3980-3987, 1996.
- Zha J., Harada H., Yang E., Jockel J. and Korsmeyer SJ., **“Serine phosphorylation of death agonist BAD in response to survival factor results in binding to 14-3-3 not BCL-X(L).”**  
Cell, vol:87, pp:619-628, 1996.
- Zieve GW., Turnbull D., Mullins JM. and McIntosh JR., **“Production of large numbers of mitotic mammalian cells by use of the reversible microtubule inhibitor nocodazole. Nocodazole accumulated mitotic cells.”**  
Exp. Cell Res., vol:126, pp:397-405, 1980.
- Zindy F., Eischen CM., Randle DH., Kamijo T., Cleveland JL., Sherr CJ. and Roussel MF., **“Myc signaling via the ARF tumor suppressor regulates p53-dependent apoptosis and immortalization.”**  
Genes Dev., vol:12, pp:2424-2433, 1998.
- Zornig M., Hueber AO., Baum W. and Evan G., **“Apoptosis regulators and their role in tumorigenesis”**  
Biochimica et Biophysica Acta, vol:1551, pp:F1-F37, 2001.

**APPENDIX**

**PUBLICATIONS**

## NAPO as a novel marker for apoptosis

Berna S. Sayan,<sup>1</sup> Gulayse Ince,<sup>1</sup> A. Emre Sayan,<sup>1</sup> and Mehmet Ozturk<sup>1,2</sup>

<sup>1</sup>Department of Molecular Biology and <sup>2</sup>BilGen Genetics and Biotechnology Center, Bilkent University, 06533 Ankara, Turkey

Apoptosis or programmed cell death plays a pivotal role in embryonic development and maintenance of homeostasis. It is also involved in the etiology of pathophysiological conditions such as cancer, neurodegenerative, autoimmune, infectious, and heart diseases. Consequently, the study of apoptosis is now at center of both basic and clinical research applications. Therefore, sensitive and simple apoptosis detection techniques are required. Here we describe a monoclonal antibody-defined

novel antigen, namely *NAPO* (negative in apoptosis), which is specifically lost during apoptosis. The anti-*NAPO* antibody recognizes two nuclear polypeptides of 60 and 70 kD. The antigen is maintained in quiescent and senescent cells, as well as in different phases of the cell cycle, including mitosis. Thus, immunodetection of *NAPO* antigen provides a specific, sensitive, and easy method for differential identification of apoptotic and nonapoptotic cells.

### Introduction

During the last decade, apoptosis has become a major focus of interest for many fields of biomedical research. Programmed cell death is required for proper embryonic development as well as for the maintenance of homeostasis in adult tissues (Vaux and Korsmeyer, 1999; Wyllie and Golstein, 2001). Moreover, apoptosis is involved in the etiology and pathophysiology of a variety of diseases, such as cancer, neurodegenerative, autoimmune, infectious, and heart diseases (Chervonsky, 1999; Roulston et al., 1999; Mattson, 2000; Narula et al., 2000; Reed, 2000). Apoptotic cell death is characterized by a series of morphological changes, including cell shrinkage, nuclear condensation, chromatin segregation, membrane blebbing, formation of membrane-bound apoptotic bodies, and internucleosomal DNA cleavage (Saraste and Pulkki, 2000). These morphological changes result from a series of genetically programmed biochemical changes initiated by either the activation of death receptors or intracellular stress conditions such as DNA damage. These proapoptotic signals are conveyed to mitochondria to cause the release of caspase-activating factors from this organelle, followed by a cascade of caspase activation which leads to cell death (Earnshaw et al., 1999; Gottlieb, 2000).

Apoptosis, as a critical component of life in multicellular organisms, is a target subject for understanding cellular mechanisms of many diseases, as well as for developing new

drugs that interfere with either proapoptotic or antiapoptotic molecular networks. Consequently, it has become important to develop reliable assays to measure cell death. Techniques currently available for apoptosis detection are based on the study of morphology of apoptotic cells (light and fluorescence microscopy coupled to nuclear staining with specific dyes and electron microscopy), DNA fragmentation detected by terminal transferase-mediated dUTP nick-end labeling (TUNEL)\* and similar techniques, membrane changes detected by annexin V in vivo labeling, and on immunological assays using antibodies directed to apoptosis-related proteins (Stadelmann and Lassmann, 2000). Essential requirements for apoptosis detection techniques include high sensitivity for apoptotic cells, the ability to differentiate between apoptosis and other forms of cellular changes, as well as distinction between different stages of the cell death process. However, we are facing a relative paucity for simple techniques fulfilling these requirements, and furthermore allowing quantitative analysis (van Heerde et al., 2000). Immunological detection of apoptosis-related proteins is probably the best approach to overcome this obstacle, but there are only a few known apoptosis marker antigens (Stadelmann and Lassmann, 2000).

Here we describe a mouse monoclonal antibody-defined nuclear antigen composed of two polypeptides that we call *NAPO* (for negative in apoptosis), which is strongly expressed in cells under many conditions (proliferation, quiescence, mitosis, and senescence) except apoptosis. The immunoreactivity of the antigen, as tested by immunofluorescence technique,

Address correspondence to Mehmet Ozturk, Department of Molecular Biology and Genetics, Bilkent University, 06533 Ankara, Turkey. Tel.: (90) 312-266-50-81. Fax: (90) 312-266-50-97. E-mail: ozturk@fen.bilkent.edu.tr

Gulayse Ince's present address is Johns Hopkins University, School of Medicine, Baltimore, MD 21205.

Key words: apoptosis; apoptotic cell death; apoptotic marker; quiescence; senescence

\*Abbreviations used in this paper: TUNEL, terminal transferase-mediated dUTP nick-end labeling.

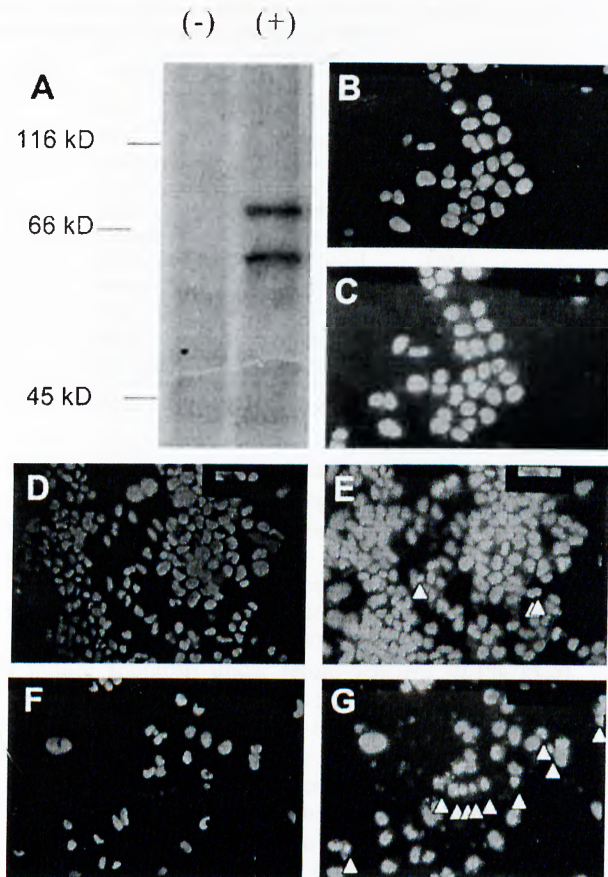


**Figure 1. Initial characterization of NAPO antigen.** Anti-NAPO monoclonal antibody recognizes two bands migrating at ~60 and 70 kD. [ $^{35}$ S]methionine-labeled Huh7 cells were subjected to immunoprecipitation with anti-NAPO antibody (+). (-) is a negative control (A). Immunofluorescence staining of Huh7 cells with anti-NAPO antibody indicates that NAPO is a nuclear antigen (B). Hoechst 33258 counterstain for nuclear DNA (C). NAPO immunofluorescence staining of SNU 398 cells growing in standard culture medium indicates that the majority of cell nuclei are positive, but occasionally some cells with small nuclei (presumably apoptotic) are negative (D), as indicated by white arrows in nuclear DNA staining (E). NAPO antigen is negative in apoptotic SNU 398 cells which are induced by growth in serum-free medium (F). Apoptotic cells are indicated by white arrows in Hoechst 33258 counterstaining (G).

is lost in apoptotic cells in a way opposite to TUNEL and annexin V staining. Thus, NAPO antigen may serve as a reliable marker for apoptosis.

## Results and discussion

### Biochemical characterization of the NAPO antigen

A mouse IgG monoclonal antibody (named anti-NAPO antibody) was generated against a nuclear antigen after immunization with human colorectal cell line COLO 320. Detergent-soluble proteins were prepared from metabolically labeled Huh7 cells and subjected to immunoprecipitation with anti-NAPO antibody. As shown in Fig. 1 A, anti-NAPO antibody recognized two proteins migrating at ~60

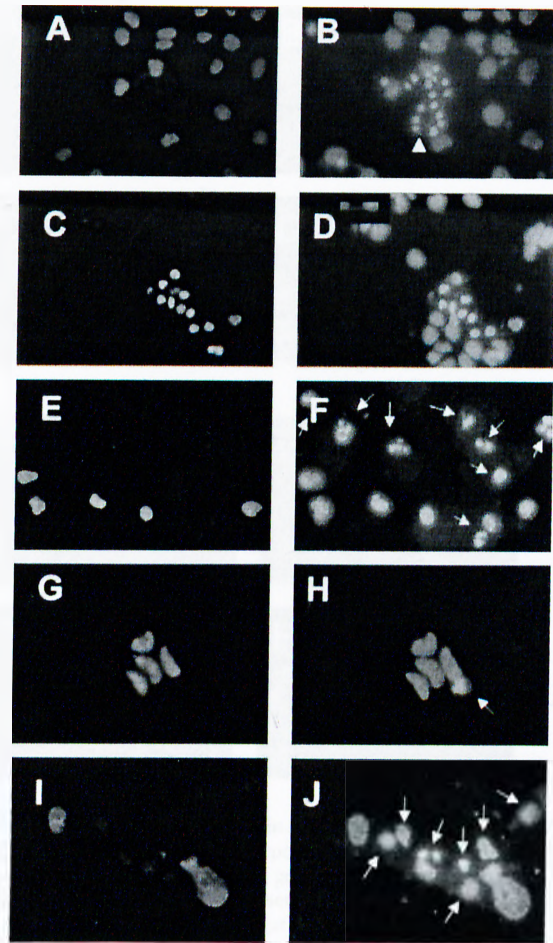


**Figure 2. Identification of NAPO as a common apoptosis marker.** NAPO is negative in 100  $\mu$ M H<sub>2</sub>O<sub>2</sub>-treated apoptotic Huh7 cells (A), in contrast to positive staining with TUNEL (C). NAPO is also lost in Fas-mediated apoptosis in Jurkat cells (E), H<sub>2</sub>O<sub>2</sub>-mediated apoptosis in 293 cells (G), and UV-C-mediated apoptosis in MRC-5 cells (I). B, D, F, H, and J show Hoechst 33258 counterstaining.

and 70 kD, respectively. Immunofluorescence studies revealed with the same cell line indicated that NAPO was a nuclear antigen (Fig. 1, B and C). This antibody was specific for human and monkey NAPO, since all human cell lines and monkey COS-7 showed positive immunostaining, but mouse (HC 11), rat (IAR-6), and hamster (CHOK-I) cell lines were negative (unpublished data).

Although NAPO antigen was ubiquitously present in all human cell lines so far tested, small nuclear fragments which are occasionally observed with some cell lines under normal culture conditions were negative (Fig. 1, D and E as an example). This suggested to us that NAPO antigen could be lost during apoptosis.

### Identification of NAPO as an apoptotic marker

Hepatocellular carcinoma-derived SNU 398 cells, which undergo apoptosis when grown under serum-free conditions were serum starved for three days and tested for NAPO antigen immunoreactivity. Cells displaying morphological char-

Table 1. List of cell lines tested for loss of *NAPO* immunoreactivity after induction of apoptosis by various stimuli

Cell line	Origin	Morphology	Apoptosis stimuli
Huh 7	HCC	Epithelial	H <sub>2</sub> O <sub>2</sub>
SNU 398	HCC	Epithelial	Serum starvation
MCF7	Breast cancer	Epithelial	TNF- $\alpha$ , UV-C
HeLa	Cervix cancer	Epithelial	UV-C
SW480	Colon cancer	Epithelial	UV-C
LNcaP	Prostate cancer	Epithelial	UV-C
U2OS	Osteosarcoma	Epithelial	UV-C
A375	Melanoma	Epithelial	UV-C
Jurkat	TCL	Lymphoid	Anti-Fas, UV-C
MRC-5	Lung	Fibroblastic	UV-C
293	Embryonal kidney	Epithelial	Cisplatin, H <sub>2</sub> O <sub>2</sub>

HCC, hepatocellular carcinoma; TCL, acute T cell leukemia.

acteristics of apoptosis (cell shrinkage, nuclear condensation, and fragmentation) displayed negative *NAPO* staining in contrast to positive nuclear staining of all nonapoptotic cells (Fig. 1, F and G).

To confirm the loss of *NAPO* antigen during apoptosis in another cellular system, hepatocellular carcinoma-derived Huh7 cells were used. H<sub>2</sub>O<sub>2</sub> (100  $\mu$ M) treatment of these cells induce apoptosis under serum-deficient (0.1% FCS) conditions (unpublished data). As shown in Fig. 2 A, *NAPO* antigen was negative in apoptotic Huh7 cells that are identified as cells with small nuclei by Hoechst 33258 counterstaining (Fig. 2 B). To test whether the loss of *NAPO* expression is specific to this antigen, rather than a common feature shared by nuclear proteins, we also tested Huh7 cells for p53 protein immunoreactivity under similar conditions. Huh7 cells express a mutant p53 protein that accumulate in their nuclei (Volkman et al., 1994). Both apoptotic and nonapoptotic Huh7 cells displayed positive staining for p53 protein. Indeed, apoptotic cells displayed a stronger p53 immunoreactivity when compared with nonapoptotic cells (unpublished data). This indicated that the loss of *NAPO* immunoreactivity in apoptotic Huh7 cells was specific to this antigen rather than a common feature of nuclear proteins.

For further characterization of *NAPO* as an apoptosis marker, additional studies were performed in different cell lines treated with different apoptosis stimuli. For all experiments *NAPO* tests were run in parallel to TUNEL or annexin V staining (TUNEL data for Huh7 shown in Fig. 2 C as an example). To show whether *NAPO* antigen is lost during death receptor-mediated apoptosis, TNF- $\alpha$ -treated MCF 7 and anti-Fas antibody-treated Jurkat cells were used. *NAPO* was lost in apoptotic Jurkat (Fig. 2 E) as well as MCF-7 cells (unpublished data). To test whether *NAPO* loss during apoptosis was common to cells of different origin, additional tumor-derived (HeLa, U2OS, A375, SW480, LN-CaP) as well as normal tissue-derived (293 and MRC-5) cell lines were induced to undergo apoptosis by H<sub>2</sub>O<sub>2</sub>, UV-C, or cisplatin treatment (Table 1). *NAPO* staining was lost in all apoptotic cells in contrast to strong nuclear staining of the nonapoptotic counterparts (example data on 293 and MRC-5 cells are shown in Fig. 2, G and I, respectively).

These results demonstrate that *NAPO* is ubiquitously expressed in living cells, but lost during apoptosis independent of the apoptosis activating pathway (Table 1). The loss of

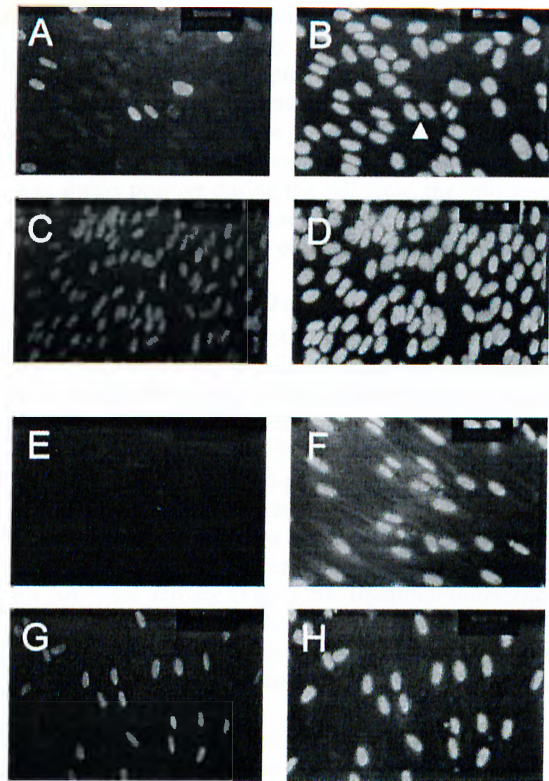
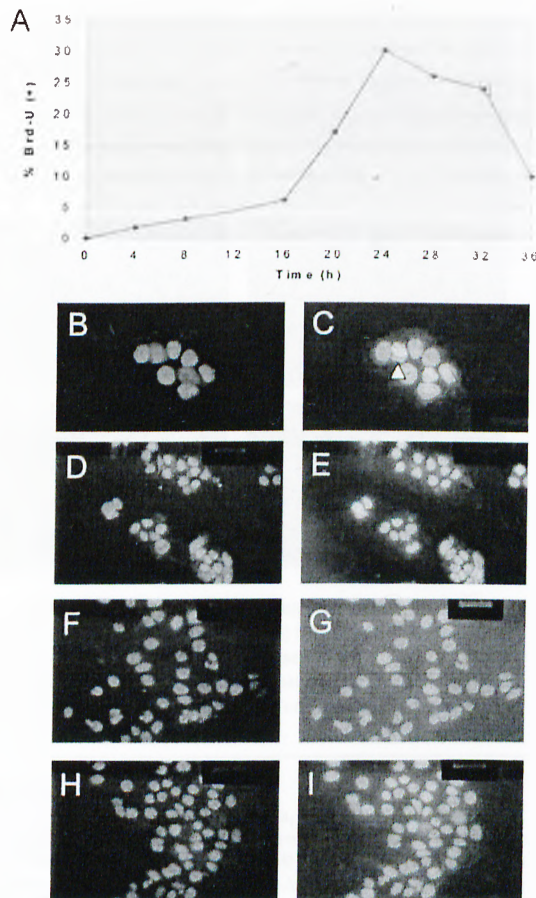


Figure 3. *NAPO* antigen is positive in quiescent cells. MRC-5 cells were tested in parallel for BrdU incorporation (A and E) or *NAPO* antigen (C and G). Cells in A–D were grown under standard culture conditions. Cells in panels E–H were serum starved for 3 d to induce a quiescent state, as indicated by negative BrdU staining in E. Note that both actively growing (C) and quiescent cells (G) are positive for *NAPO*. B, D, F, and H show Hoechst 33258 counterstaining.

*NAPO* during apoptosis strongly suggests that this antigen is a nuclear caspase substrate. The epitope recognized by anti-*NAPO* antibody on this antigen is probably lost as a result of caspase-mediated protein cleavage. However, it is presently unclear whether any of 60- and 70-kD polypeptides of the *NAPO* antigen are known caspase substrates. To our knowledge, proteins with similar molecular weight have not been described previously as apoptosis-associated proteins. Thus, *NAPO* appears to be a novel marker for apoptosis that could serve to distinguish apoptotic from nonapoptotic cells. However, it was important to know whether the antigenic reactivity is modified under different growth conditions such as quiescence, cell cycle (especially mitosis), and senescence.

#### Expression of the *NAPO* antigen in quiescent cells

MRC-5 human embryonic lung fibroblast cells (passage 18) were grown to confluency and serum starved for 3 d to induce quiescence. To show that these cells are indeed quiescent, BrdU incorporation was also tested. Our results indicate that ~15% of asynchronously growing MRC-5 cells are positive for BrdU i.e., in S phase (Fig. 3 A), whereas no BrdU labeling was observed in quiescent cells (Fig. 3 E). Under both conditions, all cells displayed a similarly positive nuclear staining for *NAPO* (Fig. 3, C and G). These obser-



**Figure 4. *NAPO* expression during cell cycle.** Huh7 cells were synchronized by nocodazole treatment, followed by mitotic shake-off. Freshly collected cells were then grown in culture for up to 36 h. The S phase was identified by BrdU incorporation assay. Time points between 0–16, 20–32, and 36 h were evaluated respectively as G1, S, and G2 phases according to the BrdU incorporation index (A). *NAPO* and BrdU staining were performed at 4 h intervals. B, D, F, and H illustrate *NAPO* staining of cells at mitotic arrest (B), 8 h (D), 24 h (F), and 36 h (H), respectively. C, E, G, and I show Hoechst 33258 counterstaining. Note diffused *NAPO* staining in mitotically arrested Huh7 cells (B and C) which were digitally magnified threefold for better visualization.

vations indicated that *NAPO* expression is not lost in nondividing quiescent cells.

#### Expression of the *NAPO* antigen during cell cycle

We also analyzed the expression pattern of *NAPO* in synchronized cells in order to follow its positivity during different phases of the cell cycle. For this purpose Huh7 cells were treated with nocodazole and mitotic cells were collected by mitotic shake-off and plated onto coverslips. Synchronized Huh7 cells were tested every 4 h for 36 h of culture for both BrdU incorporation and *NAPO* staining. BrdU incorporation was minimal until 16 h after the release from mitotic arrest with a maximum of BrdU incorporation at 24 h, followed by a significant decrease at 36 h (Fig. 4 A). According to BrdU incorporation index, cells at time points before 16 h were evaluated as G1 phase cells, cells between time points

20 and 32 h as S phase cells, and those at time point 36 h as G2 phase cells. Mitotically arrested cells showed a diffusely positive (nuclear and cytoplasmic) *NAPO* staining (Fig. 4 B). *NAPO*-staining pattern was nuclear throughout the cell cycle, at all time points (time points 8, 24, and 36 h are shown in Figs. 4, D, F, and H, respectively). Thus, *NAPO* staining was always positive during the cell cycle, the only noticeable change being a diffuse staining during mitosis, in contrast to strictly nuclear staining in other phases of the cell cycle.

#### Expression of the *NAPO* antigen in senescent cells

To test whether *NAPO* antigen expression is modified during senescence, MRC-5 cells were grown until passage 40, at which point they remain alive and attached to cell plate, but they stop dividing, a characteristic feature of senescence (Fulder and Holliday, 1975). The senescence is often accompanied by a positive SA- $\beta$ -gal activity, which is negative in presenescent cells (Dimri et al., 1995). As shown in Fig. 5, in contrast to presenescent MRC-5 cells at passage 18 (Fig. 5 A), senescent MRC-5 cells at passage 40 were positive for SA- $\beta$ -gal activity (Fig. 5 B). Immunofluorescence data shown in Fig. 5, C and D, indicated that both presenescent and senescent MRC-5 cells were positive for *NAPO* antigen immunoreactivity, demonstrating that *NAPO* expression is not lost in senescent cells.

Our observations demonstrate that *NAPO* is present in living cells in all phases of the cell cycle as well as during senescence and quiescence, getting lost only during apoptosis. When compared with other available apoptosis detection systems, *NAPO* test is highly specific for apoptosis and offers the simplicity of antibody-based assays. The anti-*NAPO* antibody can be used for detection of apoptotic cells under different conditions, such as in situ staining of cells and tissue sections, and for flow cytometry. TUNEL assay (Gavrieli et al., 1992) is widely used for the identification of apoptotic cells, even though it requires several cumbersome experimental steps. As *NAPO* and TUNEL assays provide exclusive nuclear staining of alive and apoptotic cells, respectively, we believe that both assays may be combined for better identification of apoptosis. Moreover, *NAPO* assay may detect apoptotic cells before DNA fragmentation and it does not require special pretreatment of assay samples. *NAPO* may also be used in combination with annexin V staining (Martin et al., 1995). *NAPO* differs from previously identified and antibody-defined apoptosis markers (Grand et al., 1995; Zhang et al., 1996; Hammond et al., 1998; Srinivasan et al., 1998; Leers et al., 1999) by its exclusive loss in apoptotic cells, but not in quiescent, proliferating, senescent, or even mitotic cells. We believe that this antibody will be very helpful for development of simple and easy immunoassays for measurement of apoptosis in both cell lines and tissue samples.

## Materials and methods

### Monoclonal antibody production

10,000,000 COLO 320 cells were lysed in 2 ml PBS and 0.5 ml of lysate was injected into tail vein of Balb/c mice. 1 mo later, mice were immunized twice more at 1 wk intervals, hybridomas were prepared from splenic cells, and antibody-producing clones were selected as described previously (Ozturk et al., 1989). One of the antibodies of IgG isotype, named anti-*NAPO*, was used for further studies.

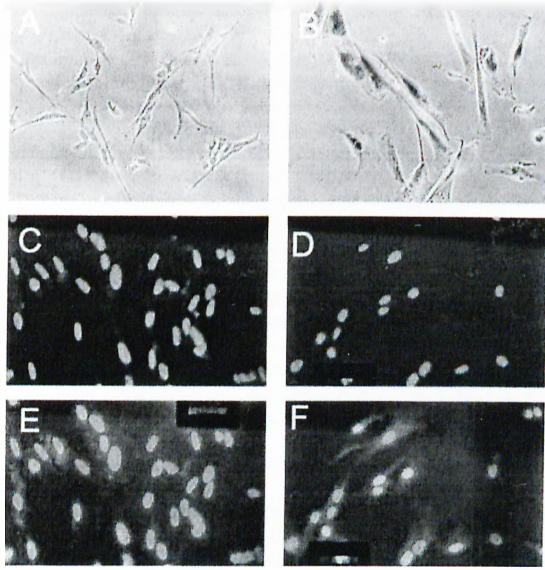


Figure 5. **NAPO antigen is positive in senescent cells.** Presenescent (A, C, and E) and senescent (B, D, and F) MRC-5 cells were stained for senescence-associated  $\beta$ -galactosidase activity (A and B), NAPO immunoreactivity (C and D), and Hoechst 33258 DNA staining (E and F). Note that senescence-associated  $\beta$ -galactosidase-positive cells are also positive for NAPO antigen.

#### Tissue culture

Huh7, SNU 398, COLO 320, MCF-7, HeLa, U2OS, SW480, A375, 293, MRC-5, COS7, IAR-6, and CHOK-1 cells were grown in DME (Biochrom or GIBCO BRL). HC11 was grown in RPMI 1640 (Biological Industries) supplemented with 10 ng/ml EGF (Sigma-Aldrich) and 5  $\mu$ g/ml insulin (Sigma-Aldrich). Jurkat and LNCaP cells were grown in RPMI 1640. All cells were grown in media supplemented with 10% FCS, 1% nonessential amino acids, 100  $\mu$ g/ml penicillin/streptomycin at 37°C and 5% CO<sub>2</sub>.

#### Induction of apoptosis

Apoptotic cell death was induced by either serum starvation or treatment with H<sub>2</sub>O<sub>2</sub>, UV-C, cisplatin, anti-Fas antibody or TNF- $\alpha$  treatment. SNU 398 hepatocellular carcinoma cells were induced in serum-free medium for 3 d and tested for apoptosis. For oxidative stress-induced apoptosis, Huh7 cells were incubated in a culture medium containing 0.1% FCS for 72 h, and treated with freshly prepared 100  $\mu$ M H<sub>2</sub>O<sub>2</sub> for at least 4 h before apoptosis assay. 293 cells were treated with 200  $\mu$ M H<sub>2</sub>O<sub>2</sub> or 100  $\mu$ M cisplatin. MCF-7, HeLa, U2OS, A375, SW480, LNCaP, Jurkat, and MRC-5 cells were treated with UV-C irradiation (60–120 mJ/cm<sup>2</sup>). For physiologically induced apoptosis studies, TNF- $\alpha$ -treated (Boehringer; 50 ng/ml for 72 h) MCF-7 and anti-fas antibody-treated (Upstate Biotechnology; clone CH11, 25 ng/ml for 24 h) Jurkat cells were used.

#### Induction of quiescence

Presenescent MRC-5 cells (passage 18) were grown to confluency on coverslips and serum starved for 3 d. At the end of 3 d, one set of cells was tested for BrdU labeling and the other set was subjected to immunofluorescence for the expression of the NAPO antigen as described later. Asynchronously growing MRC-5 cells of the same passage were used as a control.

#### Mitotic arrest and cell cycle synchronization

Huh7 cells were grown to 60% confluency and incubated with 50 ng/ml nocodazole (Sigma-Aldrich) for 18 h. Mitotic cells were collected by mitotic shake-off and replated onto coverslips. At indicated time points (between 4 and 36 h), one set of cells was tested for BrdU labeling, and the other set was subjected to immunofluorescence for the expression of the NAPO antigen.

#### Immunoprecipitation

Huh7 cells grown to 70% confluency were starved in DME lacking methionine (Sigma-Aldrich) and labeled with 200  $\mu$ Ci [<sup>35</sup>S]methionine (Amer-

sham Pharmacia Biotech) per 4 ml medium for 2 h. Cells were scraped in ice-cold PBS and lysed in NP-40 lysis buffer (150 mM NaCl, 1.0% NP-40, 50 mM Tris pH 8.0, protease inhibitor cocktail; Roche), and centrifuged at 13,000 rpm at 4°C for 30 min. The cell lysate was incubated with anti-NAPO antibody for 2 h and the NAPO antigen was immunoprecipitated by using protein G sepharose (Amersham Pharmacia Biotech).

#### Immunofluorescence

Cells were grown on coverslips and fixed with 100% ice-cold acetone for 1 min or by 4% paraformaldehyde for 1 h. When paraformaldehyde was used, cells were permeabilized for 3 min with 0.1% Triton X-100 in 0.1% sodium citrate. After saturation with 3% BSA in PBS-T (0.1%) for 15 min, fixed cells were incubated with anti-NAPO antibody for 1 h at room temperature. FITC-conjugated goat anti-mouse antibody (Dako) was used as the secondary antibody and diluted as recommended by the supplier. The immunofluorescence staining of Huh7 cells for p53 protein was tested using 6B10 monoclonal antibody (Yolcu et al., 2001). Nuclear DNA was visualized by incubation with 3  $\mu$ g/ml Hoechst 33258 (Sigma-Aldrich) for 5 min in the dark. Cover slips were then rinsed with distilled water, mounted on glass microscopic slides in 50% glycerol, and examined under fluorescent microscope (ZEISS). Jurkat cells were cytospinned (Shandon) for 3 min at 200 rpm before immunofluorescence procedures.

#### TUNEL and annexin V stainings

The TUNEL assay was performed using an in situ cell death detection kit (Roche), according to manufacturer's recommendations. The annexin V assay was performed by annexin V-PE reagent (PharMingen), according to manufacturer's recommendations, and cells were fixed in ethanol. After TUNEL and annexin V assays, cells were counterstained with Hoechst 33258 and examined as described.

#### BrdU labeling and identification of S phase cells

For BrdU incorporation, cells were incubated with 30  $\mu$ M BrdU for 1 h before fixation with ice-cold 70% ethanol for 10 min. After DNA denaturation in 2 N HCl for 20 min, cells were incubated with FITC-conjugated anti-BrdU antibody (Dako) in the dilution as recommended by the supplier, cells were counterstained with Hoechst 33258 and examined as described.

#### Senescence-associated $\beta$ -galactosidase assay

MRC-5 cells were grown to passage 40 and subjected to senescence-associated  $\beta$ -galactosidase (SA  $\beta$ -gal) assay, as described by Dimri et al. (1995). Briefly, cells were fixed in 3% formaldehyde for 5 min and incubated with SA  $\beta$ -gal solution (40 mM citric acid/sodium phosphate buffer, pH 6.0, 5 mM potassium ferro cyanide, 5 mM potassium ferric cyanide, 150 mM NaCl, 2 mM MgCl<sub>2</sub>, and 1 mg/ml X-Gal) for up to 12 h, and examined under light microscope.

We thank Rolf I. Carlson for his technical help in antibody production and Gokhan S. Hotamisligil for providing some of the cell lines used here. The present work was supported by a grant from Bilkent University.

The initial stage of this project (monoclonal antibody production) was performed at Massachusetts General Hospital Cancer Center (Charlestown, MA) and supported by a grant (CA-54567) from the National Institutes of Health to M. Ozturk.

Submitted: 6 August 2001

Revised: 14 September 2001

Accepted: 17 October 2001

## References

- Chervonsky, A.V. 1999. Apoptotic and effector pathways in autoimmunity. *Curr. Opin. Immunol.* 11:684–688.
- Dimri, G.P., X. Lee, G. Basile, M. Acosta, G. Scott, C. Roskelley, E.E. Medrano, M. Linskens, I. Rubelj, O. Pereira-Smith, et al. 1995. A biomarker that identifies senescent human cells in culture and in aging skin in vivo. *Proc. Natl. Acad. Sci. USA.* 92:9363–9367.
- Earnshaw, W.C., L.M. Martins, and S.H. Kaufmann. 1999. Mammalian caspases: structure, activation, substrates, and functions during apoptosis. *Annu. Rev. Biochem.* 68:383–424.
- Fulder, S.J., and R.A. Holliday. 1975. Rapid rise in cell variants during the senescence of populations of human fibroblasts. *Cell.* 6:67–73.
- Gavrieli, Y., Y. Sherman, and S.A. Ben-Sasson. 1992. Identification of pro-

- grammed cell death in situ via specific labeling of nuclear DNA fragmentation. *J. Cell Biol.* 119:493–501.
- Gottlieb, R.A. 2000. Mitochondria: execution central. *FEBS Lett.* 482:6–12.
- Grand, R.J., A.E. Milner, T. Mustoe, G.D. Johnson, D. Owen, M.L. Grant, and C.D. Gregory. 1995. A novel protein expressed in mammalian cells undergoing apoptosis. *Exp. Cell Res.* 218:439–451.
- Hammond, E.M., C.L. Brunet, G.D. Johnson, J. Parkhill, A.E. Milner, G. Brady, C.D. Gregory, and R.J. Grand. 1998. Homology between a human apoptosis specific protein and the product of APG5, a gene involved in autophagy in yeast. *FEBS Lett.* 425:391–395.
- Leers, M.P., W. Kolgen, V. Bjorklund, T. Bergman, G. Tribbick, B. Persson, P. Bjorklund, F.C. Ramaekers, B. Bjorklund, M. Nap, et al. 1999. Immunocytochemical detection and mapping of a cytokeratin 18 neo-epitope exposed during early apoptosis. *J. Pathol.* 187:567–572.
- Martin, S.J., C.P. Reutelingsperger, A.J. McGahon, J.A. Rader, R.C. van Schie, D.M. LaFace, and D.R. Green. 1995. Early redistribution of plasma membrane phosphatidylserine is a general feature of apoptosis regardless of the initiating stimulus: inhibition by overexpression of Bcl-2 and Abl. *J. Exp. Med.* 182:1545–1556.
- Mattson, M.P. 2000. Apoptosis in neurodegenerative disorders. *Nat. Rev. Mol. Cell Biol.* 1:120–129.
- Narula, J., F.D. Koldogje, and R. Virmani. 2000. Apoptosis and cardiomyopathy. *Curr. Opin. Cardiol.* 15:183–188.
- Ozturk, M., P. Motte, H. Takahashi, M. Frohlich, B. Wilson, L. Hill, B. Bressac, and J.R. Wands. 1989. Identification and characterization of a Mr 50,000 adrenal protein in human hepatocellular carcinoma. *Cancer Res.* 49:6764–6773.
- Reed, C.J. 2000. Apoptosis and cancer: strategies for integrating programmed cell death. *Semin. Hematol.* 37:9–16.
- Roulston, A., R.C. Marcellus, and P.E. Branton. 1999. Viruses and apoptosis. *Annu. Rev. Microbiol.* 53:577–628.
- Saraste, A., and K. Pulkki. 2000. Morphologic and biochemical hallmarks of apoptosis. *Cardiovasc. Res.* 45:528–537.
- Srinivasan, A., K.A. Roth, R.O. Sayers, K.S. Shindler, A.M. Wong, L.C. Fritz, and K.J. Tomaselli. 1998. In situ immunodetection of activated caspase-3 in apoptotic neurons in the developing nervous system. *Cell Death Differ.* 5:1004–1016.
- Stadelmann, C., and H. Lassmann. 2000. Detection of apoptosis in tissue sections. *Cell Tissue Res.* 301:19–31.
- van Heerde, W.L., S. Robert-Offerman, E. Dumont, L. Hofstra, P.A. Doevendans, J.F. Smits, M.J. Daemen, and C.P. Reutelingsperger. 2000. Markers of apoptosis in cardiovascular tissues: focus on Annexin V. *Cardiovasc. Res.* 45:549–559.
- Vaux, D.L., and S.J. Korsmeyer. 1999. Cell death in development. *Cell.* 96:245–254.
- Volkman, M., W.J. Hofmann, M. Muller, U. Rath, G. Otto, H. Zentgraf, and P.R. Galle. 1994. p53 overexpression is frequent in European hepatocellular carcinoma and largely independent of the codon 249 hot spot mutation. *Oncogene.* 9:195–204.
- Wyllie, A.H., and P. Golstein. 2001. More than one way to go. *Proc. Natl. Acad. Sci. USA.* 98:11–13.
- Yolcu, E., B.S. Sayan, T. Yagci, R. Cetin-Atalay, T. Soussi, N. Yurdusev, and M. Ozturk. 2001. A monoclonal antibody against DNA binding helix of p53 protein. *Oncogene.* 20:1398–1401.
- Zhang, C., Z. Ao, A. Seth, and S.F. Schlossman. 1996. A mitochondrial membrane protein defined by a novel monoclonal antibody is preferentially detected in apoptotic cells. *J. Immunol.* 157:3980–3987.



## Acquired expression of transcriptionally active p73 in hepatocellular carcinoma cells

A Emre Sayan<sup>1</sup>, Berna S Sayan<sup>1</sup>, Necati Findikli<sup>1</sup> and Mehmet Ozturk<sup>\*,1</sup>

<sup>1</sup>Department of Molecular Biology and Genetics, Bilkent University, 06533, Ankara, Turkey

**p53 and p73 proteins activate similar target genes and induce apoptosis and cell cycle arrest. However, p53, but not p73 is considered a tumour-suppressor gene. Unlike p53, p73 deficiency in mice does not lead to a cancer-prone phenotype, and p73 gene is not mutated in human cancers, including hepatocellular carcinoma. Here we report that normal liver cells express only ΔN-p73 transcript forms giving rise to the synthesis of N-terminally truncated, transcriptionally inactive and dominant negative p73 proteins. In contrast, most hepatocellular carcinoma cells express TA-p73 transcript forms encoding full-length and transcriptionally active p73 proteins, in addition to ΔN-p73. We also show that together with the acquired expression of TA-p73, the 'retinoblastoma pathway' is inactivated, and E2F1-target genes including cyclin E and p14<sup>ARF</sup> are activated in hepatocellular carcinoma. However, there was no full correlation between 'retinoblastoma pathway' inactivation and TA-p73 expression. Most TA-p73-expressing hepatocellular carcinoma cells have also lost p53 function either by lack of expression or missense mutations. The p73 gene, encoding only ΔN-p73 protein, may function as a tumour promoter rather than a tumour suppressor in liver tissue. This may be one reason why p73 is not a mutation target in hepatocellular carcinoma. *Oncogene* (2001) 20, 5111–5117.**

**Keywords:** liver cancer; p73; retinoblastoma; p16<sup>INK4a</sup>; p14<sup>ARF</sup>; cyclin E

### Introduction

The p53 and its newly discovered homologues, namely p73 and p63 form a family of genes that activate similar target genes, and induce apoptosis and cell cycle arrest (Marin and Kaelin, 2000; Lohrum and Vousden, 2000). However, p53, but not the other family members, is considered a tumour-suppressor gene. For example, unlike p53, p73 deficiency in mice does not lead to a cancer-prone phenotype (Yang *et al.*, 2000), and p73 gene is not mutated in human tumours, including hepatocel-

lular carcinoma (HCC) (Marin and Kaelin, 2000; Mihara *et al.*, 1999). Presently, the reasons for this discrepancy are not known. One of the major differences between p53 and the two other family members is the ability of p63 and p73 genes to encode multiple transcript isoforms (Marin and Kaelin, 2000; Lohrum and Vousden, 2000). Different p63 and p73 C-termini are generated as a result of alternative splicing between exons 10–15 and 10–14, respectively (Marin and Kaelin, 2000). In addition, p63 utilizes a cryptic promoter located in intron 3 to generate additional transcripts called ΔN-p63 isoforms (Yang *et al.*, 1998).

Our knowledge on truncated ΔN-p73 isoforms is scarce, but ΔN-p73 transcripts lacking transactivation domain were proposed to be predominant p73 gene products in some mouse tissues (Yang *et al.*, 2000). Pozniak *et al.* (2000) have recently demonstrated that p73 is primarily present in developing neurons as a truncated ΔN-p73 isoform in mouse. Like the transcripts encoding ΔN-p63 (Yang *et al.*, 1998), murine ΔN-p73 messages were derived from an alternative promoter located in intron 3, and ΔN-p73 failed to activate transcription from a p53-reporter gene, but suppressed the transactivation activity of both TA-p73α and wild-type p53 (Yang *et al.*, 2000; Pozniak *et al.*, 2000). On the other hand, most, if not all reported studies on the expression of p73 in different cancers did not distinguish between ΔN-p73 and TA-p73 isoforms (reviewed in Marin and Kaelin, 2000; Lohrum and Vousden, 2000).

With regard to p73 implications in liver malignancy, Tannapfel *et al.* (1999a,b) have reported that both p73 transcripts and protein were undetectable in most normal liver cells, but p73 protein was over-expressed in a subset of HCCs, and could serve as an indicator of poor prognosis (Tannapfel *et al.*, 1999b). On the other hand, Mihara *et al.* (1999) reported the absence of mutation, as well as absence of over-expression of p73 gene in HCC. These observations were in apparent contradiction and they did not provide evidence about the mechanisms of p73 involvement in liver malignancy. These reports, together with the identification ΔN-p73 in some mouse tissues (Yang *et al.*, 2000; Pozniak *et al.*, 2000), led us to test whether p73 expression in normal liver and HCC differs in terms of ΔN-p73 and TA-p73 isoforms. We also compared p73

\*Correspondence: M Ozturk; E-mail: ozturk@fen.bilkent.edu.tr  
Received 27 March 2001; revised 8 May 2001; accepted 24 May 2001

expression in HCC cells with the status of 'retinoblastoma pathway' and p53.

## Results

By comparison of murine p73 cDNA sequences with that of human *p73* gene, we developed assays for identification and detection of  $\Delta$ N-p73 and TA-p73 transcript isoforms (Figure 1a). Initial RT-PCR assays and nucleic acid sequencing identified  $\Delta$ N-p73 isoform in SNU 398 HCC cell line (Figure 1b). The  $\Delta$ N-p73 was also detected uniformly in mouse, rat (data not shown) and human liver tissues, as well as HCC cell lines (Figure 1c). In contrast, TA-p73 was not detectable in normal liver, but it was present in 14/15 (93%) of HCC cell lines. However, TA-p73 bands displayed various intensities. They were at the limit of detection in cDNAs from SNU 182 and SNU 423 cell lines, and there was no detectable TA-p73 expression in Mahlavu cell line (Figure 1c). p73 transcripts also differ in their 3' regions because of alternative splicing between exons 10 to 14, giving rise to  $\alpha$ ,  $\beta$ ,  $\gamma$ ,  $\delta$ ,  $\epsilon$  and  $\phi$  isoforms (Zaika *et al.*, 1999). p73 transcripts expressed in normal liver and HCC cell lines were mainly  $\alpha$ ,  $\beta$  and  $\phi$  isoforms (data not shown). To confirm the expression of  $\Delta$ N-p73 and TA-p73, we tested the presence of these protein isoforms in SNU 398 as compared to COS7 (Figure 1d), using ER 13 monoclonal antibody against amino acids 495–636 of p73- $\alpha$  (Oncogene Research Products, MA, USA). This antibody was shown to react with the  $\alpha$ , but not  $\beta$  isoform of p73 protein (Marin *et al.*, 1998). As shown in Figure 1d, ER13 antibody reacted with full-length p73- $\alpha$  (i.e. TA-p73- $\alpha$ ) in COS7 cell line which was used as a positive control (Marin *et al.*, 1998). SNU 398 cell line expressed TA-p73- $\alpha$  similar to COS7, but also a shorter polypeptide with an apparent molecular weight of 62 kD. This polypeptide can not be p73- $\beta$  because of ER 13 specificity. Its apparent molecular weight correlates with that of mouse  $\Delta$ N-p73- $\alpha$  described by Pozniak *et al.* (2000). Since, SNU 398 express both TA-p73 and  $\Delta$ N-p73 transcripts (Figure 1c), the presence of both TA-p73 and  $\Delta$ N-p73 proteins in this cell line is expected.

Next, p73 expression was studied in primary HCC tumours. As shown in Figure 1e, all tumours, as well as non tumour liver samples expressed  $\Delta$ N-p73 isoform. In addition, two of seven (29%) HCC tumour samples expressed TA-p73 isoform. An additional tumour (T1) displayed a weakly positive TA-p73 band. There was no detectable TA-p73 in the remaining T3, T4, T6 and T7 tumours, as well as in non tumour liver NT1. Thus, acquired expression of TA-p73 in HCC was demonstrated in both primary HCC tumours and HCC-derived cell lines. However, the presence of TA-p73 was more frequent in cell lines than primary tumours. The TA-p73 transcripts shown in Figure 1 were tested with a primer pair located on exons 3 and 4, respectively. It has recently been described that, in some breast carcinoma cell lines overexpressing TA-

p73, a transactivation-deficient splice variant lacking exon 2 (p73 $\Delta$ exon2) is also detected (Fillippovich *et al.*, 2001). Since our TA-p73 transcript test system would not distinguish between TA-p73 and p73 $\Delta$ exon2, we performed additional RT-PCR experiments. Using a forward primer located on exon 1 together with a reverse primer located on exon 4 (Fillippovich *et al.*, 2001), we detected mainly TA-p73 transcripts in both primary HCC and cell lines (data not shown). This confirms that TA-p73 forms described in Figure 1 are indeed full-length forms, even though one can not rule out a weak expression of p73 $\Delta$ exon2 form in some cell lines.

Induced expression of TA-p73 in some HCCs suggested that its expression is acquired during malignant transformation of hepatocytes. Recently, E2F1 transcription factor has been shown to activate p73 transcription through E2F1-binding motifs around non-coding exon 1 of p73 gene (Stiewe and Putzer 2000; Lissy *et al.*, 2000; Irwin *et al.*, 2000; Zaika *et al.*, 2001). E2F1-responsive p73 gene products have been identified as full-length p73 $\alpha$  and p73 $\beta$  proteins (Stiewe and Putzer, 2000; Lissy *et al.*, 2000; Irwin *et al.*, 2000) that can be encoded by TA-p73, but not  $\Delta$ N-p73 transcript isoforms (Figure 1a). Thus, we hypothesized that the selective induction of TA-p73 expression in HCC tumours is due to E2F1 activation. Therefore, we also tested the expression of E2F1 target genes *p14<sup>ARF</sup>* and *CCNE1* encoding cyclin E (Dyson, 1998). As shown in Figure 1e, the expression of cyclin E was induced in three tumours (T1, T2, T5), as compared to non tumour liver tissue NT1. The expression of *p14<sup>ARF</sup>* was also induced in two tumours (T1 and T2). It was also noteworthy that in TA-p73-positive T2 and T5 tumours, cyclin E expression was also induced, but only T2 showed *p14<sup>ARF</sup>* induction. Thus, three E2F1 target genes (i.e. *p73*, *Cyclin E* and *p14<sup>ARF</sup>*) were induced in some HCC tumours. However, there was no full correlation between their expression patterns in different tumours. This could be due to the quality of RNA extracted from these archival tumour tissues. (We were not able to test additional samples, because HCC is a rarely operated tumour). Alternatively, the expression of these E2F1 target genes in HCC may be under the influence of additional factors.

As the activity of E2F1 is controlled by the protein product of retinoblastoma (RB1) gene (pRb) (Dyson, 1998), we studied whether the induction of TA-p73 expression is related to the inactivation of 'retinoblastoma pathway' in HCC cells. The 'retinoblastoma pathway' in cancer cells is altered mainly by inactivation of either *RB1* or *p16<sup>INK4a</sup>* gene (Dyson, 1998). In HCC, *RB1* mutations are rare, but allelic loss and decreased pRb levels occur frequently (reviewed in Ozturk, 1999), which may be due to overexpression of gankyrin that reduces the stability of pRb, and releases 'free E2F1' (Higashitsuji *et al.*, 2000). Loss of *p16<sup>INK4a</sup>* expression by gene deletion or promoter methylation is also common in HCC (see Ozturk, 1999; Baek *et al.*, 2000). Therefore, we compared the expression of TA-p73 with the expression of pRb protein and *p16<sup>INK4a</sup>*

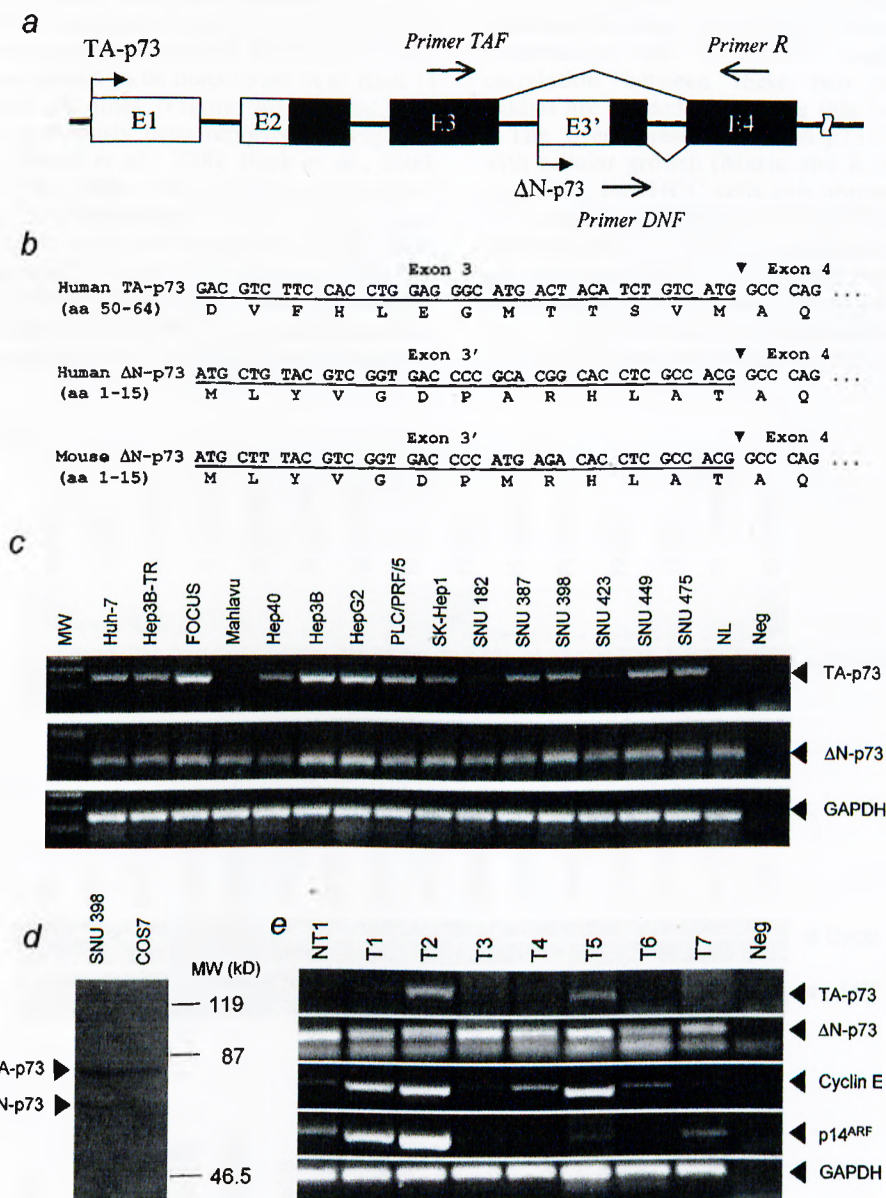


**Figure 1** Identification of TA-p73 and ΔN-p73 transcripts and their expression in normal liver, HCC cell lines and primary HCC tumours, as compared to E2F1 target genes cyclin E and p14<sup>ARF</sup>. (a) Exon-intron structure of 5' coding region of human p73 gene showing the transcription start sites and splicing events leading to TA-p73 and ΔN-p73 isoforms. Initiation of transcription in exon 1 produces the TA-isoforms, containing the transactivation (TA) domain (previously called p73), while initiation in exon 3' gives rise to the ΔN-isoforms without the TA domain. The putative transcriptional start site and exon 3' for ΔN-p73 were identified by *in silico* analysis of human p73 gene, as compared to mouse ΔN-p73 transcript sequence. Primers TAF and DNF indicate the positions of isoform-specific forward primers used to identify respectively TA-p73 and ΔN-p73 transcripts, in combination with Primer R common to both isoforms. (b) Partial nucleotide and amino acid sequences of human TA-p73 and ΔN-p73 transcript isoforms as compared to mouse ΔN-p73 isoform. Data for human ΔN-p73 was obtained from direct sequencing of a 186 bp RT-PCR product obtained from SNU 398 HCC cell line, using DNF and R primer pair. (c) As compared to normal liver (NL), the expression of TA-p73, but not ΔN-p73 is induced strongly in 14 out of 15 (93%) HCC cell lines. TA-p73 and ΔN-p73 isoforms were tested as described in a. GAPDH was used as a control for equal template loading in PCR. Neg; negative control. (d) Western blot analysis of p73 protein in SNU 398 and COS7 reveals the presence of a ~62 kD polypeptide (presumably ΔN-p73 according to Pozniak *et al.*, 2000) in SNU 398, in addition to TA-p73 protein present in both cell lines. Five-hundred μg total protein was analysed with anti-p73 ER13 monoclonal antibody which recognizes p73-α, but not p73-β isoforms (Marin *et al.*, 1998). (e) Expression of TA-p73, ΔN-p73, cyclin E and p14<sup>ARF</sup> transcripts in primary HCC tumours. RT-PCR analysis using oligonucleotide primers shown in a, reveals the expression of ΔN-p73 in all samples tested. TA-p73 is easily detected in two out of seven tumours (T2, T5), T1 shows only weak expression, non tumour liver NT1 (counterpart of T1) is negative. Similarly, cyclin E expression is also induced in T1, T2, and T5, but p14<sup>ARF</sup> transcripts are induced only in T1 and T2. GAPDH was used as a control for equal template loading in PCR. Neg; negative control

transcripts in HCC cell lines. The expression of either pRb or p16<sup>INK4a</sup> was lost in six cell lines, and significantly decreased in five others. Thus, 'retinoblastoma pathway' appeared to be inactivated in at least 11 out of 15 (73%) cell lines (Figure 2a). Indeed, this inactivation has previously been reported for eight of these cell lines (Morel *et al.*, 2000; Baek *et al.*, 2000; Puisieux *et al.*, 1993; Suh *et al.*, 2000). In support of this conclusion, the expression of E2F1 target genes *cyclin E* and *p14<sup>ARF</sup>* were also induced in all cell lines, except three for *p14<sup>ARF</sup>* (Figure 2b), due to CDKN2A gene deletion in SNU 387 and SNU 449 (Baek *et al.*, 2000), and probably in SK-Hep1. These studies showed that both the inactivation of 'retinoblastoma pathway'

and the induction of TA-p73 expression are relatively common events in HCC cell lines. However, our observations do not allow establishing a direct correlation between these two events. Additional studies are needed to address this issue.

The overexpression of TA-p73 is not compatible with cellular growth (Marin and Kaelin, 2000; Fang *et al.*, 1999), but HCC cells can apparently tolerate TA-p73 expression (Figure 1c). The ΔN-p73, co-expressed in these cells, is known to suppress both TA-p73 and p53 activities (Yang *et al.*, 2000; Pozniak *et al.*, 2000). In addition, some tumour-derived p53 mutant proteins were shown to bind and inactivate TA-p73 protein (Marin and Kaelin, 2000; Di Como *et al.*, 1999; Strano

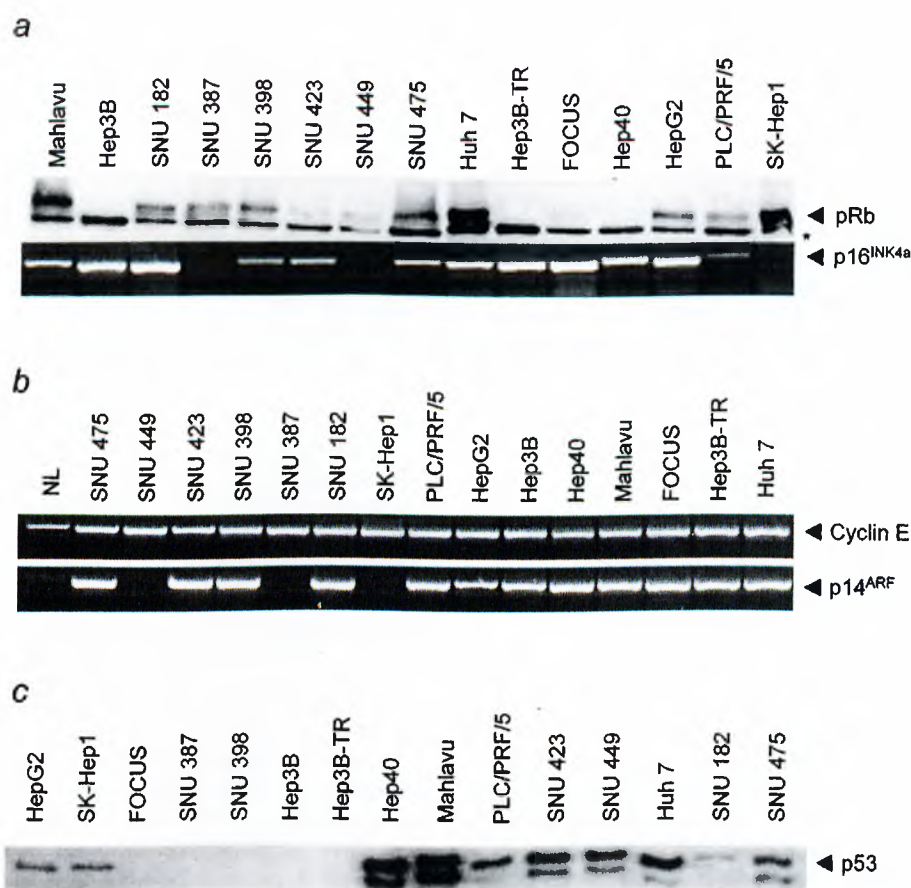


**Figure 2** Comparative analysis of the status of retinoblastoma pathway (pRb and p16<sup>INK4a</sup>), E2F1 target (cyclin E and p14<sup>ARF</sup>) and p53 genes in HCC cell lines. (a) Either pRb or p16<sup>INK4a</sup> expression is totally lost (Hep3B, SNU 387, SNU 449, Hep3B-TR, Hep40, SK-Hep1), or significantly decreased (SNU 398, SNU 423, SNU 475, FOCUS, PLC/PRF/5) in 11 out of 15 (73%) cell lines tested. Western blot analysis using antibody IF8 reveals that pRb protein is not detectable in Hep3B, Hep3B-TR and Hep40, or weakly positive in SNU 423, SNU 449 and FOCUS. The asterisk (\*) denotes a non-pRb cross-reactive antigen (Morel *et al.*, 2000), serving as a loading control for Western blot assay. RT-PCR analysis shows that p16<sup>INK4a</sup> is not detectable in SNU 387, SNU 449 and SK-Hep1, or weakly positive in SNU 398, SNU 423, SNU 475 and PLC/PRF/5. See Figure 1c for template loading control using GAPDH. Negative control for p16<sup>INK4a</sup> RT-PCR is not shown. (b) The expression of E2F1 target cyclin E and p14<sup>ARF</sup> genes is induced in HCC cell lines. RT-PCR analysis of cyclin E transcripts reveals that their expression is uniformly induced in all cell lines tested, as compared to normal liver (NL). The induction of p14<sup>ARF</sup> expression is detectable in all but three cell lines. The lack of expression in SNU 449 and SNU 387 (see Baek *et al.*, 2000), and probably SK-Hep1 (notice the lack of both p16<sup>INK4a</sup> and p14<sup>ARF</sup> expression) is due to CDKN2A gene deletion. See Figure 1c for the use of GAPDH as template loading control. Negative control is not shown. (c) Western blot assay for p53 shows no expression in FOCUS, SNU 387, SNU 398, Hep3B, Hep3B-TR, and high levels in Hep40, Mahlavu, PLC/PRF/5, SNU 423, SNU 449, Huh7, SNU 475 cell lines. Mahlavu and PLC/PRF/5 display Arg249Ser, and Huh7 Tyr220Cys mutations. HepG2 and SK-Hep1 express wild-type p53 (Puisieux *et al.*, 1993; Hsu *et al.*, 1993). pRb Western blot data was used as a loading control (as in a)

*et al.*, 2000; Marin *et al.*, 2000; Gaiddon *et al.*, 2001). Therefore, we tested whether there was a correlation between TA-p73 expression and p53 gene status in HCC cells. As shown in Figure 2c, p53 protein was either lost or mutant in at least eight out of 15 (53%) cell lines tested.

## Discussion

Our observations demonstrate that p73 gene in normal liver cells encodes only truncated  $\Delta$ N-p73 transcript isoform. In mouse, this isoform was shown to code for an inactive p73 protein, acting as a dominant negative form on the activities of full-length TA-p73 as well as wild-type p53 proteins (Yang *et al.*, 2000; Pozniak *et al.*, 2000). The dominant expression of  $\Delta$ N-p73 transcript isoform was demonstrated in normal liver tissues from human, mouse as well as rat organisms (see Figure 1c,e for human liver, other data not shown). In contrast, p73 gene encodes both TA-p73 and  $\Delta$ N-p73 isoforms in most HCC cell lines and some primary tumours. The acquired expression of TA-p73 in HCC cells appears to be transformation-related rather than proliferation-related, since Mahlavu cells did not express detectable TA-p73 transcripts, while expressing  $\Delta$ N-p73 isoform (Figure 1c). We also detected  $\Delta$ N-p73, but not TA-p73 transcripts in proliferating normal human fibroblast cell line MRC5 (data not shown).

Separate analysis of  $\Delta$ N-p73 and TA-p73 transcripts in liver and HCC has not been reported yet. However, Tannapfel *et al.* (1999a) reported the absence of p73 expression in normal hepatocytes, using an antibody directed against amino acid residues encoded by exon 3 of p73, which is absent in  $\Delta$ N-p73, but present in TA-p73 transcripts (see Figure 1b). Studies with this antibody (together with another anti-p73 antibody directed against a region common to both TA-p73 and  $\Delta$ N-p73 proteins) also demonstrated that the p73 protein was negative in non tumour liver tissues, but positive in 32% of HCCs (Tannapfel *et al.*, 1999b). Based on observations described here, it now appears that p73 detected in these HCCs is the TA-p73 form, although this requires a separate confirmation analysis with the TA-p73-specific antibody alone.

The induction of TA-p73 and the 'retinoblastoma pathway' inactivation was common in HCC cell lines (Table 1). However, comparative studies did not allow us to establish a link between the induction of TA-p73 expression and the inactivation of 'retinoblastoma pathway'. For example, the expression of E2F1-target genes was also induced in cell lines with apparently normal pRb and p16<sup>INK4a</sup> expression. Nevertheless, our results indicate that 'retinoblastoma pathway' inactivation is common in HCC cell lines and it is accompanied by an induction of E2F1 target genes (i.e. p73, cyclin E and p14<sup>ARF</sup>) in most HCCs. This may suggest that the acquired expression of TA-p73 in some HCC cell lines is due to the inactivation of 'retino-

blastoma pathway'. However, this remains to be demonstrated with further studies.

The expression of  $\Delta$ N-p73 in normal liver, and the acquired expression of TA-p73 in HCC reveal new implications for p73 in tumour biology. The p73 gene, encoding only  $\Delta$ N-p73 transcripts in normal liver, may function as a tumour promoter rather than a tumour suppressor in this tissue, by interfering with wild-type p53 function (Yang *et al.*, 2000; Pozniak *et al.*, 2000). This could explain why p73 is not mutated in HCC (Mihara *et al.*, 1999). However, p53 gene is frequently mutated in HCC (Ozturk, 1999), as also demonstrated here in HCC-derived cell lines (Figure 2c). Thus,  $\Delta$ N-p73 protein may not completely neutralize wild-type p53 activity. Alternatively, the induction of TA-p73 transcription in tumour cells may redirect  $\Delta$ N-p73 protein from wild-type p53 to newly expressed TA-p73 proteins.

On the other hand, the expression of TA-p73 transcripts in HCC cells is puzzling, based on the fact that TA-p73 overexpression is known to induce growth arrest and apoptosis (Marin and Kaelin, 2000; Lohrum and Vousden, 2000). Therefore, HCC cells expressing TA-p73 need to equip themselves with mechanism(s) to tolerate TA-p73 protein expression. In addition to a possible role of  $\Delta$ N-p73 protein for TA-p73 inactivation (Yang *et al.*, 2000; Pozniak *et al.*, 2000), mutant p53 proteins may also inactivate TA-p73, as reported previously (Di Como *et al.*, 1999; Strano *et al.*, 2000; Marin *et al.*, 2000; Gaiddon *et al.*, 2001). Accordingly, several HCC cell lines reported here (Mahlavu, PLC/PRF/5, Huh7 etc.) express mutant p53 proteins that may inactivate TA-p73 protein. However, some other cell lines (FOCUS, Hep3B, SNU 387, SNU 398 etc.) have lost p53 expression. In this later group of cell lines, the tolerance of TA-p73 expression may require mutant p53-independent mechanisms. One additional hypothesis is that TA-p73 protein levels and/or its growth suppressive activities are regulated by post-translational mechanisms, independent of both  $\Delta$ N-p73 and mutant p53. For example, endogenous p73 protein in a tumour cell line was shown to be stabilized by cisplatin and by c-Abl kinase, with no change in p73 transcript levels (Gong *et al.*, 1999). Moreover, the apoptosis-inducing function of p73 was demonstrated to be dependent to or enhanced by the c-Abl kinase in different cell types (Yuan *et al.*, 1999; Agami *et al.*, 1999; Gong *et al.*, 1999). Thus, some HCC cell lines may tolerate TA-p73 expression, if, for example, they are deficient in c-Abl kinase activity.

## Materials and methods

### Tissues and cell lines

Normal liver tissues from Balb/c mice and Sprague-Dawley rats were obtained after ether anaesthesia. Normal human liver tissue was obtained from discarded surgical material from a patient operated for hepatic hydatid cyst. Primary HCC tumours and non tumour liver were freshly frozen

**Table 1** Comparative analysis of TA-p73 induction, E2F1 target gene activation and the retinoblastoma (*RBI*) pathway inactivation in HCC cell lines

Cell lines	<i>pRb</i>	<i>RBI</i> pathway genes <i>p16<sup>INK4a</sup></i>	TA-p73	E2F1 target genes <i>p14<sup>ARF</sup></i>	Cyclin E
<i>Group I: Inactivated RBI pathway</i>					
hep3B	ND	Positive	Positive	Positive	Positive
Hep3B-TR	ND	Positive	Positive	Positive	Positive
hep40	ND	Positive	Positive	Positive	Positive
FOCUS	Traces	Positive	Positive	Positive	Positive
SNU-449	Positive	ND	Positive	ND	Positive
SNU-387	Positive	ND	Positive	ND	Positive
SK-hep1	Positive	ND	Positive	ND	Positive
PLC/PRF/5	Positive	Traces	Positive	Positive	Positive
SNU-475	Positive	Traces	Positive	Positive	Positive
SNU-398	Positive	Traces	Positive	Positive	Positive
SNU-423	Traces	Traces	Traces	Positive	Positive
<i>Group II: Normal RBI pathway</i>					
Mahlavu	Positive	Positive	ND	Positive	Positive
SNU-182	Positive	Positive	Traces	Positive	Positive
HepG2	Positive	Positive	Positive	Positive	Positive
Huh-7	Positive	Positive	Positive	Positive	Positive

ND: not detected

archival materials. Fifteen human hepatoma-derived cell lines (14 HCC and one hepatoblastoma), MRC5 and COS7 were grown in culture as described (Morel *et al.*, 2000). Most cell lines were from ATCC, the others have been previously described (Morel *et al.*, 2000; Baek *et al.*, 2000; Puisieux *et al.*, 1993; Bouzahzah *et al.*, 1995).

#### RNA and cDNA preparations

Total RNA from cell lines and tissues was extracted using NucleoSpin RNA II Kit (MN Macherey-Nagel, Duren, Germany) and TriPure reagent (Boehringer Mannheim, Indianapolis, IN, USA), respectively. The cDNAs were prepared from total RNA (5 µg) using RevertAid First Strand cDNA Synthesis Kit (MBI-Fermentas, Vilnius, Lithuania).

#### Transcript analysis by RT-PCR

For the identification of TA-p73 and ΔN-p73 forms, we used the available human p73 genomic sequence and mouse ΔN-p73 cDNA sequence data and designed two forward and one reverse (Primer R; 5'-GCGACATGGTGTCGAAGGTG-GAGC-3') primers to specifically amplify these forms from human, mouse and rat tissues. These sequences were selected on the basis of highest homology between mouse and human DNA sequences (maximum one mismatch, data not shown). The forward primers TAF (5'-AACCAGACGACCT-ACTTCGACC-3') and DNF (5'-ACCATGCTG TAC-GTCGGTGACCCC-3') were used for specific amplification of TA-p73 and ΔN-p73 forms, respectively. For the detection of p73 isoforms generated by differential splicing between exons 10 to 14, a forward primer from exon 10 (5'-CGCCATATT GGTGCCGACCCACTGGTG-3') and two different reverse primers were used. A reverse primer from exon 13 (5'-GTTTGGCACCCCAATCCTGT-3') was used for specific amplification of transcripts containing this exon, i.e. p73α, p73ε, and p73γ (see Zaika *et al.*, 1999 for terminology). Another reverse primer, encompassing sequences from exon 12 followed by exon 14 (5'-AGGGCCCC-CAGTCTGAGC-3'), was used for specific amplification of p73β and p73φ isoforms (Zaika *et al.*, 1999) that contain

this particular sequence. p16<sup>INK4a</sup> and p14<sup>ARF</sup> RT-PCRs were done using a specific forward primer for each transcript (5'-CGGAGAGGGGGAGAACAGAC-3' for p16<sup>INK4a</sup> and 5'-TCACCTCTGGTGCCAAAGGG-3' for p14<sup>ARF</sup>) and a common reverse primer (5'-GGCAGTTGTGGCCCTG-TAGG-3'). For the detection of cyclin E mRNA levels, cyclin E-F (5'-TTGACCGGTATATGGCGACACAAG-3') and cyclin E-R (5'-ATGATACAAGGCCGAAGCAG-CAAG-3') primers were used. All RT-PCR reactions were done using appropriate annealing and extension conditions (additional information is available upon request). Equal amount of RNA was used in cDNA synthesis and the quality of cDNA was initially tested by GAPDH RT-PCR amplification with primer pair F (5'-GGCTGAGAACGG-GAAGCTTGTTCAT-3') and R (5'-CAGCCTTCTCCAT-GGTGGTGAAGA-3'), using 1/40 vol-ume of cDNA preparation. Further PCR studies were performed with cDNA preparations yielding equal amounts of GAPDH amplification products. Total PCR cycle numbers have been defined following an initial study at 22, 26, 30 and 34 cycles, in order to remain in the logarithmic phase of amplification. All RT-PCR results have been repeated several times from different batches of RNA preparations except primary tumours for which single RNA preparations were used. The expression of TA-p73 isoform was confirmed with an additional pair of primers, as described by Fillippovich *et al.* (2001). The identity of different p73 isoforms (TA-p73, ΔN-p73, p73α, p73β, p73γ, p73φ) has been confirmed by restriction enzyme mapping and automated sequencing (PE, ABI PRISM 377 automated sequencer) techniques.

#### Western blotting

The expression of retinoblastoma (pRb) and p53 proteins in different cell lines was studied by Western blotting, using anti-pRb IF8 (SC102, Santa Cruz Biotechnology) and anti-p53 6B10 (Yolcu *et al.*, 2001) monoclonal antibodies, respectively, as described previously (Morel *et al.*, 2000). Equal protein loading was confirmed by blotting with control antibody against cytokeratin 18 (JAR13 clone, gift from D Bellet, Institut Gustave Roussy, France). p73 protein Western

blot assays were done with ER13 (Ab-1, Oncogene Research Products, MA, USA) using the experimental procedure described by Marin *et al.* (1998).

#### Abbreviations

HCC, hepatocellular carcinoma; RBI, retinoblastoma gene; pRb, retinoblastoma protein.

#### Acknowledgements

This work was supported by a grant from TUBITAK (Turkey). We would like to thank B Carr (University of Pittsburgh, PA, USA) for providing Hep40 and Hep3B-TR

cell lines, D Bellet (Institut Gustave Roussy, France) for JAR13 antibody, R Cetin-Atalay for critical reading of the manuscript, T Cagatay for DNA sequencing work, C Akcali's group for animal surgery, and G Tuncman for help in RNA studies.

#### Accession numbers

The following sequences were deposited in the GenBank database. Human DNA sequence from clone RP5-1092A11 on chromosome 1p36.2-36.33 containing p73 gene: AL136528; Mouse mRNA for p73 delta-N protein: Y19235; Homo sapiens p73 gene: AH007820.

#### References

- Agami R, Blandino G, Oren M and Shaul Y. (1999). *Nature*, **399**, 809–813.
- Baek MJ, Piao Z, Kim NG, Park C, Shin EC, Park JH, Jung HJ, Kim CG and Kim H. (2000). *Cancer*, **89**, 60–69.
- Bouzahzah B, Nishikawa Y, Simon D and Carr BI. (1995). *J. Cell Physiol.*, **165**, 459–467.
- Di Como CJ, Gaiddon C and Prives C. (1999). *Mol. Cell Biol.*, **19**, 1438–1449.
- Dyson N. (1998). *Genes Dev.*, **12**, 2245–2262.
- Fang L, Lee SW and Aaronson SAJ. (1999). *J. Cell Biol.*, **147**, 823–830.
- Fillippovich I, Sorokina N, Gatei M, Haupt Y, Hobson K, Moallem E, Spring K, Mould M, McGuckin MA, Lavin MF and Khanna KK. (2001). *Oncogene*, **20**, 514–522.
- Gaiddon C, Lokshin M, Ahn J, Zhang T and Prives C. (2001). *Mol. Cell Biol.*, **21**, 1874–1887.
- Gong JG, Costanzo A, Yang HQ, Melino G, Kaelin Jr WG, Levvero M and Wang JY. (1999). *Nature*, **399**, 806–809.
- Higashitsuji H, Itoh K, Nagao T, Dawson S, Nonoguchi K, Kido T, Mayer RJ, Arii S and Fujita J. (2000). *Nat. Med.*, **6**, 96–99.
- Hsu IC, Tokiwa T, Bennett W, Metcalf RA, Welsh JA, Sun T and Harris CC. (1993). *Carcinogenesis*, **14**, 987–992.
- Irwin M, Marin MC, Phillips AC, Seelan RS, Smith DI, Liu W, Flores ER, Tsai KY, Jacks T, Vousden KH and Kaelin WG. (2000). *Nature*, **407**, 645–648.
- Lissy NA, Davis PK, Irwin M, Kaelin WG and Dowdy SF. (2000). *Nature*, **407**, 642–645.
- Lohrum MA and Vousden KH. (2000). *Trends Cell Biol.*, **10**, 197–202.
- Marin MC, Jost CA, Irwin MS, DeCaprio JA, Caput D and Kaelin WG. (1998). *Mol. Cell Biol.*, **18**, 6316–6324.
- Marin MC and Kaelin Jr WG. (2000). *Biochim. Biophys. Acta*, **1470**, M93–M100.
- Marin MC, Jost CA, Brooks LA, Irwin MS, O'Nions J, Tidy JA, James N, McGregor JM, Harwood CA, Yulug IG, Vousden KH, Allday MJ, Gusterson B, Ikawa S, Hinds PW, Crook T and Kaelin WG. (2000). *Nat. Genet.*, **25**, 47–54.
- Mihara M, Nimura Y, Ichimiya S, Sakiyama S, Kajikawa S, Adachi W, Amano J and Nakagawara A. (1999). *Br. J. Cancer*, **79**, 164–167.
- Morel AP, Unsal K, Cagatay T, Ponchel F, Carr B and Ozturk M. (2000). *J. Hepatol.*, **33**, 254–265.
- Ozturk M. (1999). *Semin. Liver Dis.*, **19**, 235–242.
- Pozniak CD, Radinovic S, Yang A, McKeon F, Kaplan DR and Miller FD. (2000). *Science*, **289**, 304–306.
- Puisieux A, Galvin K, Troalen F, Bressac B, Marçais C, Galun E, Ponchel F, Yakicier C, Ji J and Ozturk M. (1993). *FASEB J.*, **7**, 1407–1413.
- Stiewe T and Putzer BM. (2000). *Nat. Genet.*, **26**, 464–469.
- Strano S, Munarriz E, Rossi M, Cristofanelli B, Shaul Y, Castagnoli L, Levine AJ, Sacchi A, Cesareni G, Oren M and Blandino G. (2000). *J. Biol. Chem.*, **275**, 29503–29512.
- Suh S, Pyun H, Cho J, Baek W, Park J, Kwon T, Park JW, Suh MH and Carson DA. (2000). *Cancer Lett.*, **160**, 81–88.
- Tannapfel A, Engeland K, Weinans L, Katalinic A, Hauss J, Mossner J, Engeland K and Wittekind C. (1999a). *Br. J. Cancer.*, **80**, 1069–1074.
- Tannapfel A, Wasner M, Krause K, Geissler F, Katalinic A, Hauss J and Wittekind C. (1999b). *J. Natl. Cancer Inst.*, **91**, 1154–1158.
- Yang A, Kaghad M, Wang Y, Gillett E, Fleming MD, Dotsch V, Andrews NC, Caput D and McKeon F. (1998). *Mol. Cell*, **3**, 305–316.
- Yang A, Walker N, Bronson R, Kaghad M, Oosterwegel M, Bonnin J, Vagner C, Bonnet H, Dikkes P, Sharpe A, McKeon F and Caput D. (2000). *Nature*, **404**, 99–103.
- Yolcu E, Sayan BS, Yagci T, Cetin-Atalay R, Soussi T, Yurdusev N and Ozturk M. (2001). *Oncogene*, **20**, 1398–1401.
- Yuan ZM, Shioya H, Ishiko T, Sun X, Gu J, Huang YY, Lu H, Kharbanda S, Weichselbaum R and Kufe D. (1999). *Nature*, **399**, 814–817.
- Zaika A, Irwin M, Sansome C and Moll UM. (2001). *J. Biol. Chem.*, **276**, 11310–11316.
- Zaika AI, Kovalev S, Marchenko ND and Moll UM. (1999). *Cancer Res.*, **59**, 3257–3263.



## SHORT REPORT

# A monoclonal antibody against DNA binding helix of p53 protein

Esma Yolcu<sup>1,2</sup>, Berna S Sayan<sup>1</sup>, Tamer Yağci<sup>2</sup>, Rengul Cetin-Atalay<sup>1</sup>, Thierry Soussi<sup>3</sup>, Nevzat Yurdusev<sup>2</sup> and Mehmet Ozturk<sup>\*1,2</sup>

<sup>1</sup>Department of Molecular Biology and Genetics and BilGen Genetics and Biotechnology Center, Bilkent University, 06533, Ankara, Turkey; <sup>2</sup>TUBITAK-MRC, Research Institute for Genetic Engineering and Biotechnology, Department of Molecular Oncology, Gebze, Kocaeli, Turkey; <sup>3</sup>Institut Curie, Paris, France

Three monoclonal antibodies (Mabs) were generated against p53 DNA-binding core domain. When tested by immunoprecipitation, Western blot and immunofluorescence techniques, Mab 9E4, as well as 7D3 and 6B10 reacted with both wild-type and various mutant p53 proteins. The epitopes recognized by Mabs 7D3, 9E4 and 6B10 were located respectively within the amino acid residues 211–220, 281–290 and 291–300 of human p53 protein. The epitope recognized by 9E4 Mab coincides with helix 2, also called p53 DNA binding helix, which allows the direct contact of the protein with its target DNA sequences. This antibody may be useful to study transcription-dependent and transcription-independent activities of wild-type and mutant p53 proteins. *Oncogene* (2001) 20, 1398–1401.

**Keywords:** p53; hybridoma; DNA binding helix

Encoded by a tumor suppressor gene, p53 protein is one of the most intensively investigated molecules in the tumor biology field (Levine, 1997). Wild-type p53 protein is a transcription factor that regulates the expression of a large list of genes involved in many different cellular processes such as growth arrest, apoptosis, senescence, DNA repair and tumor metastasis. The best-described functions of wild-type p53 are cell cycle arrest and apoptosis as a response to DNA damage. Cell cycle arrest is mediated by p53-induced transcriptional activation, whereas apoptosis was reported to be induced by both transcription-dependent and transcription-independent pathways (Agarwal *et al.*, 1998).

In normal cells, p53 protein is actively degraded by a mechanism involving p53-mdm2 interaction. Following DNA damage or oncogene activation, p53 is stabilized and accumulates in cells (Oren, 1999). Transcriptional activation induced by p53 results from its nuclear localization and binding, as a tetramer, to specific p53-binding pentamers (PuPuPuCA/T) located at the regulatory regions of different p53-responsive genes (Levine, 1997). The central core region of p53 is

directly involved in its binding to target DNA motifs. This region is known as an independently folded, compact structural domain. Cho *et al.* (1994) demonstrated that the structure of the p53 core domain contains a  $\beta$  sandwich composed of two antiparallel  $\beta$  sheets, and a loop- $\beta$  – sheet- $\alpha$  – helix motif that packs tightly against one end of the  $\beta$  sandwich. At this end of the  $\beta$  barrel, there are two long loop regions (L2 and L3) that are stabilized by a tetrahedrally coordinated zinc atom. Although the  $\beta$  barrel comprises a major part of the core domain structure, two loops and one  $\alpha$  helix of p53 are directly involved in DNA binding. Protein-DNA interactions are composed of major groove contacts with C-terminal sequence of the  $\alpha$  helix H2 (aa 278–286) and loop L1 (aa 112–124) of the loop-sheet-helix motif; minor groove interactions which take place in the A:T-rich region of the DNA and involve Arg<sup>248</sup> from L3 loop (aa 236–251), and interactions of p53 with the phosphate backbone connecting major and minor grooves (Cho *et al.*, 1994). The majority of p53 gene alterations are missense mutations leading to the synthesis of mutant proteins. These mutant proteins are unable to bind the target DNA sequences due to the substitutions at key amino acid residues of the DNA binding core domain (Soussi *et al.*, 2000).

Monoclonal antibodies directed against linear and conformational epitopes at different domains of p53 protein are highly useful tools to investigate structure-function relationship of wild-type and mutant p53 proteins. Most of these antibodies react with epitopes located at the antigenically dominant N-terminal and C-terminal regions of p53 (Legros *et al.*, 1994). The centrally located core region is poorly antigenic, and only a few monoclonal antibodies have been generated to this critical DNA binding domain (Legros *et al.*, 1994). We generated three monoclonal antibodies against p53 DNA binding domain, from mice immunized with recombinant full length human p53 protein, by selective screening of antibody-producing hybridomas using a truncated p53 polypeptide lacking both N-terminal and C-terminal regions (a histidine-tagged 237 amino acid polypeptide spanning residues 72–308 of human p53 protein).

Three hybridoma clones (named 6B10, 7D3 and 9E4) producing monoclonal anti-p53 antibodies were selected for further studies. All three Mabs were first

\*Correspondence: M Ozturk  
Received 4 December 2000; revised 8 January 2001; accepted 8 January 2001

tested for their ability to recognize human p53 protein using western immunoblotting technique (Figure 1). Both 9E4 and 6B10 recognized wild-type p53 expressed in HepG2 cells, but 7D3 reacted only weakly. All three antibodies also reacted with two different mutant p53 proteins, p53-Y220C and p53-R249S, expressed in Huh-7 and Mahlavu cells, respectively. p53-deleted Hep3B cells were used as a negative control (Hsu *et al.*, 1993). Interestingly, 9E4 reacted with three antigens in these p53-deficient cells, as well as three other cell lines tested (Figure 1). These antigens showed a different migration pattern than wild-type or mutant p53 proteins (compare 9E4 with 6B10 in Figure 1), and appear to be unrelated to p53 protein. The apparent molecular weights of two antigens were higher than that of p53. The nature of these antigens recognized by 9E4 is presently unknown. On the other hand, 9E4 antibody reacted only with p53 when tested by immunoprecipitation after <sup>35</sup>S-methionine labelling of transfected Saos cells (Figure 2). This suggests that 9E4 recognizes several cross-reacting antigens under denaturing conditions of Western blot assay, but not in their native form. The immunoprecipitation experiments with both 9E4 and 6B10, in comparison with DO7 antibody (Vojtesek *et al.*, 1992) also indicated that their immunoreactivities with different p53 proteins were weaker, probably because their respective epitopes are less accessible under non-denaturing conditions of immunoprecipitation assay (Figure 2). Figure 2 shows that all tested p53 mutants are recognized by 9E4, and to a lesser degree by 6B10. Some of these mutants such as p53-R175P retain transcriptional activity and the ability to induce G1 arrest, but have lost apoptotic activity, while others such as p53-R175Y and p53-R175 W have lost both activities (Ryan and Vousden, 1998).

We also tested 9E4, 6B10 and 7D3 antibodies by indirect immunofluorescence after fixation and permeabilization of cells with methanol. A strongly positive nuclear staining was observed with 9E4 and 6B10 in many cell lines expressing different mutant p53 proteins. The 9E4 Mab also reacted strongly with a cytoskeleton-associated antigen in different cell lines tested, including p53-negative Hep3B cells, under these conditions. These observations confirm our hypothesis that antigens cross-reacting with 9E4 antibody are recognized only under denaturing conditions. The immunoreactivity observed by 7D3 was weak in indirect immunofluorescence assay, similarly to Western blot data (data not shown).

The main characteristics of our antibodies are summarized in Table 1. The epitopes recognized by these antibodies were determined by Pepscan ELISA, as previously described (Legros *et al.*, 1994). The 7D3 Mab reacted with an epitope located within amino acid residues 211–220 (TFRHSVVVPY) of human p53. This 10 amino-acid fragment carries epitopes for two previously identified antibodies, namely Pab240 that recognizes the residues 213–218 (Stephen and Lane, 1992) and HO13.1 (Legros *et al.*, 1994). The 6B10 Mab recognizes amino acids residues 291–300 (KKGEPH-

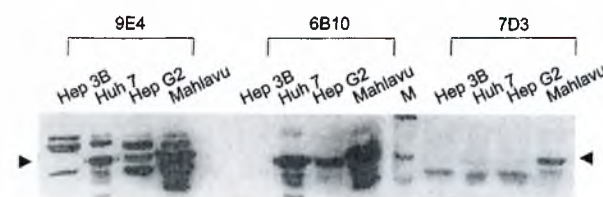


**Figure 1** Immunoreactivities of 6B10, 7D3 and 9E4 monoclonal antibodies with wild-type and mutant p53 protein as tested by Western immunoblotting. Cell lysates were prepared from indicated cell lines using a buffer containing 150 mM NaCl, 1 mM EDTA, 1.0% NP-40, 10 mM Tris (pH 8.0), 1.0% sodium deoxycolate and 1×complete EDTA-free protease inhibitor cocktail (Roche). A total of 30 μg protein was loaded from each lysate and subjected to 10% SDS-PAGE. Transfer of the proteins to PVDF membrane (Millipore) was performed by Bio-Rad semi-dry transfer cell. Membranes were blocked in TBS-T containing 3% dried non-fat milk powder and incubated with the indicated anti-p53 antibodies. Detection was performed with Lumilight-plus kit (Roche). Black arrows indicate p53 protein. Note that Hep 3B cells are p53-negative, while HepG2, Huh-7 and Mahlavu cells express wild-type, mutant p53-Y220C and mutant p53-R249S, respectively (Hsu *et al.*, 1993)

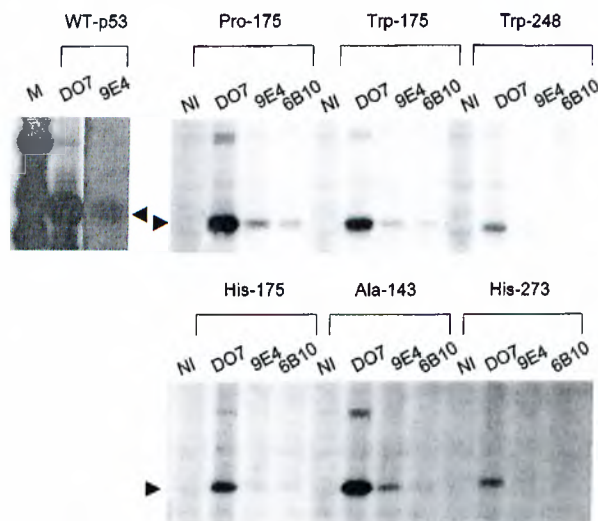


**Figure 2** Immunoprecipitations of wild-type and mutant p53 proteins with 9E4 and 6B10 monoclonal antibodies indicate that both 9E4 and 6B10 recognize both wild-type and mutant p53 proteins, although their immunoreactivities are weak in comparison to DO7 monoclonal antibody. The experiments for wild-type p53 protein were performed with in-vitro translated human p53. All other experiments were performed with p53 negative SaOs cells following transient transfection with the indicated mutant forms of human p53. Following transfections, cells were metabolically labelled with <sup>35</sup>S-methionine, and lysed in a buffer containing 150 mM NaCl, 1 mM EDTA, 1.0% NP-40, 10 mM Tris (pH 8.0), 1.0% sodium deoxycholate, 10 μg/ml leupeptine, 1 μg/ml pepstatin and 10 μg/ml aprotinin. Following centrifugation, supernatants were immunoprecipitated with the indicated antibodies and Protein G agarose, run on SDS-PAGE and subjected to autoradiography

HELP), similar to HO7.1 and HO33.8 antibodies described by Legros *et al.* (1994).

The Mab 9E4 recognizes a new epitope located within amino acids residues 281–290 (DRRTEENLR). This epitope comprises six (DRRTEE) of the nine amino acid

Table 1 Characteristics of monoclonal antibodies 6B10, 7D3 and 9E4

Monoclonal antibodies	Ig isotype (light chain) <sup>a</sup>	Epitope on human p53 (amino acid residues) <sup>b</sup>	Related structural motifs (amino acid residues)
7D3	IgG2a ( $\kappa$ )	TFRHSVVVPY (211–220)	Pab240 epitope <sup>c</sup> (213–218)
9E4	IgG1 ( $\kappa$ )	DRRTEENLR (281–290)	H2 Helix <sup>d</sup> (278–286)
6B10	IgG1 ( $\kappa$ )	KKGEPHHELP (291–300)	HO7.1 and HO33.8 epitopes <sup>b</sup> (291–300)

<sup>a</sup>Isotypes were determined by 'Mouse-Hybridoma Subtyping Kit' (Boehringer). <sup>b</sup>Epitopes were mapped by Pepsan ELISA assay (Legros *et al.*, 1994). <sup>c</sup>Stephen and Lane (1992). <sup>d</sup>Cho *et al.* (1994)

residues (PGRDRRTEE) that form the DNA binding H2  $\alpha$  helix motif (H2) of human p53 (residues 278–286). p53 interactions with its target pentamer involve both major and minor groove contacts. Several amino acid residues of H2 motif are involved in these contacts. The Arg<sup>280</sup> residue, reinforced by Asp<sup>281</sup>, makes the most critical major groove contact with the invariant C:G base pair of the pentamer consensus. The Asp<sup>281</sup>, does not participate directly to DNA contacts, but it forms salt bridges with both Arg<sup>280</sup>, and Arg<sup>273</sup> which itself binds to a phosphate group in the consensus motif. Finally, Arg<sup>283</sup> of H2 helix participates to DNA backbone contacts by binding to another phosphate of the consensus motif. A fourth residue of H2 helix, Arg<sup>282</sup>, one of the six mutational hotspots of p53, plays a structural role in the loop-sheet-helix motif, being involved in the packing of H2 helix against the  $\beta$  hairpin and L1 loop (Cho *et al.*, 1994). Thus, the epitope recognized by 9E4 harbors several key amino acid residues directly involved in specific binding of p53 to its target DNA sequences.

The positions of epitopes recognized by 7D3 and 9E4 Mabs are shown in Figure 3. We believe that the 9E4 antibody will be a quite useful tool for different studies related to the specific binding of p53 to its target DNA sequences, as well as for the comparison of its transcription-dependent and transcription-independent cellular activities. It is expected that 9E4 antibody will block both specific DNA-binding and transcriptional regulatory activities of p53, when introduced into cells by micro-injection or as an intracellular antibody (Cohen *et al.*, 1998; Caron de Fromentel *et al.*, 1999). By the same methods, 9E4 may also be useful to test whether certain p53 mutants display any transcriptional activity, either as a repressor or activator, directly or indirectly (Blandino *et al.*, 1999). Finally, two recently discovered p53 homologue proteins, namely p63 and p73, are known to display p53-like transcriptional activities. These new proteins have different amino acid sequences in the region homologous to 9E4 antibody epitope on p53

## References

- Agarwal ML, Taylor WR, Chernov MV, Chernova OB and Stark GR. (1998). *J. Biol. Chem.*, **273**, 1–4.  
Blandino G, Levine AJ and Oren M. (1999). *Oncogene*, **18**, 477–485.

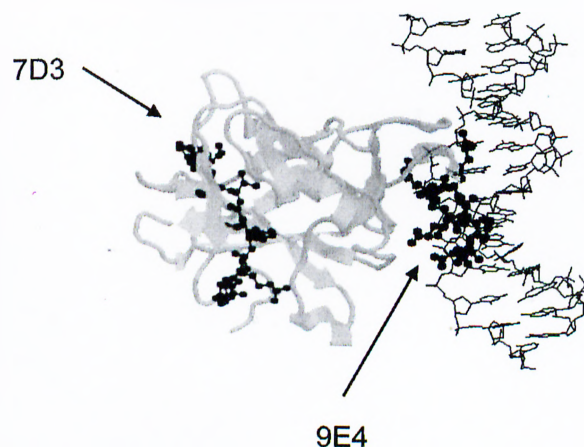


Figure 3 The location of p53 protein epitopes recognized by 7D3 and 9E4 mouse monoclonal antibodies on the p53 core domain. The three dimensional model of the core domain of human p53 and its DNA binding site (Cho *et al.*, 1994), illustrating the epitope structures (ball and stick in black) involved in direct interaction with 7D3 and 9E4 monoclonal antibodies

protein. In contrast to the DRRTEENLR sequence on p53, p63 and p73 have respectively DRKADEDSIR and DRKADEDHYR sequences (underlined residues differ from that of p53) at the same region (Kaghad *et al.*, 1997; Osada *et al.*, 1998). It is highly unlikely that 9E4 will be able to recognize these corresponding amino acid residues on p63 and p73. Therefore, 9E4 may be used to block specifically any p53-related transcriptional activity, when studying cellular activities of p63 or p73 under experimental conditions. Such studies are under investigation.

## Acknowledgments

This work is supported by grants from ICGB and TUBITAK.

- Caron de Fromentel C, Gruel N, Venot C, Debussche L, Conseiller E, Dureau C, Teillaud JL, Tocque B and Bracco L. (1999). *Oncogene*, **18**, 551–557.



- Cho Y, Gorina S, Jeffrey PD and Pavletich NP. (1994). *Science*, **265**, 346–355.
- Cohen PA, Mani JC and Lane DP. (1998). *Oncogene*, **17**, 2445–2456.
- Hsu IC, Tokiwa T, Bennett W, Metcalf RA, Welsh JA, Sun T and Harris CC. (1993). *Carcinogenesis*, **14**, 987–992.
- Kaghad M, Bonnet H, Yang A, Creancier L, Biscan JC, Valent A, Minty A, Chalon P, Lelias JM, Dumont X, Ferrara P, McKeon F and Caput D. (1997). *Cell*, **90**, 809–819.
- Legros Y, Meyer A, Ory K and Soussi T. (1994). *Oncogene*, **9**, 3689–3694.
- Levine AJ. (1997). *Cell*, **88**, 323–331.
- Oren M. (1999). *J. Biol. Chem.*, **274**, 36031–36034.
- Osada M, Ohba M, Kawahara C, Ishioka C, Kanamaru R, Katoh I, Ikawa Y, Nimura Y, Nakagawara A, Obinata M and Ikawa S. (1998). *Nat. Med.*, **4**, 839–843.
- Ryan KM and Vousden C. (1998). *Mol. Cell. Biol.*, **18**, 3692–3698.
- Soussi T, Dehouche K and Bérout C. (2000). *Hum. Mutat.*, **15**, 105–113.
- Stephen CW and Lane DP. (1992). *J. Mol. Biol.*, **225**, 577–583.
- Vojtesek B, Bartek J, Midgley CA and Lane DP. (1992). *J. Immunol. Methods*, **151**, 237–244.